N° d'ordre: 254-2008   Année 2008

THESE

Présentée devant

Jilin University

et

Université Claude Bernard Lyon 1,

Pour l'obtention

Du DIPLOME DE DOCTORAT

(Arrêté du 7 août 2006 et arrêté du 6 janvier 2005)

Présentée et soutenue publiquement le 14 Décembre 2008

Par

Lina LI

Specific recognition and enzymatic inhibition: Chemical and biochemical aspects of mineralization mechanisms

Directeurs de thèse:

Pr René Buchet et Pr Yuqing Wu

JURY: Mme le Pr. Yanmei LI – rapporteur

M le Pr. M Slawomir PIKULA- rapporteur

M le Pr. Marc LEMAIRE

M le Pr. Junqiu LIU

M le Dr.Stéphane PELLET-ROSTAING

M le Pr. Peiyi WU

Mme le Pr. Yuqing WU

M le Pr. René BUCHET

UNIVERSITE CLAUDE BERNARD - LYON I

Président de l'Université	**M. le Professeur L. COLLET**
Vice-Président du Conseil Scientifique	M. le Professeur J.F. MORNEX
Vice-Président du Conseil d'Administration	M. le Professeur J. LIETO
Vice-Président du Conseil des Etudes et de la Vie Universitaire	M. le Professeur D. SIMON
Secrétaire Général	M. G. GAY

SECTEUR SANTE

Composantes

UFR de Médecine Lyon R.T.H. Laënnec	Directeur : M. le Professeur P. COCHAT
UFR de Médecine Lyon Grange-Blanche	Directeur : M. le Professeur X. MARTIN
UFR de Médecine Lyon-Nord	Directeur : M. le Professeur J. ETIENNE
UFR de Médecine Lyon-Sud	Directeur : M. le Professeur F.N. GILLY
UFR d'Odontologie	Directeur : M. O. ROBIN
Institut des Sciences Pharmaceutiques et Biologiques	Directeur : M. le Professeur F. LOCHER
Institut Techniques de Réadaptation	Directeur : M. le Professeur MATILLON
Département de Formation et Centre de Recherche en Biologie Humaine	Directeur : M. le Professeur P. FARGE

SECTEUR SCIENCES

Composantes

UFR de Physique	Directeur : Mme. le Professeur S. FLECK
UFR de Biologie	Directeur : M. le Professeur H. PINON
UFR de Mécanique	Directeur : M. le Professeur H. BEN HADID
UFR de Génie Electrique et des Procédés	Directeur : M. le Professeur G. CLERC
UFR Sciences de la Terre	Directeur : M. le Professeur P. HANTZPERGUE
UFR de Mathématiques	Directeur : M. le Professeur M. CHAMARIE
UFR d'Informatique	Directeur : M. le Professeur S. AKKOUCHE
UFR de Chimie Biochimie	Directeur : Mme. le Professeur H. PARROT
UFR STAPS	Directeur : M. C. COLLIGNON
Observatoire de Lyon	Directeur : M. le Professeur R. BACON
Institut des Sciences et des Techniques de l'Ingénieur de Lyon	Directeur : M. le Professeur J. LIETO
IUT A	Directeur : M. le Professeur M. C. COULET
IUT B	Directeur : M. le Professeur R. LAMARTINE
Institut de Science Financière et d'Assurances	Directeur : M. le Professeur J.C. AUGROS

Acknowledgements

This thesis was prepared at the University Claude Bernard Lyon 1, UMR 5246 CNRS, in Lyon (France) and at Jilin University, Key Laboratory for Supramolecular Structure and Materials, in Changchun (China) under the co-supervision of Professors Rene Buchet and Yuqing Wu. I would like to thank them for their extraordinary guidance and encouragement during the research process.

I wish to thank the following people who have been a valuable source of information and inspiration and who helped me in various ways through teaching, discussions and assistance during experiments:

University Claude Bernard Lyon 1	Jilin University
Jacqueline Radisson	Lixin Wu
Anne Briolay	Junqiu Liu
Laurence Bessueille	Junqi Sun
Françoise Besson	
Marc Lemaire	
Stephane Pellet Rostaing	

My thanks also to other colleagues of ICBMS laboratory in University Claude Bernard Lyon 1, all of whom were so friendly and gave me much help not only with regard to research but also to many aspects concerning my stay in France.

I thank also my colleagues in Jilin University Lei Wang and Liping Zhang, both good friends, who helped me in many ways during the course of my Ph.D.

I would like to express my gratitude to the China Scholarship Council which supported the scholarship during my research period in France.

Finally, my very warm thank to my mother and father for their support and encouragement throughout the different stages of my studies. I must not forget my boyfriend Lei, whose affectionate attention has accompanied me throughout these years.

Lina LI

October, 14th, 2008

CONTENTS

Abbreviations

ADP   - Adenosine 5′-diphosphate

ADPR   - Adenosine 5′-diphosphoribose

AMP   - Adenosine 5′-monophosphate

AP   - Alkaline phosphatase (EC 3.1.3.1)

ATP   - Adenosine 5′-triphosphate

BIAP   - Bovine intestinal alkaline phosphatase

BSA   - Bovine serum albumin

CIAP   - Calf intestinal alkaline phosphatase

Da   - Dalton

DDP   - Dansyl-D-phenylalanine

DDS   - Dansyl-D-serine

DDT   - Dansyl-D-tryptophan

DLP   - Dansyl-L-phenylalanine

DLS   - Dansyl-L-serine

DLT   - Dansyl-L-tryptophan

DPs   - Dansyl-D, L-phenylalanine

DSs   - Dansyl-D, L-serine

DTs   - Dansyl-D, L-tryptophan

DMSO   - Dimethyl Sulphoxide

E. coli   - *Escherichia coli*

FTIR   - Fourier transform infrared spectroscopy

GTP   - Guanosine 5′-triphosphate

HA   - Hydroxyapatite $Ca_{10}(PO_4)(OH)_2$

K - Association constant

K_i - Inhibition constant

K_L/K_D - Enantioselectivity ratio of association constant

MV   - Matrix vesicle

P_i - Inorganic phosphate (orthophosphate)

PBS   - phosphate-buffered saline

PME   - Phosphomonoesterase

pNPP   - *para*-Nitrophenyl Phosphate

PP_i - Inorganic pyrophosphate

SCL   - Synthetic cartilage lymph

SD   - Standard deviation

SDS   - Sodium dodecyl sulfate

SDS-PAGE   - Sodium dodecyl sulfate polyacrylamide gel electrophoresis

TES   - N-Tris(hydroxymethyl)methyl-2-aminoethane sulfonic acid

TNAP   - Tissue non-specific alkaline phosphatase

Tris   - Tris-(hydroxymethyl) aminomethane

UTP   - Uridine 5′-triphosphate

v/v   - Volume/volume

CHAPTER I

Introduction

1. Molecular recognition

Molecular recognition is the specific interaction of one molecule with another through noncovalent bonding including hydrogen bonding, metal coordination, hydrophobic forces, van der Waals forces, pi-pi interactions, and/or electrostatic effects [1]. Since the host and guest involved in molecular recognition exhibit molecular complementarities, the essential factor in the recognition process is the appropriate tridimensional structure of the guest which can be recognized specifically by the host [1,2]. Among the numerous molecular specific recognitions, chiral recognition is the most attractive one. Indeed, during the past 15 years, intensive research has provided new insight into the mechanism of molecular recognition in biological systems. In addition, it provided new opportunities for developing molecular devices for biochemical and pharmaceutical applications as well as for separation processes, catalysis and sensing [3-8].

2. Chiral recognition

Chirality is a common property of biological molecules which plays a fundamental role in the recognition processes. Chiral recognition, the process in which a particular molecular group (host) specifically recognizes a stereoisomer (guest), is one of the essential reaction processes occurring in living systems, especially in the case of enzymatic catalysis, protein–DNA interaction, antibody activity, etc. Therefore, the biological activity of a compound often depends upon its stereochemistry in living organisms, having consequences in the design of drugs [9-11]. In this respect, chiral discrimination can be applied in drug–target interactions or separating chiral drugs from their enantiomers, which may show striking differences in terms of biological activity, potency, toxicity, transport mechanisms, and routes of metabolism [12,13].

Enantiomeric recognition of biologically important substrates and enzyme inhibitors is a very important research area since the detailed molecular mechanisms involved in these specific interactions in biological systems are often only partially elucidated and are complicated [14-16]. Modified chiral amino acids can offer potential information in the rational design of novel drugs. For example, L-phenylalanine and L-tryptophan are two inhibitors for tissue-specific alkaline phosphatase, whereas their enantiomers are not [17,18].

Various methods are used to characterize the enantiomeric recognition such as chromatography [19], ^{1}H-NMR [20], LB films [21], UV-visible [22] or FAB-MS [23], ESI-MS [24] and fluorescent sensing [25]. Among these methods the fluorescence technique is the most attractive method to monitor the interaction between enantiomers and receptors [25-28] due to its ease of measurement and high sensitivity, especially for the determination of association constant K [25,26].

Receptor systems [29-31] such as cyclodextrins (CDs) and calixarenes have been observed to selectively bind enantiomers and produce a complex that can be detected by fluorescence techniques. Unfortunately, this approach is often not sufficiently reliable to serve as a simple and quick analytical method for enantiomer determinations. The centrality of chiral recognition in biology has prompted these investigators to explore the use of biomolecules as receptors.

3. Chiral recognition in biological systems: the case of enzymes

One of the best examples of chiral recognition in biology is the case of enzymes. The enormous variety of biochemical reactions that comprise life are nearly all mediated by a series of biological catalysts known as enzymes [32]. The rates of enzymatically catalyzed reaction are typically 10^6 to 10^{12} greater than those of the corresponding uncatalyzed reactions. Enzymatically catalyzed reactions occur under relatively mild conditions (nearly neutral pH, temperature around 37 °C and atmospheric pressure). Enzymes have generally great specificity with respect to the identities of both their substrates (reactants) and their products. The substrate specificity is controlled mainly by noncovalent forces (van der Waals, electrostatic, hydrogen bonding and hydrophobic interactions). In general, a substrate-binding site consists of an indentation or cleft on the surface of an enzyme molecule that is complementary in shape to the substrate [32]. There are many examples of enantiomeric substrates that can be recognized by enzymes or proteins. Just to mention one among these, bovine serum albumin (BSA), due to its enantioselectivity, has been utilized as chiral stationary phase (CSP) for years in HPLC [33-34]. In this work, alkaline phosphatase was selected for the following reasons. 1) There are at least four isozymes of alkaline phosphatase in mammals, permitting us to investigate specific recognition for one type of isozyme. 2) Tissue non-specific alkaline phosphatase (TNAP), present in

bones, is a biological marker of mineralization process. Soluble TNAP inhibitors could serve as drugs for treating pathological soft tissue mineralization disorders.

4. Alkaline phosphatases - structure and general properties

The alkaline phosphatases (E.C.3.1.3.1; APs) are metalloenzymes expressed in various species, including bacteria, mammals, reptiles, amphibians, nematodes, and insects [35]. APs from all sources are homodimeric enzymes, and each catalytic site contains three metal ions (two Zn ions and one Mg ion) that are necessary for enzymatic activity (Fig.1). APs catalyze the hydrolysis of almost any phosphomonoester by releasing inorganic phosphate (P_i) and alcohol at alkaline pH [36].

Mammalian alkaline phosphatases which are anchored to the exterior of the cytoplasmic membrane via a phosphatidylinositol glycan moiety [37] have low sequence identity with the *Escherichia coli* enzyme (25–30%) [38], but the residues involved in the active site of the enzyme and those coordinating the two zinc atoms and the magnesium ion are largely conserved [39,40]. In mammals, the AP family consists of two groups, tissue non-specific alkaline phosphatase and the tissue-specific alkaline phosphatases. The number of tissue-specific alkaline phosphatases expressed depends on the species. In humans, APs are encoded by four distinct loci. Three isozymes are tissue-specific, *i.e.* intestinal AP (IAP), placental AP (PLAP), and germ cell AP (GCAP). They are 90–98% homologous, and their genes are clustered on chromosome 2 [41-45]. The fourth AP isozyme is tissue non-specific (TNAP) and is expressed in a variety of tissues including liver, bone, and kidney. TNAP is about 50% identical to the other three isozymes, and its gene is located on chromosome 1 [46,47].

The catalytic mechanism was first deduced from the structure of the bacterial enzyme and was recently confirmed from the structure of a human isozyme. It involves the activation of a serine by a zinc atom, the formation of a phosphorylenzyme, the hydrolysis of the phosphoseryl by a water molecule activated by a second zinc atom and the release of the phosphate or its transfer to an acceptor [48]. Four main catalytic functions have been attributed to these enzymes: hydrolase activity on low molecular weight phosphomonoesters, phosphotransferase activity, protein phosphatase activity and pyrophosphatase activity.
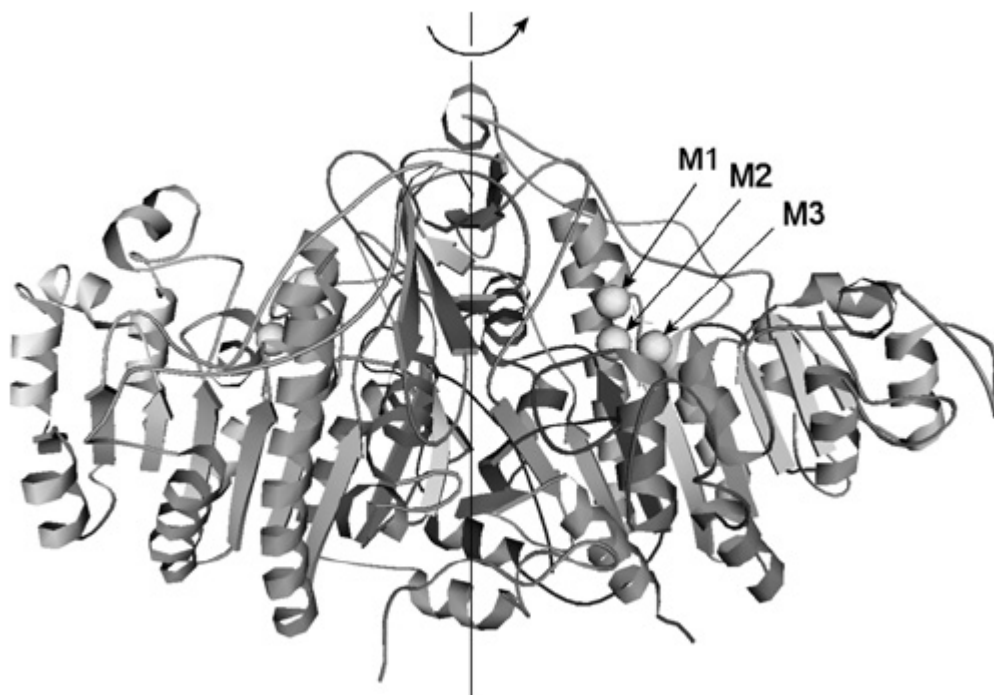
Figure 1 Ribbon diagram of *E. Coli* alkaline phosphatase structure with three metal-binding sites (M1, M2 and M3) indicated in one monomer active-site. Adapted from [49].

TNAP and the tissue-specific isozymes have different sensitivities to chemical inhibition by various L-form amino acids and other inhibitors, such as L-phenylalanine [17,50], L-cysteine [52-54], L-homoarginine [17,50], and levamisole [50,51]. TNAPs are particularly sensitive to inhibition with levamisole [50,51], L-cysteine [54], L-homoarginine [17,50], and are comparatively insensitive to L-phenylalanine [17,50]. The tissue-specific isozymes are comparatively insensitive to levamisole [51] and L-homoarginine [17], and sensitive to L-phenylalanine inhibition [17], L-cysteine can also inhibit tissue-specific AP but is less sensitive [52,53]. However, both of them can be inhibited by inorganic phosphate [55,56], vanadate [55,57], arsenate [55,57] and theophylline [55,57-58] at a similar level.

Nevertheless, the physiological role of different APs is still not well known, except for the TNAP isoenzyme implicated in skeletal maturation and mineralization of bone tissue [59-61]. Here our attention is focused on TNAP and its related mineralization process especially on matrix vesicles (MVs) which is described in detail below.

5. The role of alkaline phosphatase and related proteins in mineralization

TNAP is one of the most frequently used biochemical markers of mineralization induced by osseous cells such as osteoblasts and chondrocytes [62-64]. Osseous TNAP, localized in plasma membrane and in Matrix Vesicles (MVs), is a glycosylphosphatidylinositol (GPI)-anchored protein [37,65]. Given the different solubilization of TNAP from osteoblast plasma membrane, obtained from human primary bone cell culture, it was suggested that changes in TNAP activity result from age-related modifications. These changes could be associated with the posttranslational modification of TNAP or with the membrane constituents [66,67]. The role of TNAP in mineral formation was evidenced in the case of the hereditary disease hypophosphatasia, an inheritable disorder leading to a defective bone formation and characterized by a deficiency in TNAP [68]. Mice deficient in the gene encoding TNAP mimic a severe form of hypophosphatasia, indicating the importance of TNAP in hydrolyzing phosphate substrates, including pyrophosphate (PP_i), during mineral formation [69].

TNAP appears to be a multifunctional enzyme and several of its properties are important for the mineralization process [70]. Although TNAP is a well-known biochemical marker of mineralization, the nature of the substrate hydrolyzed by TNAP is not clearly established. It was proposed a long time ago that TNAP may supply P_i by hydrolyzing phosphate substrates [71]. This proposal was further substantiated by the observation that supplementation of culture media with β-glycerophosphate, an exogenous TNAP substrate, induced osteogenesis and HA deposition [72]. Addition of levamisole, a specific inhibitor of TNAP activity, prevented β-glycerophosphate induced mineralization *in vitro* [73].

Other enzymes producing P_i as TNAP such as 5'-AMPase, nucleoside [74], Ca-stimulated ATPase [75] etc…are present at the membrane of the matrix vesicle (extracellular organelles involved in the initial step of mineral formation). Therefore, not only TNAP but also other enzymes are involved in the P_i homeostasis. The local concentration of P_i can be increased by the activities of 5'-AMPases and ATPases, while nucleoside triphosphate phosphodiesterase contributes to the production of PP_i, which is an inhibitor of mineral formation [62].

P_i arising from extracellular matrix and from the hydrolytic activities of enzymes located either in matrix vesicles (MVs) or in the plasma membrane of chondrocytes or osteoblast cells, is transported into the MVs to initiate the first stage of the mineralization process. Indeed, sodium-dependent P_i transporter responsible for the Pi uptake inside MVs has been identified. Other P_i transporters, not strictly sodium-dependent, are also involved in the Pi uptake inside the MVs [62,74].

6. Matrix vesicles

Since MVs are enrichied in TNAP as well as in other enzymes implicated in the mineralization, they will be used as a primary source of TNAP to test inhibitors and their abilities to mineralize will be monitored. Therefore, this chapter contains some information on MVs. MVs are submicroscopic extracellular membrane-invested particles, released by budding from the surfaces of chondrocytes, osteoblasts, and odontoblasts [76-78]. Their diameters range from 100 nanometers (nm) at the smallest to about 300 nm [79] [Fig.2].

Matrix vesicles serve as the initial site of calcification in all skeletal tissues, including growth plate cartilage, embryonic and growing bone, and odontoblastic predentin. Matrix vesicles are released into the extracellular matrix carrying cell-derived molecules that endow matrix vesicles with a remarkable mineral-initiating ability [74,80]. Recently, proteome analysis of MVs revealed more than 200 proteins, some of them are involved in the process of biomineralization [81].
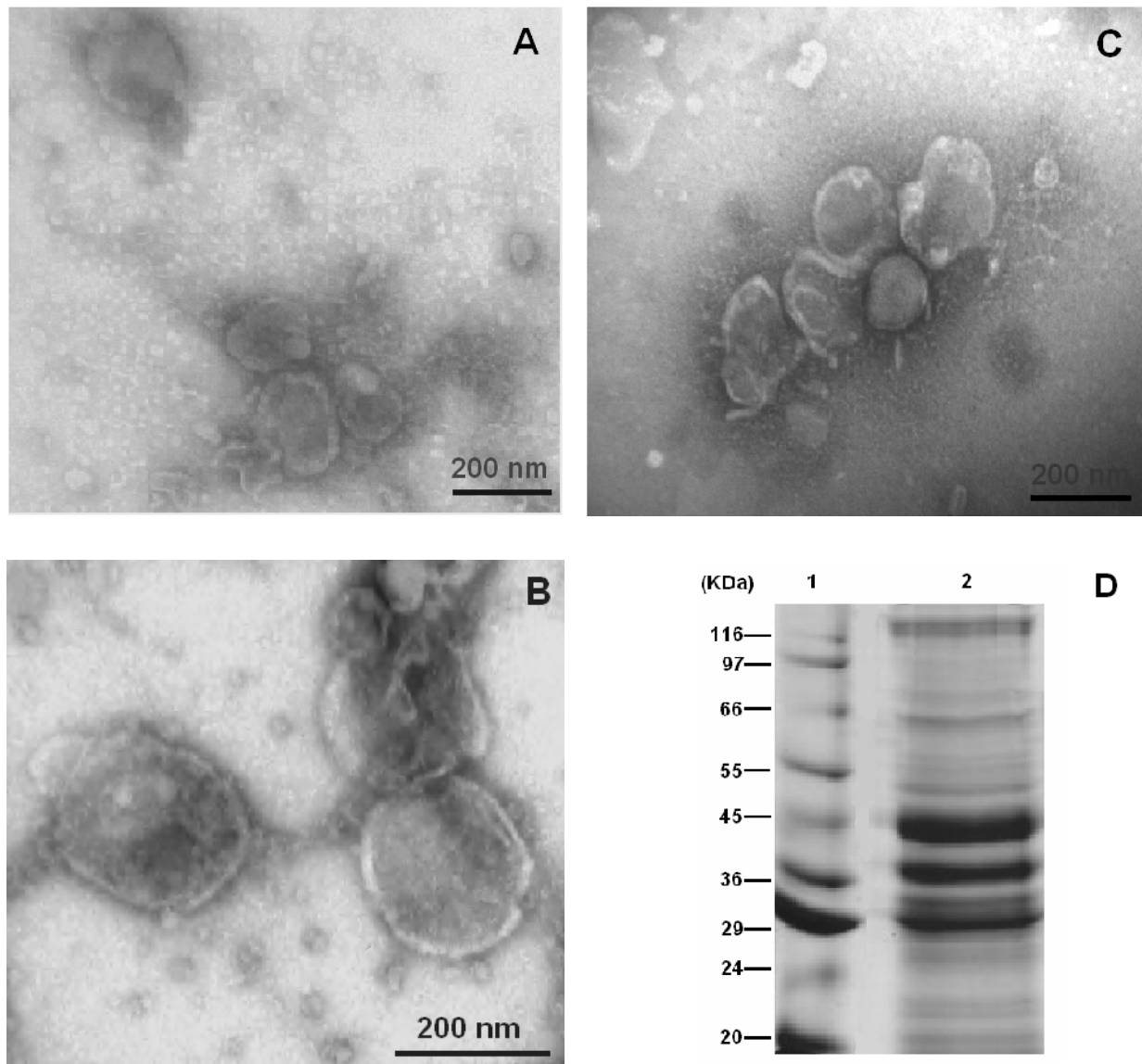
Figure 2. A-C, Transmission electron micrographs of MVs negatively stained with uranyl acetate. Scale bar is as indicated. D, Gel electrophoresis (10% SDS–PAGE and stained with Coomassie brilliant blue) of MVs. *Lane 1*, protein standards; *lane 2*, 30μg of MV protein profiles.

7. Mineralization process

Mineralization which is initiated by matrix vesicles is essentially a biphasic phenomenon [74]. During the first step of mineral initiation, Ca^{2+} accumulates into MVs at calcium-binding molecules that are concentrated in the MV structure. These include 1) calcium-binding acidic phospholipids, especially phosphatidyl serine (PS) [82], which are localized at the inner surface of the MV membrane, thus promoting the

14

accumulation of Ca^{2+}; and 2) calcium-binding proteins enriched in MVs, including annexin II (calpactin), annexin V (anchorin CII), and annexin VI. Annexins also can function as transmembrane Ca^{2+} channels. The local intra- and perivesicular PO_4^{3-} concentration is raised by the enzymatic activity of phosphohydrolases that are enriched in the MV membrane, especially alkaline phosphatase, adenosine monophosphate phosphodiesterase, adenosine triphosphatase, and indirectly by nucleoside triphosphate pyrophosphohydrolase [83-85]. The uptake of PO_4^{3-} also is facilitated by the action of a sodium-dependent P_i transporter that is present in MVs [86] as well by other transporters. Elevation of Ca^{2+} and PO_4^{3-} within the protective microenvironment of the lumen of matrix vesicle, when exceeding the solubility product of calcium and PO_4^{3-} ions, leads to the formation of needle-like crystals of hydroxyapatite $(Ca_{10}(PO_4)_6(OH)_2)$. Mineral deposits near the inner surface of the MV membrane. The intravesicular pH is adjusted by the action of carbonic anhydrase that is concentrated in MVs [87], which could also stabilize the pH.

The second step begins with crystal penetration of the matrix vesicle membrane, exposing preformed mineral to the extracellular fluid. The rate of mineral crystal proliferation from this point will be governed by extracellular conditions such as the levels of ionic Ca^{2+} or PO_4^{3-} in the extracellular fluid, the pH of the extracellular fluid, and the presence of molecules in the extracellular fluid that can control the rate of crystal proliferation such as anionic proteoglycans [88,89] and/ or calcium-binding noncollagenous matrix protein [90], most of which are believed to retard crystal proliferation. On the other hand, there are several proteins, such as bone salioprotein, matrix extracellular phosphorylglycoprotein, highly phosphorylated osteopontin, etc. in the extracellular matrix which are nucleating proteins [91]. The biphasic nature of the mineralization process has been confirmed in several biologic systems. Electron microscope studies of calcifying cartilage, bone, dentin, and turkey tendon have shown that the deposition of mineral occurs first within and then around matrix vesicles [92-97]. The second phase is somewhat physicochemical because its rate is governed by the presence of nucleating proteins as well as by nonenzymatic extracellular molecules including collagen. HA crystals grow and propagate between collagen fibers due to a continuous supply of Ca^{2+} and PO_4^{3-} in extracellular matrix [98]. In calcified diseases (unwanted calcification) such as chondrocalcinosis, osteoarthritis, crystal deposition arthritis, and atherosclerosis, MVs or vesicles are

accidentally produced by cells which can initiate pathologic calcification. Therefore, the calcification is under tight cellular control. It is also regulated at molecular levels by enzymes, proteins, and the phospholipid membrane of the matrix vesicle, all provided by the cell. Chondrocytes or osteoblasts must be mineralization competent, to be able to release MVs having the ability to initiate calcification. For example, chondrocytes at the cartilage are not able to mineralize during adult life.

8. Matrix vesicle and alkaline phosphatase involvement in osteoarthritis

The pioneering studies of Ali and Wisby showed that the pathogenesis of osteoarthritis is associated with excessive and uneven calcification of the deep, tidemark zone of articular cartilage [99]. Matrix vesicles, isolated from the articular cartilage of patients with osteoarthritis, were shown to possess a markedly increased alkaline phosphatase activity, and were more prone to initiate *in vitro* calcification [100]. These observations support the hypothesis that an irregular, hypercalcified, and physically hardened subchondral tidemark in osteoarthritis joints creates abnormal and excessive mechanical stress, which leads to premature erosion of the overlying articular cartilage. Recent reports of osteoarthritis cartilage also have demonstrated an abnormally increased rate of chondrocyte maturation and apoptosis [101,102]. Premature maturation of chondrocytes in osteoarthritis would be expected to increase the release of alkaline phosphatase-enriched, mineralization-competent MVs. Furthermore, an excessive number of apoptotic chondrocytes in osteoarthritis would release more proteolytic enzymes into the matrix, especially matrix metalloproteinases and cathepsins [103,104]. These enzymes digest proteoglycans, elastin, and collagen, thus provoking further degradation of the articular cartilage matrix, as well as further mineral propagation in the tidemark area because of the removal of mineral-inhibiting proteoglycans. These observations indicate that MV-mediated mineralization and tissue non-specific alkaline phosphatase are very important targets for osteoarthritis therapy.

REFERENCE

[1] Lehn, J.M. (1993) Supramolecular Chemistry. Science; 260: 1762-1763.

[2] Gellman, S.H. (1997) Introduction: Molecular Recognition. Chem. Rev.; 97(5): 1231-1232.

[3] Reinhoudt, D.N. (1996) Supramolecular Technology. «Comprehensive Supramolecular Chemistry» Pergamon Press, New York, vol. 10.

[4] Kubo, Y., Maeda, S., Tokita, S. and Kubo, M. (1996) Colorimetric chiral recognition by a molecular sensor. Nature; 382: 522-524.

[5] Murakami, Y., Kikuchi, J., Hisaeda, Y. and Hayashida, O. (1996) Artificial Enzymes. Chem. Rev.; 96: 721-758.

[6] Sanders, J.K.M. (1998) Supramolecular Catalysis in Transition. Chem. Eur. J.; 4: 1378-1383.

[7] Peczuh, M.W. and Hamilton, A.D. (2000) Peptide and Protein Recognition by Designed Molecules. Chem. Rev.; 100: 2479-2494.

[8] Al Rabaa, A.R., Tfibel, F., Mérola, F., Pernot, P. and Fontaine-Aupart M.P. (1999) Spectroscopic and photophysical study of an anthryl probe: DNA binding and chiral recognition. J. Chem. Soc. Perkin Trans.; 2: 341-351.

[9] Schneider, H.J. (1991) Mechanisms of Molecular Recognition: Investigations of Organic Host-Guest Complexes. Angew. Chem., Int. Ed. Engl.; 30: 1417-1436.

[10] Lehn, J.M. (1988) Supramolecular Chemistry - Scope and Perspectives Molecules, Supermolecules, and Molecular Devices. Angew. Chem. Int. Ed. Engl.; 27: 89-112.

[11] Testa, B. (2004) Mechanisms of chiral recognition in xenobiotic metabolism and drug-receptor interactions. Chirality; 1: 7-9.

[12] Crossley, R. (1995) Chirality and the Biological Activity of Drugs. CRC Press: Boca Raton, FL.; Chapter 2.

[13] Scott, A.K. (1993) Stereoisomers and drug toxicity. The value of single stereoisomer therapy. Drug Saf.; 8: 149-159.

[14] Booth, T.D., Wahnon, D. and Wainer, I.W. (1997) Is Chiral Recognition a Three-Point Process? Chirality; 9: 96-98.

[15] Henriksson, H., Ståhlberg, J., Isaksson, R., Pettersson, G. (1996) The active sites of cellulases are involved in chiral recognition: a comparison of cellobiohydrolase 1 and endoglucanase 1. FEBS Letters; 390: 339-344.

[16] Bachmann, S., Knudsen, K.R. and Jørgensen, K.A. (2004) Mimicking enzymatic transaminations: attempts to understand and develop a catalytic asymmetric approach to chiral α-amino acids. Org. Biomol. Chem.; 2: 2044-2049.

[17] Fishman, W.H., Sie, H.G. (1971) Organ-specific inhibition of human alkaline phosphatase isoenzymes of liver, bone, intestine and placenta; L-phenylalanine, L-tryptophan and L-homoarginine. Enzymologia; 41: 140-167.

[18] Lin, C.W., Sie, H.G., Fishman, W.H. (1971) L-tryptophan. A non-allosteric organ-specific uncompetitive inhibitor of human placental alkaline phosphatase. Biochem. J.; 124: 509-516.

[19] Peyrin, E., Guillaume, Y.C. Morin, N., Guinchard, C. (1998) Retention behavior of D,L-dansyl-amino acids on a human serum albumin chiral stationary phase: effect of a mobile phase modifier. Journal of Chromatography A; 808: 113-120.

[20] Bang, E., Jung, J.W., Lee, W., Lee, D.W. and Lee, W. (2001) Chiral recognition of (18-crown-6)-tetracarboxylic acid as a chiral selector determined by NMR spectroscopy. J. Chem. Soc. Perkin Trans.; 2: 1685-1692.

[21] Qian, P., Matsuda, M., Miyashita, T. (1993) Chiral molecular recognition in polymer Langmuir-Blodgett films containing axially chiral binaphthyl groups. J. Am. Chem. Soc.; 115: 5624-5628.

[22] Wang, C.Z., Zhu, Z.A., Li, Y., Chen, Y.T., Wen, X., Miao, F.M., Chan, W.L. and Chan, A.S.C. (2001) Chiral recognition of amino acid esters by zinc porphyrin derivatives. New J. Chem.; 25: 801-806.

[23] Motohiro, S. (2003) Evaluation of Chiral Recognition of Oligosaccharides using FABMS. J Mass Spectrom Soc Jpn; 51: 330-333.

[24] Sawada, M., Takai, Y., Kaneda, T., Arakawa, R., Okamoto, M., Doe, H., Matsuo, T., Naemura, K., Hirose K. and Tobe, Y. (1996) Chiral molecular recognition in electrospray ionization mass spectrometry. Chem. Commun.; 1735-1736.

[25] Wong, W.L., Huang, K.H., Teng, P.F., Lee C.S. and Kwong H.L. (2004) A novel chiral terpyridine macrocycle as a fluorescent sensor for enantioselective recognition of amino acid derivatives. Chem. Commun.; 384-385.

[26] Abe, Y., Fukui, S., Koshiji, Y., Kobayashi, M., Shoji, T., Sugata, S., Nishizawa, H., Suzuki, H., Iwata, K. (1999) Enantioselective binding sites on bovine serum albumin to dansyl amino acids. Biochimica et Biophysica Acta; 1433: 188-197.

[27] James, T.D., Sandanayake, K., Shinkai, S. (1995) Chiral discrimination of monosaccharides using a fluorescent molecular sensor. Nature; 374: 345-347.

[28] a. Takeuchi, M., Yoda, S., Imada, T., Shinkai, S. (1997) Chiral Sugar Recognition by a Diboronic-Acid-Appended Binaphthyl Derivative through Rigidification Effect. Tetrahedron; 53: 8335-8348.

b. Parker, K.S., Townshend, A., Bale, S.J. (1995) Determination of the enantiomeric composition of 1-phenylethylamine based on its quenching of the fluorescence of 2,2'-dihydroxy-1,1'-binaphthalene. Anal. Proc.; 32: 329-332.

c. Parker, K.S., Townshend, A., Bale, S.J. (1996) Simultaneous determination of the concentrations of each enantiomer of 1-phenylethylamine using their quenching of the fluorescence of two chiral fluorophores. Anal. Commun.; 33: 265-267.

[29] Grady, T., Harris, S. J., Smyth, M.R., Diamond, D. and Hailey, P. (1996) Determination of the Enantiomeric Composition of Chiral Amines Based on the Quenching of the Fluorescence of a Chiral Calixarene. Anal. Chem.; 68: 3775-3782.

[30] Schuette, J.M., Will, A.Y., Agbaria, R.A., Warner, I.M. (1994) Fluorescence Characterization of the Cyclodextrin/Pyrene Complex Interaction with Chiral Alcohols and Diols. Appl. Spectrosc.; 48: 581-586.

[31] Yang, H., Bohne, C. (1995) Chiral discrimination in the fluorescence quenching of pyrene complexed to β-cyclodextrin. J. Photochem. Photobiol. A; 86: 209-217.

[32] Voet, D., Voet, J.G. (1995) Biochemistry. Ed. John Wiley & Sons, Inc.; New York (USA).

[33] Allenmark, S., Bomgren, B., Boren, H. (1983) Direct liquid chromatographic separation of enantiomers on immobilized protein stationary phases III. Optical resolution of a series of N-aroyl D,L-amino acids by high-performance liquid chromatography on bovine serum albumin covalently bound to silica. J. Chromatogr. A; 264: 63-68.

[34] Allenmark, S. (1986) Optical Resolution by Liquid Chromatography on Immobilized Bovine Serum Albumin. J. Liq. Chromatogr.; 9: 425-442.

[35] Schwartz, J.H. and Lipmann, F. (1961) Phosphate incorporation into alkaline phosphatase of *E. coli.* Proc. Natl. Acad. Sci. U.S.A.; 47: 1996-2005.

[36] Hull, W.E., Halford, S.E., Gutfreund, H. and Sykes, B.D. (1976) ^{31}P nuclear magnetic resonance study of alkaline phosphatase: the role of inorganic phosphate in limiting the enzyme turnover rate at alkaline pH. Biochemistry; 15: 1547-1561.

[37] Noda, M., Yoon, K., Rodan, G.A., Koppel, D.E. (1987) High lateral mobility of endogenous and transfected alkaline phosphatase: a phosphatidylinositol-anchored membrane protein. J. Cell Biol.; 105: 1671-1677.

[38] Bradshaw, R.A., Cancedda, F. and Ericsson, L.H. (1981) Amino acid sequence of Escherichia coli alkaline phosphatase. Proc. Natl. Acad. Sci. U.S.A.; 78: 3473-3477.

[39] Kim, E.E. and Wyckoff, H.W. (1989) Structure of alkaline phosphatase. Clin. Chim. Acta; 186: 175–188.

[40] Kim, E.E. and Wyckoff, H.W. (1991) Reaction mechanism of alkaline phosphatase based on crystal structures: two-metal ion catalysis. J. Mol. Biol.; 218: 449-464.

[41] Harris, H. (1989) The human alkaline phosphatases: what we know and what we don't know. Clin. Chim. Acta; 186:133-150.

[42] Kam, W., Clauser, E., Kim, Y.S., Kan, Y.W., Rutter, W. (1985) Cloning, sequencing, and chromosomal localization of human term placental alkaline phosphatase cDNA. Proc. Natl. Acad. Sci. U.S.A.; 82: 8715-8719.

[43] Millan, J.L. (1986) Molecular cloning and sequence analysis of human placental alkaline phosphatase. J. Biol. Chem.; 261: 3112-3115.

[44] Henthorn, P.S, Raducha, M, Edwards, Y.H., Weiss, M.J., Slaughter, C., Lafferty, M.A., Harris, H. (1987) Nucleotide and amino acid sequences of human intestinal alkaline phosphatase: close homology to placental alkaline phosphatase. Proc. Natl. Acad. Sci. U.S.A.; 84: 1234-1238.

[45] Millan, J.L., Manes, T. (1988) Seminoma-derived Nagao isozyme is encoded by a germ-cell alkaline phosphatase gene. Proc. Natl. Acad. Sci. U.S.A.; 85: 3024-3028.

[46] Weiss, M.J., Henthorn, P.S., Lafferty, M.A., Slaughter, C., Raducha, M. and Harris, H. (1986) Isolation and characterization of a cDNA encoding a human liver/bone/kidney-type alkaline phosphatase. Natl. Acad. Sci. U.S.A.; 83: 7182-7186.

[47] Moss, D.W. (1992) Perspectives in alkaline phosphatase research. Clin. Chem.; 38: 2486-2492.

[48] Murphy, J.E. and Kantrowttz, E.R. (1994) Why are mammalian alkaline phosphatases much more active than bacterial alkaline phosphatases? Molecular Microbiology; 12: 351-357.

[49] Zhang, L., Buchet, R. and Azzar G. (2005) Distinct structure and activity recoveries reveal differences in metal binding between mammalian and Escherichia coli alkaline phosphatases. Biochem. J.; 392: 407-415.

[50] Kozlenkov, A., Du, M.H., Cuniasse, P., Ny, T., Hoylaerts, M.F. and Millan, J.L. (2004) Residues Determining the Binding Specificity of Uncompetitive Inhibitors to Tissue-Nonspecific Alkaline Phosphatase. J. Bone. Miner. Res.; 19: 1862-1872.

[51] Van Belle, H. (1976) Alkaline phosphatase. I. Kinetics and inhibition by levamisole of purified isoenzymes from humans. Clin Chem; 22: 972-976.

[52] Cox, R.P., Macleod, C.M. (1963) Repression of alkaline phosphatase in human cell cultures by cystine and cysteine. Proc. Nat. Acad. Sci. U.S.A.; 49: 504-510.

[53] Zhu, C.M., Chen, Q.C., Lin, H.N., Yang, Y., Park, Y.D., Zhang, R.Q., Zhou, H.M. (1999) Kinetics of inhibition of green crab (Scylla serrata) alkaline phosphatase by L-cysteine. J. Protein Chem.; 18: 603-607.

[54] So, P.P., Tsui, F.W., Vieth, R., Tupy, J.H., Pritzker, K.P. (2007) Inhibition of Alkaline Phosphatase by Cysteine: Implications for Calcium Pyrophosphate Dihydrate Crystal Deposition Disease. J. Rheumatol.; 34: 1313-1322.

[55] Cyboron, G.W., Vejins, M.S., Wuthier, R.E. (1982) Activity of epiphyseal cartilage membrane alkaline phosphatase and the effects of its inhibitors at physiological pH. J. Biol. Chem.; 257: 4141-4146.

[56] Zhang, L., Buchet, R. and Azzar, G. (2004) Phosphate Binding in the Active Site of Alkaline Phosphatase and the Interactions of 2-Nitrosoacetophenone with Alkaline Phosphatase-Induced Small Structural Changes. Biophysical Journal; 86: 3873-3881.

[57] Whisnant, A.R. and Gilman, S.D. (2002) Studies of reversible inhibition, irreversible inhibition, and activation of alkaline phosphatase by capillary electrophoresis. Anal. Biochem.; 307: 226-234.

[58] Glogowski, J., Danforth, D.R., Ciereszko, A. (2002) Inhibition of alkaline phosphatase activity of boar semen by pentoxifylline, caffeine, and theophylline. J. Androl.; 23: 783-792.

[59] Yoon, K., Golub, E., Rodan, G. (1989) Alkaline phosphatase cDNA transfected cells promote calcium and phosphate deposition. Connect. Tissue. Res.; 22: 17-25.

[60] Beertsen, W., van den Bos, T. (1992) Alkaline phosphatase induces the mineralization of sheets of collagen implanted subcutaneously in the rat. J. Clin. Invest.; 89: 1874-1980.

[61] Fedde, K.N., Blair, L., Silverstein, J., Coburn, S.P., Ryan, L.M., Weinstein, R.S., Waymire, K., Narisawa, S., Millan, J.L., MacGregor, G.R., Whyte, M.P. (1999) Alkaline phosphatase knock-out mice recapitulate the metabolic and skeletal defects of infantile hypophosphatasia. J. Bone. Miner. Res.; 14: 2015-2026.

[62] Balcerzak, M., Hamade, E., Zhang, L., Pikula, S., Azzar, G., Radisson, J., Bandorowicz-Pikula, J. and Buchet, R. (2003) The roles of annexins and alkaline phosphatase in mineralization process. Acta. Biochimica. Polonica.; 50: 1019-1038.

[63] Risteli, L., Risteli, J. (1993) Biochemical markers of bone metabolism. Ann. Med.; 25: 385-393.

[64] Garnero, P., Delmas, P.D. (1996) New developments in biochemical markers for osteoporosis. Calcif. Tissue Int.; 59: 2–9.

[65] Pizauro, J.M., Ciancaglini, P., Leone, F.A. (1994) Osseous plate alkaline phosphatase is anchored by GPI. Braz. J. Med. Biol. Res.; 27: 453-456.

[66] Radisson, J., Angrand, M., Chavassieux, P., Roux, B., Azzar, G. (1996) Differential solubilization of osteoblastic alkaline phosphatase from human primary bone cell cultures. Int. J. Biochem. Cell Biol.; 28: 421-430.

[67] Bourrat, C., Radisson, J., Chavassieux, P., Azzar, G., Roux, B., Meunier, P.J. (2000) Activity increase after extraction of alkaline phosphatase from human osteoblastic membranes by nonionic detergents: influence of age and sex. Calcif. Tissue Int.; 66: 22-28.

[68] Whyte, M.P. (1994) Hypophosphatasia and the role of alkaline phosphatase in skeletal mineralization. Endocrinol. Rev.; 15: 439-461.

[69] Narisawa, S., Frohlander, N., Millan, J.L. (1997) Inactivation of two mouse alkaline phosphatase genes and establishment of a model of infantile hypophosphatasia. Dev. Dyn.; 208: 432-446.

[70] Bellows, C.G., Aubin, J.E., Heersche, J.N. (1991) Initiation and progression in mineralization of bone nodules formed in vitro: the role of alkaline phosphatase and organic phosphate. Bone Miner.; 14: 27-40.

[71] Robison, R. (1924) The possible significance of hexosephosphoric esters in ossification. Biochem. J.; 17: 286-293.

[72] Tenenbaum, H.C. (1981) Role of organic phosphate in mineralization of bone in vitro. J. Dent. Res.; 60: 1586-1589.

[73] Tenenbaum, H.C. (1987) Levamisole and inorganic pyrophosphate inhibit beta-glycerophosphate induced mineralization of bone formed in vitro. Bone Miner.; 3: 13-26.

[74] Anderson, H.C. (1995) Molecular Biology of Matrix Vesicles. Clin. Orthop. Relat. Res.; 314: 266-280.

[75] Hsu, H.H. (1992) Further studies on ATP-mediated Ca deposition by isolated matrix vesicles. Bone Miner.; 17: 279-283.

[76] Akisaka, T., Gay, C.V. (1985) The plasma membrane and matrix vesicles of mouse growth plate chondrocytes during differentiation as revealed in freeze-fracture replicas. Am. J. Anat.; 173: 269-286.

[77] Borg, T.F., Runyon, R., Wuther, R.E. (1981) A freeze-fracture study of avian epiphyseal cartilage differentiation. Anat. Rec.; 199: 449-457.

[78] Cecil, R.N., Anderson, H.C. (1978) Freeze-fracture studies of matrix vesicle calcification in epiphyseal growth plate. Metab. Bone Dis. Rel. Res.; 1: 89-97.

[79] Anderson, H.C. (1969) Vesicles associated with calcification in the matrix of epiphyseal cartilage. J. Cell Biol.; 41: 59-72.

[80] Anderson, H.C. (2003) Matrix vesicles and calcification. Curr. Rheumatol. Rep.; 5: 222-226.

[81] Balcerzak, M., Malinowska, A., Thouverey, C., Sekrecka, A., Dadlez, M., Buchet, R. and Pikula, S. (2008) Proteome analysis of matrix vesicles isolated from femurs of chicken embryo. Proteomics; 8: 192-205.

[82] Peress, N.S., Anderson, H.C., Sajdera, S.W. (1974) The lipids of matrix vesicles from bovine fetal epiphyseal cartilage. Calcif. Tiss. Res.; 14: 275-281.

[83] Ali, S.Y., Sajdera, S.W., Anderson, H.C. (1970) Isolation and characterization of calcifying matrix vesicles from epiphyseal cartilage. Proc. Nat. Acad. Sci. U.S.A.; 67: 1513-1520.

[84] Kanabe, S., Hsu, H.H., Cecil, R.N., Anderson, H.C. (1983) Electron microscopic localization of adenosine triphosphate (ATP) hydrolyzing activity in isolated matrix vesicles and reconstituted vesicles from calf cartilage. J. Histochem. Cytochem.; 31: 462-470.

[85] Hsu, H.H. (1983) Purification and partial characterization of ATP pyrophosphohydrolase from fetal bovine epiphyseal cartilage. J. Biol. Chem.; 258: 3463-3468.

[86] Montessuit, C., Caverzasio, J., Bonjour, J.P. (1991) Characterization of a Pi transport system in cartilage matrix vesicles: potential role in the calcification process. J. Biol. Chem.; 266: 17791-17797.

[87] Stechschulte, D.J., Morris, D.C., Silverton, S.F., Anderson, H.C., Väänänen, H.K. (1992) Presence and specific concentration of carbonic anhydrase II in matrix vesicles. Bone Miner.; 17: 187-191.

[88] Campo, R.D., Romano, J.E. (1986) Changes in cartilage proteoglycans associated with calcification. Calcif. Tissue Int.; 39: 175-184.

[89] Dziewaitkowski, D.D., Majznerski, L.L. (1985) Role of proteoglycans in endochondral ossification: Inhibition of calcification. Calcif. Tissue Int.; 37: 560-564.

[90] Boskey, A.L. (1989) Non-collagenous matrix proteins and their role in mineralization. Bone Miner.; 6: 111-123.

[91] Van de Lest, C.H.A., Vaandrager, A.B. (2007) Mechanism of cell-mediated mineralization. Curr. Opin. Orthop.; 18: 434-443.

[92] Anderson, H.C. (1969) Vesicles associated with calcification in the matrix of epiphyseal cartilage. J. Cell. Biol. 41:59-72.

[93] Anderson, H.C., Cecil, R., Sajdera, S.W. (1975) Calcification of rachitic rat cartilage in vitro by extracellular matrix vesicles. Am. J. Pathol.; 79: 237-254.

[94] Bernard, G.W. (1972) Ultrastructural observations of initial calcification in dentine and enamel. J. Ultrastr. Res.; 41: 1-17.

[95] Arsenault, A.L., Frankland, B.W., Ottsenmeyer, F.P. (1991) Vectorial sequence of mineralization in the turkey leg tendon determined by electron microscopic imaging. Calcif. Tissue Int.; 48: 46-55.

[96] Johnson, T.F., Morris, D.C., Anderson, H.C. (1989) Matrix vesicles and calcitication of rachitic rat osteoid. J. Exp. Pathol.; 4: 123-132.

[97] Sela, J., Schwartz, Z., Amir, D., Swain, L.D., Boyan, B.D. (1992) The effect of bone injury on extracellular matrix vesicle proliferation and mineral formation. Bone Miner.; 17: 163-167.

[98] Arsenault, A.L. (1989) A comparative electron microscopic study of apatite crystals in collagen fibrils of rat bone, dentin and calcified turkey leg tendons. Bone Miner.; 6: 165-177.

[99] Ali, S.Y., Wisby, A. (1978) Apatite crystal nodules in arthritic cartilage. Europ. J. Rheumatol. Inflam.; 1: 115-119.

[100] Einhorn, T.A., Gordon, S.L., Siegel, S.A., Hummel, C.F., Avitable, M.J., Carty, R.P. (1985) Matrix vesicle enzymes in human osteoarthritis. J. Orthop. Res.; 3: 160-169.

[101] Hoyland, J.A., Thomas, J.T., Denn, R., Marriott, A., Ayad, S., Boot-Handford, R.P., Grant, M.E., Freemont, A.J. (1991) Distribution of type X collagen mRNA in normal and osteoarthritic human cartilage. Bone Miner.; 15: 151-163.

[102] Hashimoto, S., Ochs, R.L., Komiza, S., Lotz, M. (1998) Linkage of chondrocyte apoptosis and cartilage degradation in human osteoarthritis. Arthritis Rheum.; 41: 1632-1638.

[103] Masuhara, K., Bak Lee, S., Nakai, T., Sugano, N., Ochi, T., Sasaguri, Y. (2000) Matrix metalloproteinases in patients with osteoarthritis of the hip. Int. Orthop.; 24: 92-96.

[104] Lang, A., Hörler, D., Baici, A. (2000) The relative importance of cysteine peptidases in osteoarthritis. J. Rheumatol.; 27: 1970-1979.

CHAPTER II

Aims

My Ph D thesis is focused on distinct topics starting from molecular recognition, especially on chiral molecules interacting specifically with proteins such as bovine serum abumin. A second part of my Ph D thesis is centered on finding inhibitors that can interact selectively with enzymes implicated in the mineralization process. More precisely our aim was to find inhibitors which can inhibit pathological mineralization by acting in different ways, for example, by inhibiting HA formation, Pi transporter or Ca transport channel, and by altering alkaline phosphatase activity, a biological marker of mineral formation. Four specific aims formed the basis of my thesis.

1) Molecular recognition.

Dansyl group was employed to modify several chiral amino acids, since it has a high sensitivity to the environment and exhibits strong fluorescence in a hydrophobic environment. Dansyl-D-phenylalanine, dansyl- D-tryptophan, and dansyl-D-serine were synthesized (because L-isomers are commercially available), specific recognition and chiral discrimination were investigated on bovine serum albumin (BSA), using fluorescence.

2) Search for alkaline phosphatase inhibitors.

The benzothiophene-tetramisole assembling was selected from a preliminary screening of a library of over 130 benzothiophenes. The inhibition effects of all the compounds, synthesized for investigating the molecular recognition, were tested on porcine kidney TNAP and bovine intestinal AP.

3) Development of a new model to induce mineralization and screen inhibitors of mineral formation.

One efficient way to inhibit mineralization is to find inhibitors such as PP_i, which can directly inhibit HA formation. A simple biological model mimicking the mineralization process was developed by addition of DMSO (4% v/v) in synthetic cartilage lymph (SCL) medium containing calcium and inorganic phosphate at pH 7.6 and 37 °C. This new model can produce HA similarly in the same way as matrix vesicles (MVs) under physiological conditions, which could serve to screen putative inhibitors of mineral formation. Such a model also has the great advantage of monitoring the HA

nucleation process to elucidate the inhibition mechanisms of hydroxyapatite formation, especially without interfering with other processes at cellular or enzymatic levels.

4) Chinese medicines, which have been recognized as having beneficial effects for curing arthritis, were tested on the activity of alkaline phosphatase and on the mineralization induced by matrix vesicles.

MVs isolated from chichen embryo bone were used. A comparative analysis of different effects of Chinese medicines and alkaline phosphatase inhibitors on the mineralization process was performed by using turbidity. To understand the inhibition mechanism of these molecules on mineralization, different substrates were employed.

CHAPTER III

Methods and results

Chiral Discrimination of Bovine Serum Albumin toward Dansyl-derivatives of D,L-phenylalanine, D,L-tryptophan and D,L-serine in Solution

Lina LI[1-6], Yuqing Wu[1*] and Rene Buchet[2-6]

[1]State Key Laboratory for Supramolecular Structure and Materials, Jilin University, ChangChun, 130012, China.

[2]Université de Lyon, Villeurbanne, F-69622, France; [3]Université Lyon 1, Villeurbanne, F-69622, France; [4]INSA de Lyon, Villeurbanne, F-69621, France; [5]CPE Lyon, Villeurbanne, F-69616, France; [6]CNRS UMR 5246 ICBMS, Villeurbanne, F-69622, France.

Abstract: The chiral discrimination of bovine serum albumin in recognizing dansyl-D, L-phenylalanine, dansyl-D, L-tryptophan and dansyl-D, L-serine was monitored by fluorescence spectroscopy. Large differences of enantioselectivity ratios (K_L/K_D) were detected for different dansyl amino acids.

Keywords: chiral discrimination, bovine serum albumin, fluorescence, dansyl, enantioselectivity,

Introduction

Although chiral recognition of biologically important substrates by enzymes and other biological macromolecular is well known, the detailed molecular mechanisms involved in these specific interactions in biological systems are often only partially elucidated and are complicated [1-3]. Serum Albumin is the most abundant plasma protein which transports fatty acids along with other small molecules throughout the circulatory system. Chiral biochromatography with bovine serum albumin (BSA) has been reported to be useful in separating the optical isomers of drugs, amino acids and other small molecules, thereby indicating the utility of such recognition in a variety of

applications [4-6]. Dansyl amino acids are selected as the guests because of their important biological function and fluorescence property [7-8]. Three dansyl modified amino acids, different in structural features, lipophilicity and hydrophobicity, served to investigate the effect of different side groups on the recognition binding sites of BSA.
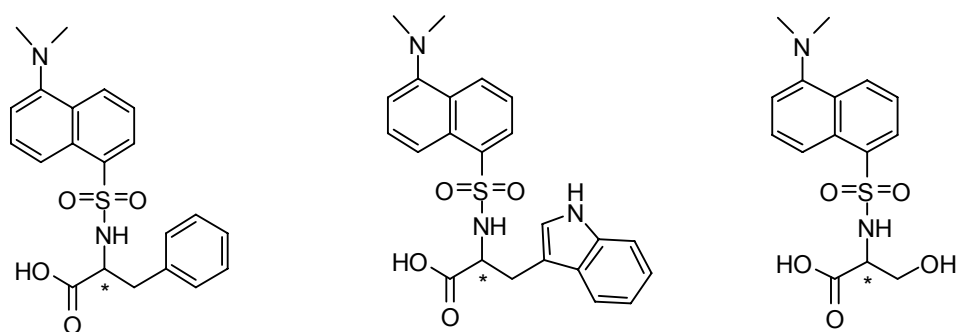
Dansyl-phenylalanine (DPs)   **Dansyl-tryptophan (DTs)**   **Dansyl-serine (DSs)**

Scheme 1. Chemical structure of Dansyl-phenylalanine, Dansyl-tryptophan, and Dansyl-serine. The abbreviations: DPs, DTs and DSs hold for both enantiomers.

Materials and Methods

The L-enantiomers: dansyl-L-phenylalanine (DLP), dansyl-L-tryptophan (DLT) and dansyl-L-serine (DLS) were purchassed from Sigma. The dansyl-D-phenylalanine (DDP), dansyl-D-tryptophan (DDT) and dansyl-D-serine (DDS) were synthesized by reacting the D-amino acids (D-phenylalanine, D-tryptophan and D-serine) in $NaHCO_3$ with dansyl-Cl in acetone for 2 hours at room temperature with continuous stirring and avoiding exposition to light. This method is analogous to the procedure of synthesis of mono-dansyl derivatives of basic amino acids reported by Joseph [9], with some modification. After removal of the excess dansyl-Cl by extracting three times with diethyl ether, the pH of the aqueous layer was adjusted to 1 with 1M hydrochloric acid. Excess CH_3CN was added to the aqueous solution to form a lower-boiling azeotrope. During the evaporation the temperature was always under 60 °C, and the CH_3CN was continually added so that the solution was evaporated to remove all the water. The crude products were purified by column chromatography on silica gel, elution with Ethyl acetate (EtOAc) –$CHCl_3$–Methanol (MeOH)–acetic acid (AcOH) 50:30:20:1 for DDP, with EtOAc–MeOH–AcOH 100:60:1.4 for DDT and with $CHCl_3$-MeOH 10:7 for DDS. The yield is about 38-39%. The products were characterized by UV-Vis,

fluorescence, polarimeter (DLP: [α] = -60.6°, DDP: [α] = +58.2°; DLT: [α] = -62.97°, DDT: [α] = +59.21°; DLS: [α] = +68.17°, DDS: [α] = -65.3°), HPLC (≥95%) and ^{1}H NMR (500MHz), DDP (DMSO): δ 8.44 (d, 2H); 8.16 (d, 4H); 8.10 (d, 8H); 7.58 (d, 3H); 7.53 (d, 7H); 7.24 (m, 6H); 7.05 (m, ph); 4.21 (t, CH); 3.00, 2.80 (2m, CH$_2$), 2.81 (s, Me$_2$N). DDT ([2]H$_2$O): δ 8.02 (d, 2H); 7.89 (d, 4H); 7.69 (d, 8H); 7.31 (t, 3H); 7.28 (d, 7H); 7.25 (d, 6H); 6.98 (d, 13H); 6.92 (d, 10H); 6.87 (t, 9H); 6.79 (s,11H) 6.66 (t, 13H); 3.78 (m, CH); 3.07,2.74 (2m, CH$_2$); 2.79 (s, Me$_2$N). DDS ([2]H$_2$O): δ 8.42 (d, 2H); 8.29 (d, 4H); 8.22 (d, 8H); 7.64 (t, 3H); 7.61 (t, 7H); 7.38 (d, 6H); 3.57 (s, CH$_2$); 3.07 (s, CH); 2.70 (s, Me$_2$N).

Results and discussion:

The fluorometric titration experiments were carried out with the concentration of dansyl amino acids fixed at 10 µM in PBS buffer with 2% ethanol (v/v) at pH7.0, and the concentrations of BSA were varied from 0 to 80 µM in aqueous solution. The emission band of the dansyl derivative was excited at 340 nm with slit width of 5 nm. The addition of a known amount of BSA to either of the 10 µM DLP solution (Fig. 1A) or to 10 µM DDP solutions (Fig. 1B) caused a significant blue shift and emission enhancement. This indicated that the inclusion complex is formed between BSA and both DLP and DDP. The DPs or part of DPs probably bound to the hydrophobic domain of BSA, as previously suggested in the case of other dansyl derivatives [10-11]. The same phenomenon for both DTs and DSs was detected.

A

B
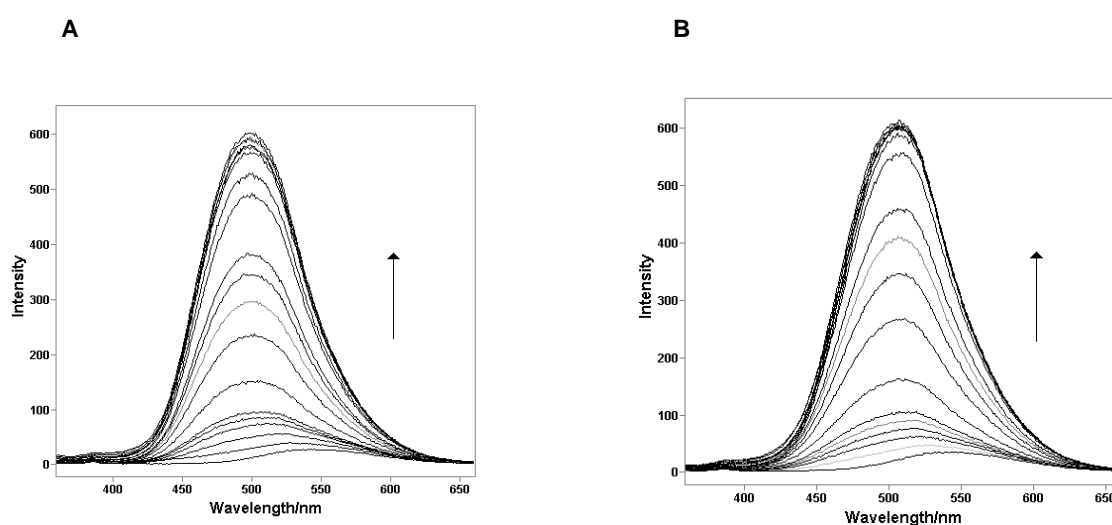
Fig.1 Emission spectra of A) DLP and B) DDP (10 µM) in the absence and presence of BSA in PBS at PH 7.0, [BSA] = 0, 0.2, 0.4, 0.6, 0.8, 1, 2, 4, 6, 8, 10, 20, 30, 40, 50, 60, 70, 80 µM, respectively. The excitation wavelength is 340 nm.

The fluorescence of BSA as function of dansyl derivative concentration served to determine the association constant K. The concentration of BSA was fixed at 1 μM, while the concentrations of DPs, DTs and DSs were varied from 0 to 10 μM in PBS solution with 2% ethanol (v/v) at pH7.0. BSA was excited at 280 nm with slit width of 5 nm.
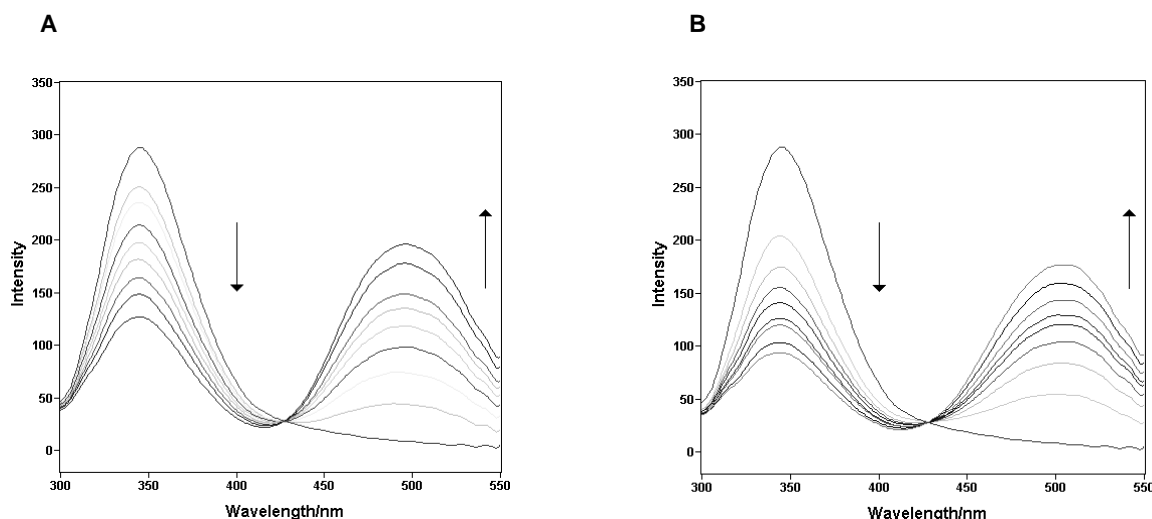
A

B

Fig.2 Emission spectra of BSA (1 μM) in the absence and in the presence of A) DLP; and B) DDP in PBS at PH 7.0. The concentrations of both enantiomers of DPs were 0, 1, 2, 3, 4, 5, 6, 8, 10 μM. The excitation wavelength is 280 nm.

An energy transfer process between BSA and each enantiomer of DPs was observed (Fig. 2A and B). The tryptophan fluorescence intensity at 340 nm decreased upon the addition of the dansyl derivative, whereas a new peak occured at around 500 nm. Dansyl amino acids alone were also excited at 280 nm under the same condition as Fig. 2, but no peak was detectable at 500 nm (data not shown). Therefore, we concluded that there was fluorescence energy transfer from the tryptophan of BSA to the dansyl group. BSA has two tryptophan residues at the sequences of 134 (subdomain IB) and 212 (hydrophobic subdomain of IIA). Large band-shifts and intensity enhancements (Fig. 1) suggested that the binding sites are located in one hydrophobic subdomain of BSA, while the decreased intensity of 340 nm (Fig. 2) confirmed that the binding site is within the hydrophobic subdomain IIA (containing Trp-212), which is analogous to IIA subdomain of HSA (containing Trp-214) [12-13]. The decrease in the 343 nm intensity was plotted as function of concentration of each enantiomeric form of dansyl derivatives (Fig. 3).
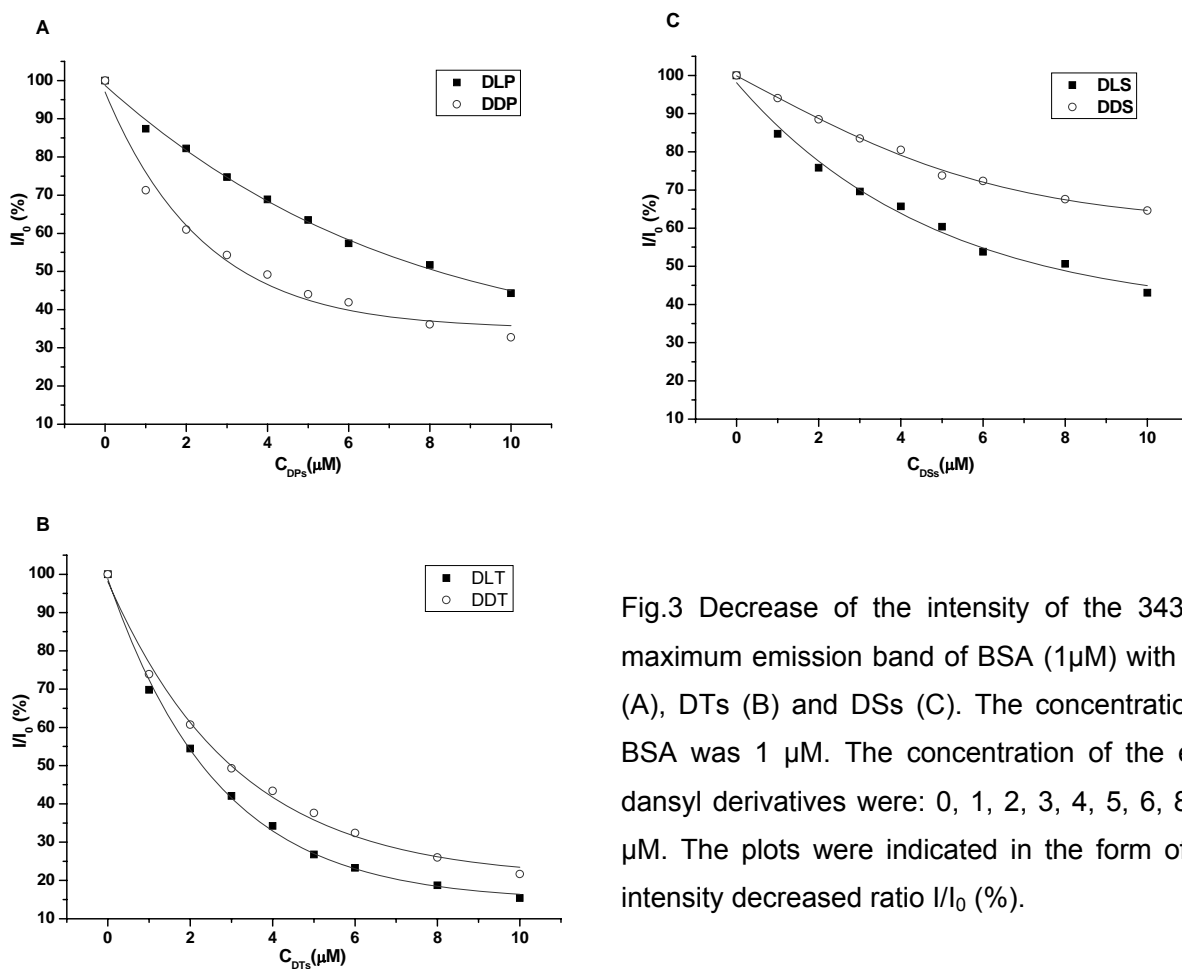
Fig.3 Decrease of the intensity of the 343 nm maximum emission band of BSA (1μM) with DPs (A), DTs (B) and DSs (C). The concentration of BSA was 1 μM. The concentration of the each dansyl derivatives were: 0, 1, 2, 3, 4, 5, 6, 8, 10 μM. The plots were indicated in the form of the intensity decreased ratio I/I_0 (%).

The decrease of emission maximum (λ_{em} = 343 nm) of BSA was more sensitive to DDP, DLT and DLS than their respective enantiomers (Figure 3). From on the plots in Figure 3, their association constant (K), their corresponding statistical number of binding sites (n) [14-16] as well as their discrimination ratio (K_L/K_D) were determined (Table).

Table: Association constants of dansyl amino acid derivatives.

Guest	K(L·mol^{-1})	n	K_L/K_D
DLP	7.74×10^4	0.965	10.32
DDP	0.75×10^4	0.713	
DLT	2.70×10^6	1.137	6.43
DDT	0.42×10^6	1.017	
DLS	2.17×10^4	0.849	0.58
DDS	3.73×10^4	0.958	（K_D/K_L =1.72）

From the Table, it is clearly seen that the DTs possess the largest association constant K at around 10^6 L·mol^{-1}. The order of K value is: DLT > DDT > DLP > DDS > DLS >DDP, whereas the increasing order of enantioselectivity ratios of K_L/K_D is DPs > DTs > DSs. Both the side groups of amino acids (including dansyl moiety) and their chirality can influence the complex binding. The L-enantiomers of DLP and DLT with aromatic side-chain were more selective to bind to BSA in comparison to DLS with aliphatic side-chain. This finding proved again that the steric bulkiness and polarizability of the side group are important parameters in the chiral recognition mechanism [17]. It was also noticed that the enantiomer with the larger fluorescence decrease didnot possess the larger K, except DLT. The level of fluorescent intensity changes does not always parallel the association constant value, as previously reported in the case of glycoprotein and saccharide [7,18]. This can be explained by the fact that the substrate binding does not occur in the same manner or in the same environment for all the substrates, affecting Trp or dansyl fluorescence distinctly.

Concluding remarks:

In summary, BSA has been demonstrated to be an enantiomeric selective sensor for DPs, DTs, and DSs. It was found to be an efficient enantiomeric discrimination of modified amino acids and also a useful host in fluorescent sensing. We propose that the mechanism of fluorescence change in DPs, DTs and DSs caused by the BSA binding is a BSA-binding-induced change in the local environment of dansyl group from a water-dominated hydrophilic solution sphere to a strongly hydrophobic binding domain of BSA. The spectroscopic fluorescence changes were not only indicative of solvation sphere dependence (wavelength shift of the maximum emission), but also revealed that the energy transfer from BSA to dansylated amino-acid derivative played a significant role in the recognition process. Our findings indicate that there is great potential for pharmaceutical applications of BSA, especially in the separation, protection, and delivery of chiral drugs.

Acknowledgement

REFERENCE

[1] Booth, T.D., Wahnon D., and Wainer, I.W. (1997) Is Chiral Recognition a Three-Point Process? Chirality; 9: 96–98.

[2] Henriksson, H., Ståhlberg, J., Isaksson, R., Pettersson, G. (1996) The active sites of cellulases are involved in chiral recognition: a comparison of cellobiohydrolase 1 and endoglucanase 1. FEBS Letters; 390: 339-344.

[3] Bachmann, S., Knudsen, K.R., and Jørgensen, K.A. (2004) Mimicking enzymatic transaminations: attempts to understand and develop a catalytic asymmetric approach to chiral α-amino acids. Org. Biomol. Chem.; 2: 2044-2049.

[4] Allenmark, S., Bomgren, B., Boren, H. (1983) Direct liquid chromatographic separation of enantiomers on immobilized protein stationary phases III. Optical resolution of a series of N-aroyl D,L-amino acids by high-performance liquid chromatography on bovine serum albumin covalently bound to silica. J. Chromatogr. A; 264: 63-68.

[5] Allenmark, S., Andersson, S. (1992) Some mechanistic aspects on chiral discrimination of organic acids by immobilized bovine serum albumin (BSA). Chirality; 4: 24-29.

[6] Lepri, L., Coas, V., Del Bubba, M., Cincinelli, A. (1999) Reversed phase planar chromatography of optical isomers with bovine serum albumin as mobile phase additive. J. Planar. Chromatogr. Mod. TLC; 12: 221–224.

[7] Yan, Y. and Myrick, M.L. (1999) Simultaneous Enantiomeric Determination of Dansyl-D,L-Phenylalanine by Fluorescence Spectroscopy in the Presence of α-Acid Glycoprotein. Anal. Chem.; 71, 1958-1962.

[8] Jia, S.Y., Hao, Y.Q., Li, L.N., Chen, K., Wu, Y.Q., Liu, J.Q., Wu, L.X. and Ding, Y.H. (2005) High Chiral Discrimination of 2,2'-Ditellurobis (2-deoxy-β-cyclodextrin) in Recognition of Dansyl-D/L-phenylalanine. Chem. Lett.; 34: 1248-1249.

[9] LeFevre, J.W. (1993) Reversed-phase thin-layer chromatographic separations of enantiomers of dansyl-amino acids using β-cyclodextrin as a mobile phase additive. J. Chromatogr. A; 653: 293-302.

[10] Wang, R. and Bright, F.V. (1993) Effects of Protein Denaturation on the Rotational Reorientation Kinetics of Dansylated Bovine Serum Albumin. J. Phys. Chem.; 97: 10872-10878.

[11] Ueno, A., Ikeda, A., Ikeda, H., Ikeda, T. and Toda, F. (1999) Fluorescent Cyclodextrins Responsive to Molecules and Metal Ions. Fluorescence Properties and Inclusion Phenomena of N^{α}–Dansyl–L–lysine-β-cyclodextrin and Monensin-Incorporated N^{α}–Dansyl–L–lysine-β-cyclodextrin. J. Org. Chem.; 64: 382-387.

[12] He, X.M. and Carter, D.C. (1992) Atomic structure and chemistry of human serum albumin. Nature; 358: 209–215.

[13] Peters, T.J. (1985) Serum Albumin. Adv. Protein Chem.; 37: 161–245.

[14] FENG, X.Z., JIN R.X., QU Y., HE X.W. (1996) Studies on the Ion's Effect on the Binding Interaction Between HP and BSA. Chem. J. Chinese Univ.; 17: 866-869.

[15] ZHANG, H.R., GUO S.Y., LI L., CAI M.Y., JIN W.J. and LIU C.S. (2001) Study on the Interaction between Sparfloxacin and Serum Albumins by Fluorescence. Spectrosc. Spect. Anal.; 21: 829-832.

[16] Du, H.Y., Xiang, J.F., Zhang, Y.Z., and Tang, Y.L. (2007) A spectroscopic and molecular modeling study of sinomenine binding to transferrin. Bioorganic & Medicinal Chemistry Letters; 17: 1701-1704.

[17] Peyrin, E., Guillaume, Y.C., Guinchard, C. (1998) Peculiarities of dansyl amino acid enantioselectivity using human serum albumin as a chiral selector. J. Chromatogr. Sci.; 36: 97-103.

[18] Takeuchi, M., Yoda, S., Imada, T., Shinkai, S. (1997) Chiral sugar recognition by a diboronic-acid-appended binaphthyl derivative through rigidification effect. Tetrahedron; 53: 8335-8348.

Benzo[*b*]thiophene derivatives as inhibitors of tissue non-specific alkaline phosphatase and of basic calcium phosphate crystals

Lina Li[1-6], Lei Chang[1-5], Stéphane Pellet-Rostaing[1-5*], François Ligier[1-5], Marc Lemaire[1-5*], René Buchet[1-5*] and Yuqing Wu[6]

[1]Université de Lyon, Villeurbanne, F-69622, France; [2]Université Lyon 1, Villeurbanne, F-69622, France; [3]INSA de Lyon, Villeurbanne, F-69621, France; [4]CPE Lyon, Villeurbanne, F-69616, France; [5]CNRS UMR 5246 ICBMS, Villeurbanne, F-69622, France.

[6]State Key Laboratory for Supramolecular Structure and Materials, Jilin University, ChangChun, 130012, China.

(I did not do the organic synthesis)

Abstract: Presence of basic calcium phosphate in knee joints of osteoarthritis patients could be prevented by inhibiting tissue non-specific alkaline phosphtase (TNAP) activity. Levamisole or the L stereoisomer of tetramisole (a known TNAP inhibitor) has been used as a treatment for curing rheumatoid arthritis but its therapeutical use is limited due to side effects. We report the synthesis and the TNAP inhibition property of benzo[*b*]thiophene derivatives, among which benzothiopheno-tetramisole and benzothiopheno- 2,3-dehydrotetramisole, which could be involved in a drug therapy for osteoarthritis. Two water soluble racemic benzothiopheno –tetramisole and -2,3-dehydrotetramisole with apparent inhibition constants K_i = 85 $\pm$ 6 μM and 135 $\pm$ 3 μM (n=3) comparable to that of enantiomeric levamisole 93 $\pm$ 4 μM were found.

Introduction

Calcium-containing crystals are present in synovial fluid extracted from the knee joints of up to 70 % of osteoarthritis patients, indicating that pathological calcification occurs in the majority of osteoarthritis.[1-4] Calcified diseases associated with osteoarthritis are correlated with the presence of calcium pyrophosphate dihydrate (CPPD) crystals (25-55 % of the time) and/or of the occurence of basic calcium phosphate (BCP)

crystals (35-70 % of the time) consisting of carbonate-substituted hydroxyapatite (HA) and octacalcium phosphate.[5-8] The origin of CPPD crystals is associated with the increase in inorganic pyrophosphate (PP_i) concentration. Upregulation of nucleotide pyrophosphatase phosphodiestrase 1 (NPP1) and of ankilosis protein (ANK, a PP_i transporter) expressions in articular cartilage can contribute to an extracellular PP_i excess,[9] leading possibly to CPPD deposition. Consistent with this mechanism, some mutations affecting *ank* gene, upregulating ANK activity, cause chondrocalcininosis in humans.[10-11] In addition, matrix vesicles of affected cartilage in osteoarthritis increase tissue non-specific alkaline phosphatase (TNAP) activity as much as 30-fold and induce HA deposition.[12] TNAP is among the first functional genes expressed in the process of calcification. The crucial role of TNAP in the mineralization process is evidenced in the case of hypophosphatasia patients, whose disease results from mutations in the gene coding TNAP leading to a decreased or absent TNAP activity.[13,14] Therefore, the formation of BCP crystals could be prevented by inhibiting TNAP activity. Levamisole (Figure 1) or the L stereoisomer of tetramisole (a known TNAP inhibitor[15]) have been used as a treatment for curing rheumatoid arthritis.[16-18] However, skin rashes and agranulocytosis reported as side effects for Levamisole[19-20] have limited its therapeutical use. Although numerous levamisole analogs (6-aryl,heteroarylimidazo[2,1-b]thiazole) have been described in the literature as anthelmintics,[21-33] few of them have been tested as inhibitors of alkaline phosphatase[22,30] and, as far as we know, none of these contained heterocyclic moities (thiophen, pyridine, benzofuran…). Here, we present the synthesis and the BIAP (bovine intestinal alkaline phosphatase)/TNAP (tissue non-specific alkaline phosphatase) inhibition properties of a library of benzothiophene derivatives among which the 6-benzothiopheno-imidazo[2,1-b]thiazole derivatives (benzothiopheno-tetramisole and benzothiopheno-2,3-dehydrotetramisole), which could be implemented in a drug therapy for osteoarthitis.

Levamisole (L-tetramisole)
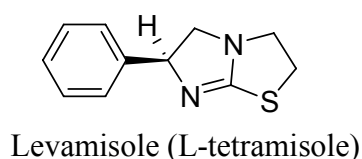
Figure 1. Structure of levamisole

Results and discussion

Chemistry.

Benzothiophene derivatives **7**-**124** were synthesized as previously described in the literature.[34-39] 2- and 3-aryl-Benzo[*b*]thiophenes **7**-**56** were synthesized from the corresponding benzo[*b*]thiophene and 2- or 3-cyano, methoxy, carbaldehyde, and (2,2,2-trifluoroethoxy) -benzo[*b*]thiophene by a one-step palladium coupling with various aryl bromides as described in previous works[34,38,39](scheme 1).

Compounds **57**-**63** were obtained as described in the literature[39] from the corresponding 2-arylbenzo[*b*]thiophenes-3-carbaldehydes involving an Erlenmeyer condensation with hippuric acid, followed by an electrophilic opening of azalactone intermediates and a hydrogenation of the alkenes. 2-aryl-3-amino or phenoxybenzo[*b*]thiophenes **78**-**111**[35] were obtained from the starting 3-bromo-benzo[*b*]thiophene 1-oxide **77** (Table 2) by using an aromatic nucleophilic substitution reaction affording the 3-amino and 3-phenoxybenzo[*b*]thiophenes 1-oxide followed by a palladium coupling involving the corresponding aryl-bromides. Aroyl-Benzo[*b*]thiophenes **112**-**124** were synthesized by a direct acylation of benzo[*b*]thiophene or 2-aryl-benzo[*b*]thiophene.[36]
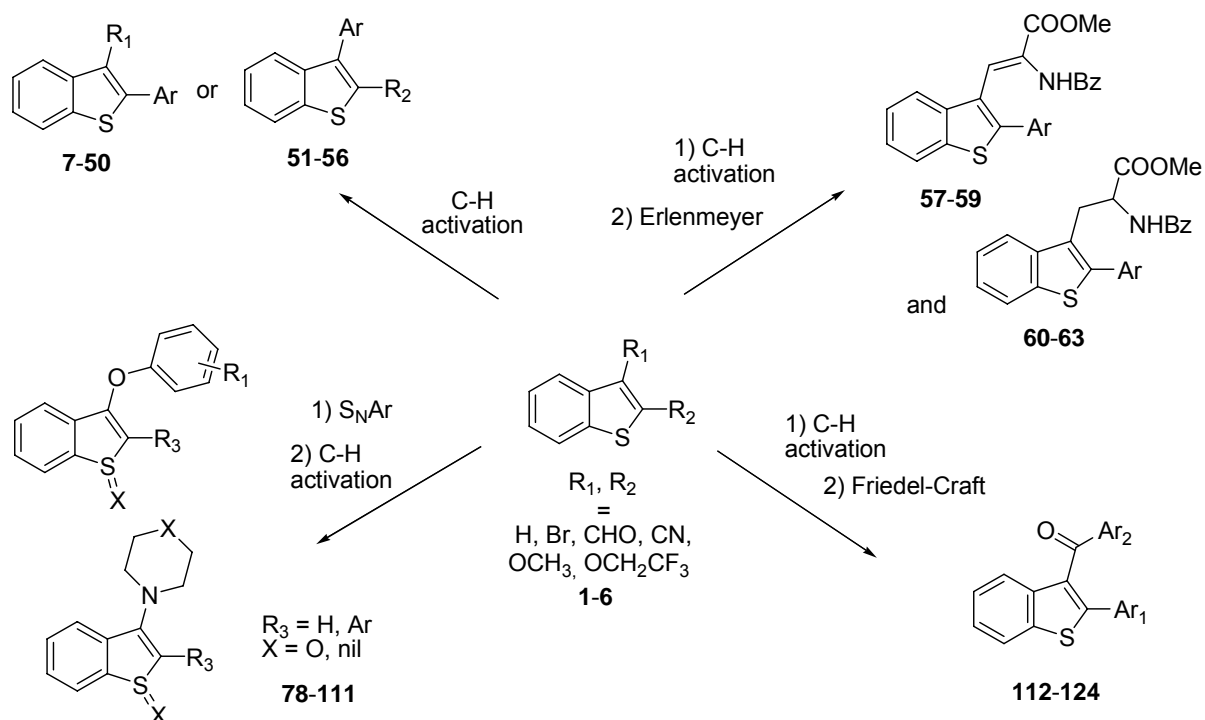

Scheme 1. General syntheses of benzo[*b*]thiophene derivatives **7**-**63** and **78**-**124**

Moreover, 2-aryl-3-methylamino-benzo[b]thiophene type-intermediates **72-76** (Table 2) were obtained by the reduction of the corresponding 2-aryl-3-cyano-benzo[b]thiophene derivatives with BH$_3$-THF.[37] Finally, 2-aryl-benzothiophenes **65-71** were synthesized from the 2-phenyl-benzo[b]thiophene -3-carbaldehyde **21** and the 2-(3'-pyridine)-benzo[b]thiophene -3-carbaldehyde **24** (scheme 2). Fluorination with DAST and amination with hydroxylamine afforded new benzo[b]thiophenes **64, 67, 68** and **71**. Reduction of **21** and **24** with sodium borohydride gave the corresponding hydroxymethyl derivatives **66**[40] and **70**. Although it was already synthesized from thianaphthen-2-one,[41] the carboxylic acid **65** was easily obtained by oxidation of **21** with sodium chlorite and sulfamic acid. Finally, oxidation of **24** with manganese dioxide in the presence of sodium cyanide afforded benzo[b]thiophene methyl ester **70**.

Benzo[b]thiopheno-2,3-dehydrotetramisole **129** and –tetramisole **133** were obtained in 5 steps from the known 3-(2-bromoacetyl)benzo[b]thiophene **125** previously synthesised from benzo[b]thiophene as reported in the literature[42] (scheme 3). Following the synthetic methodology already described in the literature,[21,22] **129** was prepared in an overall yield of 14% by condensation of **125** with the 2-aminothiazole followed by the acylation of **126**, sodium borohydride reduction of **126** and ring closure of **128** with thionyl chloride and acetic anhydride. Following the similar strategy, the condensation of **125** with the 2-aminothiazoline gave the intermediate **130** which was converted into the levamisole derivative **133**.
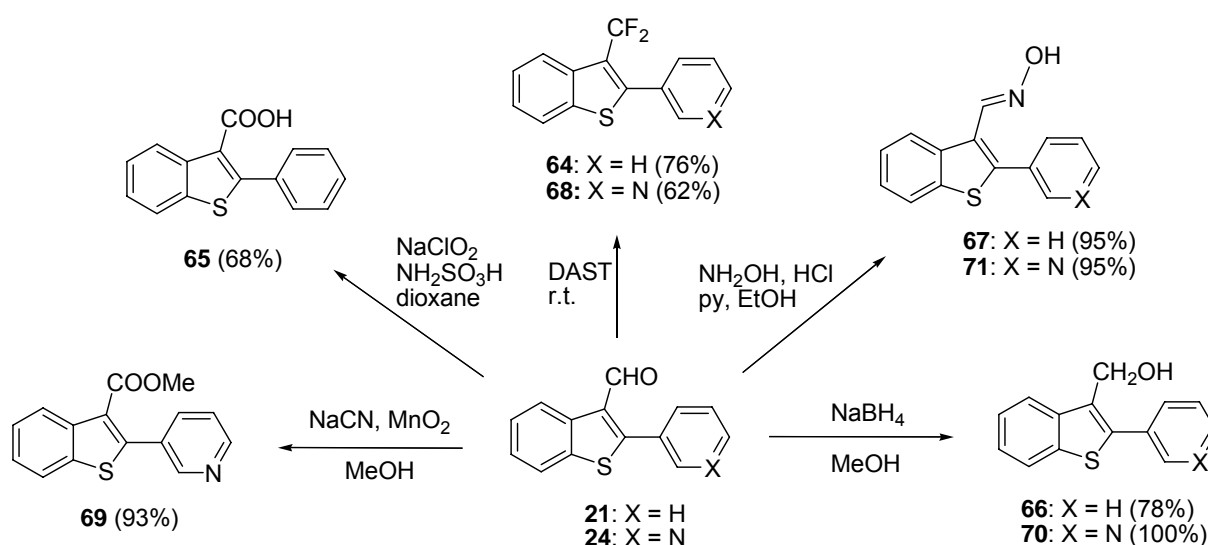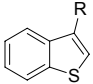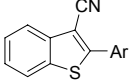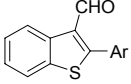

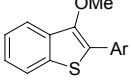
Scheme 2. Synthesis of compounds **65-71**
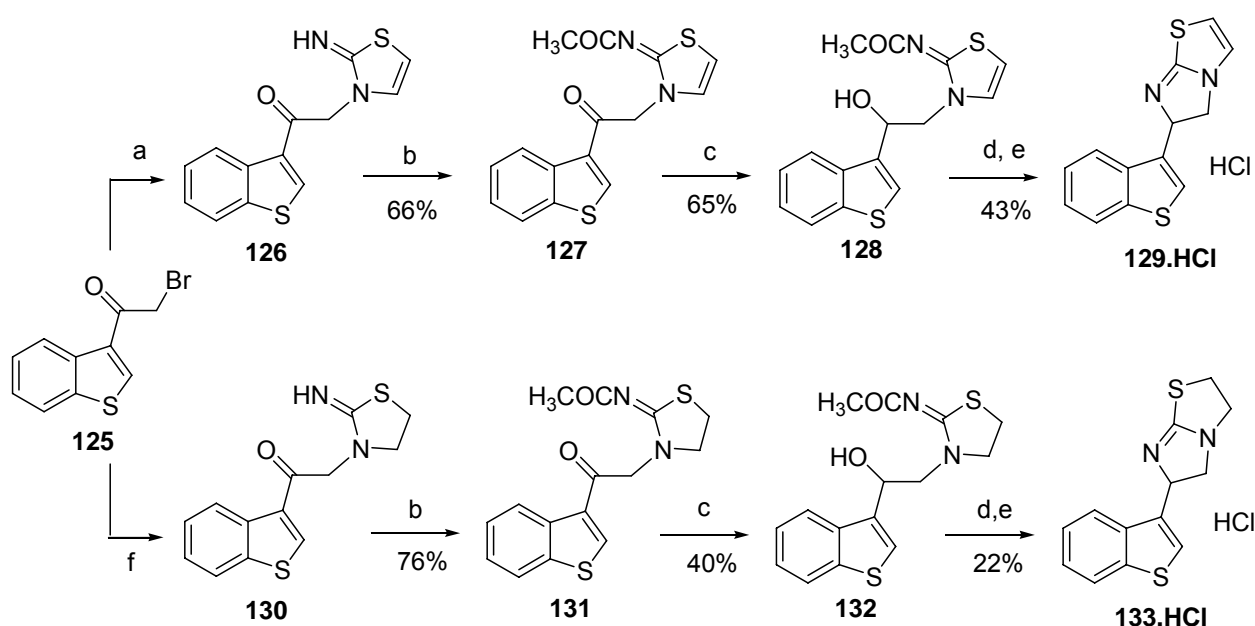
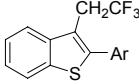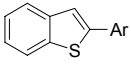**Scheme 3.** (a) 2-aminothiazole, 2-propanol, reflux, (78%); (b) Ac₂O, pyridine, chloroform, reflux; (c) NaBH₄, MeOH, r.t.; (d) SOCl₂, Ac₂O, reflux; (e) HCl, MeOH (f) 2-aminothiazoline, CH₃CN, reflux, (89%).

Evaluation of BIAP and TNAP inhibition

The library of benzothiophene compounds **1**-**124** (0.1 mM in bovine intestinal alkaline phosphatase (BIAP) reactive medium with final DMSO 1% (v/v) and 0.4 mM in TNAP reactive medium with final DMSO 4% (v/v) respectively) was tested for the potential inhibition activity of bovine intestinal alkakine phosphatase BIAP and of TNAP respectively (Tables 1-4). Among the 2-arylbenzo[*b*]thiophenes **7**-**50** (Table 1), **14** and **23** presented the more interesting effect with 95% and 91% inhibition of BIAP, while in this series **35** was the best TNAP inhibitor with 56% inhibition while it did not inhibit BIAP. Globally, 2-aryl-benzo[b]thiophene -3-carbaldehydes are more efficient than the 3-H, 3-cyano, 3-methoxy and 3-OCH₂CF₃ analogs. In this series, 2-phenyl-benzo[b]thiophen-3-oxime **67** was one of the most promising. 0.1mM of it inhibited almost totally the *p*NPP hydrolysis by BIAP (Figure 2A) and 0.4mM of it caused 32 % inhibition of TNAP (Table 2). Figure 2B shows the inhibition effect of **67** on the TNAP activity of matrix vesicles (MVs). The inhibition effect was found to be dependent on the concentration of DMSO (data not shown), while a low concentration of DMSO (up to 4% v/v) alone had nearly no effect on BIAP or TNAP.

Table 1 Inhibition effects of benzo[*b*]thiophene derivatives **1**-**50** on BIAP and on TNAP activities at pH 10.4 and at 37°C. A relative activity of 100 ± 5 % indicated no significant inhibition effects. Values greater than 105 % indicated activation, while values smaller than 95% indicated inhibition.

General Structures	Compound number	BIAP + 0.1 mM inhibitor with 1% DMSO Relative Activity (%)	TNAP + 0.4 mM inhibitor with 4% DMSO Relative Activity (%)
	CN : **1**	92	92
	CHO : **2**	120	85
	OMe : **3**	90	93
	Ph: **7**	76	-
	4-OMe-Ph : **8**	94	-
	4-CF$_3$-Ph : **9**	96	97
	2-napht : **10**	18	99
	3-py: **11**	106	-
	2-py: **12**	94	-
	2-CN-Ph: **13**	90	-
	2-Me-Ph: **14**	5	85
	3-Quinoline: **15**	95	-
	3-Cl-Ph: **16**	115	-
	4-Cl-Ph: **17**	69	-
	3-OMe-Ph: **18**	97	-
	3,4,5-OMe-Ph: **19**	88	91
	4-N(Me)$_2$-Ph: **20**	82	83
	Ph: **21**	41	77
	4-OMe-Ph: **22**	37	99
	4-Cl-Ph: **23**	9	-
	3-Py: **24**	119	93
	2-CN-Ph: **25**	110	79
	3-Quinoline: **26**	110	-
	4-CN-Ph: **27**	92	105
	2-NO$_2$-Ph: **28**	116	78
	4-CF$_3$-Ph: **29**	30	80
	3-Cl-Ph: **30**	62	95
	2-Cl-Ph: **31**	63	97
	Ph: **32**	80	87
	2-CN-Ph: **33**	57	79
	4-OMe-Ph: **34**	78	97
	3-Py: **35**	112	44
	2-napht: **36**	102	-
	2-Me-Ph: **37**	73	96
	3-Quinoline: **38**	64	86
	2-Py: **39**	99	90
	2-CN-Ph: **40**	70	87
	3-Py: **41**	122	84
	4-OMe-Ph: **42**	107	94
	2-Py: **43**	119	94
	2-NO$_2$-Ph: **44**	121	86
	2-NH$_2$-Ph: **45**	93	70
	2-NO$_2$-4-Me-Ph: **46**	127	97
	2-NO$_2$-4-Cl-Ph: **47**	107	93
	2-NH$_2$-4-Me-Ph: **48**	107	93
	3-Cl-Ph: **49**	95	96
	2-NO$_2$-4-OMe-Ph: **50**	99	96

Table 2. Inhibition effects of benzo[*b*]thiophene derivatives **4-6** and -**51-76** on BIAP and on TNAP activities at pH 10.4 and at 37°C. A relative activity of 100 ± 5 % indicated no significant inhibition effects. Values greater than 105 % indicated activation, while values smaller than 95% indicated inhibition.
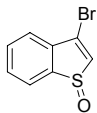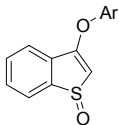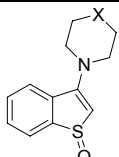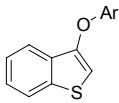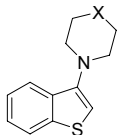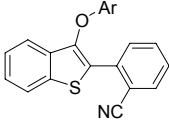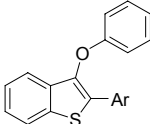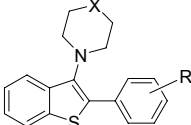
General Structures	Compound number	BIAP + 0.1 mM inhibitor with 1% DMSO Activity (%)	TNAP + 0.4 mM inhibitor with 4% DMSO Activity (%)
	I : **4**	41	54
	OCH$_2$CF$_3$: **5**	116	100
	CN : **6**	103	105
	R = H, Ar =4-OMe-Ph: **51**	100	-
	R = CN, Ar = 4-CF$_3$-Ph: **52**	115	-
	Ar = 3-Py: **53**	120	-
	R = OCH$_2$CF$_3$, Ar = 2-CN-Ph: **54**	101	87
	Ar = 3-Py: **55**	102	97
	R = 2-NO$_2$-Ph Ar = 2-NO$_2$-Ph: **56**	108	88
	4-CN-Ph: **57**	108	-
	4-CF$_3$-Ph: **58**	35	87
	4-OMe-Ph: **59**	77	91
	4-CN-Ph: **60**	115	-
	4-CF$_3$-Ph: **61**	63	-
	4-OMe-Ph: **62**	91	86
	H: **63**	116	74
	CF$_2$: **64**	94	90
	COOH: **65**	113	78
	CH$_2$OH: **66**	103	87
	C=N-OH: **67**	1	68
	CF$_2$: **68**	103	79
	COOMe: **69**	117	98
	CH$_2$OH: **70**	104	106
	C=N-OH: **71**	103	71
	Ph: **72**	148	76
	3-Py: **73**	105	111
	2,3,4-(OMe)3-Ph: **74**	142	94
	2-NH$_2$-4-OMe-Ph: **75**	103	103
	3-N(CH$_3$)$_2$: **76**	134	84
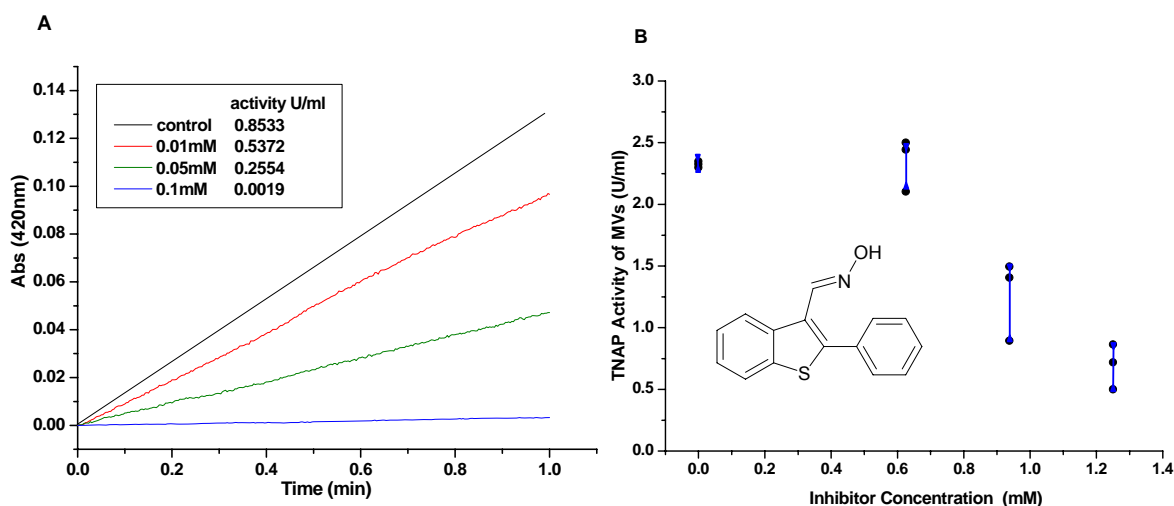
Figure 2. Inhibition of *p*NPP hydrolysis by 0.2 µg ml^{-1} BIAP with 0 to 0.1 mM benzothiophenyl compound **67** in 1% DMSO (v/v) (A) and 10 µg ml^{-1} matrix vesicles with 1% DMSO (v/v) (B) at pH 10.4 and at 37°C. *p*NPP concentration was 0.1 mM. Three independent measurements were made.
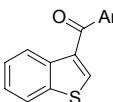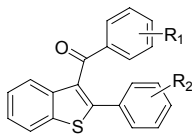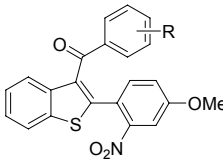
Whatever the nature of the phenolic or amino moieties incorporated in the benzo[*b*]thiophene-sulfoxyde **78**-**86** (Table 3) and 2-aryl-benzo[*b*]thiophene **100**-**110**, no significant inhibition was observed on BIAP and TNAP with compound concentrations of 0.1 mM and 0.4 mM respectively. Only the cyano derivative **81** exhibited a modest inhibition of TNAP (32%) and the carbaldehyde **90** a noticeable inhibition of BIAP (91%). Finally, in the series of 3-aroyl compounds **112**-**124** (Table 4), only 2-H derivatives **112** and **113** gave noticeable BIAP inhibitions respectively of 57% and 60%. No broad inhibition was observed on TNAP with compounds **112**-**124**.

Table 3. Inhibition effects of benzo[*b*]thiophene derivatives **77**-**111** on BIAP and on TNAP activities at pH 10.4 and at 37°C. A relative activity of 100 ± 5 % indicated no significant inhibition effects. Values greater than 105 % indicated activation, while values smaller than 95% indicated inhibition.

General structures	Compound number	BIAP + 0.1 mM inhibitor with 1% DMSO Relative Activity (%)	TNAP + 0.4 mM inhibitor with 4% DMSO Relative Activity (%)
	77	105	100
	Ph: **78**	102	104
	4-OMe-Ph: **79**	107	100
	4-Cl-Ph: **80**	122	103
	4-CN-Ph: **81**	106	67
	4-F-Ph: **82**	109	79
	3,4,5-(OMe)$_3$-Ph: **83**	127	101
	CH$_2$: **84**	110	101
	N-CH$_3$: **85**	102	95
	O: **86**	97	111
	Ph: **87**	104	89
	4-OMe-Ph: **88**	96	82
	4-F-Ph: **89**	104	78
	4-CHO-Ph: **90**	9	-
	4-Cl-Ph: **91**	107	94
	t-Bu-Ph: **92**	113	100
	4-CH$_2$NH$_2$-Ph: **93**	105	83
	4-CN-Ph: **94**	87	85
	3,4,5-(OMe)$_3$-Ph: **95**	129	101
	N-(2-OH)-Ph: **96**	49	109
	N-CH$_3$: **97**	107	97
	O: **98**	108	99
	CH$_2$: **99**	92	80
	4-F-Ph: **100**	66	85
	Ph: **101**	110	91
	2,3,4-(OMe)$_3$-Ph: **102**	121	106
	4-Cl-Ph: **103**	101	79
	4-OMe-Ph: **104**	106	98
	4-CN-Ph: **105**	82	97
	4-OMe-Ph: **106**	105	94
	Ph: **107**	104	91
	X=CH$_2$; R=2-CN: **108**	99	100
	X=CH$_2$; R=4-OMe: **109**	106	91
	X=CH$_2$; R=H: **110**	99	81
	X=O; R=2-CN: **111**	107	93

As well as for the most promising compounds **35** and **81** (inhibiting specifically TNAP) or **4** and **67** (inhibiting both BIAP and TNAP), the solubilities of benzothiophene derivatives **1**-**124** were not high enough in aqueous buffer and DMSO (up to 4% v/v) was generally added to solubilize them. Addition of 4 % v/v DMSO into aqueous mineralization medium induced spontaneously hydroxyapatite formation[43] as in the case of matrix vesicles which are released from hypertrophied chondrocytes during physiological endochondral ossification[44-46] or from osteoarthritic articular chondrocytes.[47-50]

Table 4. Inhibition effects of benzo[*b*]thiophene derivatives **112**-**124** on BIAP and on TNAP activities at pH 10.4 and at 37°C. A relative activity of 100 ± 5 % indicated no significant inhibition effects. Values greater than 105 % indicated activation, while values smaller than 95% indicated inhibition.
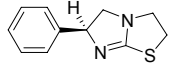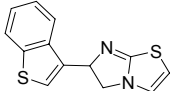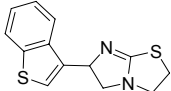
General Structures	Compound number	BIAP + 0.1 mM inhibitor with 1% DMSO Relative activity (%)	TNAP + 0.4 mM inhibitor with 4% DMSO Relative activity (%)
	Ph: **112**	43	80
	4-OMe-Ph: **113**	40	96
	R_1=H, R_2=2-CN: **114**	91	92
	R_1=4-OMe,R_2=4-OMe: **115**	70	108
	R_1=2-OMe,R_2=2-NO2: **116**	92	98
	R_1=3-OMe,R_2=2-NO$_2$: **117**	98	96
	R_1=4-OMe,R_2=2-NO$_2$: **118**	107	101
	H: **119**	114	97
	3-OMe: **120**	116	100
	4-OMe: **121**	95	100
	2-OMe: **122**	117	111
	3, 5-(OMe)$_2$-4-OH: **123**	125	95
	3,4,5-(OMe)3: **124**	124	92

DMSO is very often used as solvent for water- insoluble drugs and in several human therapeutic situations.[51]Although DMSO has some beneficial effects,[51] several reports indicate that care must be taken in the experiments with DMSO[52,53] or using DMSO as a drug vehicle.[54] DMSO induced hydroxyapatite formation in synthetic cartilage lymph.[43] Although we found that several water-insoluble benzothiophene molecules could inhibit TNAP, their effects were difficult to determine correctly since it was dependent on the DMSO concentration. Since DMSO is a promoter of mineralization, water-soluble benzothiophene derivatives have to be synthesized. We reasoned that water-soluble tetramisole could be derivatized with benzothiophene

compounds to increase the solubity of benzothiophene moiety in water and to increase the inhibition effect having two active sites in one molecule. Therefore, we designed and synthesized water-soluble benzothiophene compounds.

As levamisole, **129** and **133** hydrochloride salt did not inhibit intestinal alkakine phosphatase (Table 5). However, levamisole chlorhydrate (Figure 3), **129.HCl** (Figure 4) and **133.HCl** (Figure 5) inhibited the TNAP. Both samples as levamisole inhibited, in an uncompetitive manner, TNAP activity, being consistent with the fact that the location of the binding site of the inhibitor is controlled by the tetramisole moiety. Their plots of v_{max}^{-1} vs inhibitor concentration (Figure 3B, 4B and 5B) allowed us to determine their apparent inhibition constants K_i (pH =7.8; 37°C and without DMSO). Small differences in their apparent inhibitor constants (K_i) were observed. A better stabilization of the interactions between inhibitor and TNAP was evidenced for **129.HCl** (K_i = 85 μM) as compared with **133.HCl** (K_i = 135 μM) (Table 6).

Table 5. Inhibition effects of levamisole derivatives on BIAP and on TNAP activities at pH 10.4 and at 37°C. A relative activity of 100 ± 5 % indicated no significant inhibition effects. Values greater than 105 % indicated activation, while values smaller than 95% indicated inhibition.

General Structures	Compound number	BIAP + 0.1 mM inhibitor with 1% DMSO Relative activity (%)	TNAP + 0.4 mM inhibitor with 4% DMSO Relative activity (%)
	Levamisole.HCl	99	10
	129.HCl	99	11
	133.HCl	100	19

Comparison of inhibition effects of levamisole and benzothiopheno-tetramisole derivatives.

Although TNAP activity is usually measured at alkaline pH as to screen putative inhibitors, the inhibitor activity of samples was determined at pH = 7.8 and at 37°C to match physiological conditions.[55] The apparent K_i of porcine TNAP for levamisole was 93 μM at pH =7.8 and at 37°C (Table 6). The K_i of human TNAP for levamisole

amounted to 16 μM or to 136 μM for that of chicken TNAP measured at pH=9.8.[56] The difference in K_i of human TNAP and that of chicken TNAP was attributed to the presence of His-434 residue.[56] The K_i of racemic **129.HCl** (K_i = 85 μM) and that of racemic **133.HCl** (K_i = 135 μM) were slightly distinct from that of enantiomeric levamisole (K_i = 93 μM) indicating that there is some potential to synthesize and optimize enantiomeric levamisole derivatives. The strategy to develop drug-like-TNAP soluble inhibitors for therapeutic use for treating pathological soft tissue mineralization disorders[55,56] looks promising.

Table 6. Apparent inhibition constants (K_i) of TNAP activity determined at pH 7.8 and at 37°C without DMSO.

Inhibitors	Inhibition Type	K_i (mM) ± SD
Levamisole.HCl	Uncompetitive	93 ± 4 (n=3)
129.HCl	Uncompetitive	85 ± 6 (n=3)
133.HCl	Uncompetitive	135 ± 3 (n=3)
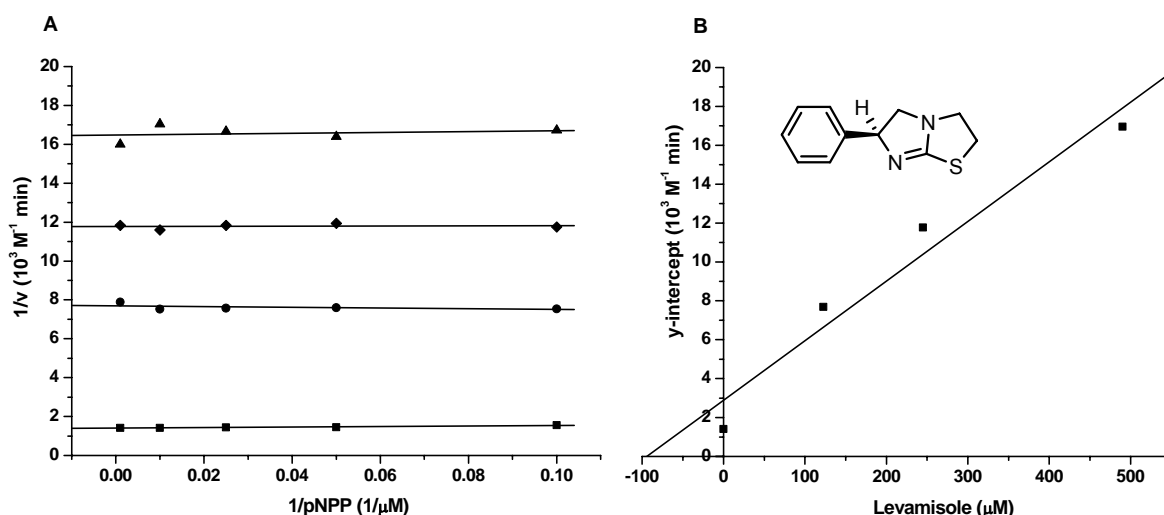
Figure 3. Inhibition of pNPP hydrolysis of TNAP by levamisole.HCl at pH=7.8 and at 37°C without DMSO. A) Linewaever-Burk plot in the presence of 6 μg ml^{-1} TNAP with 10, 20, 40, 100 and 1000 μM pNPP and increasing concentration of 0 μM (■), 122.5 μM (●), 245 μM (◆) and 490 μM (▲) levamisole. B) Plot of v_{max}^{-1} vs levamisole concentration that enabled us to determine apparent K_i. The x intercept gives the negative value of K_i.
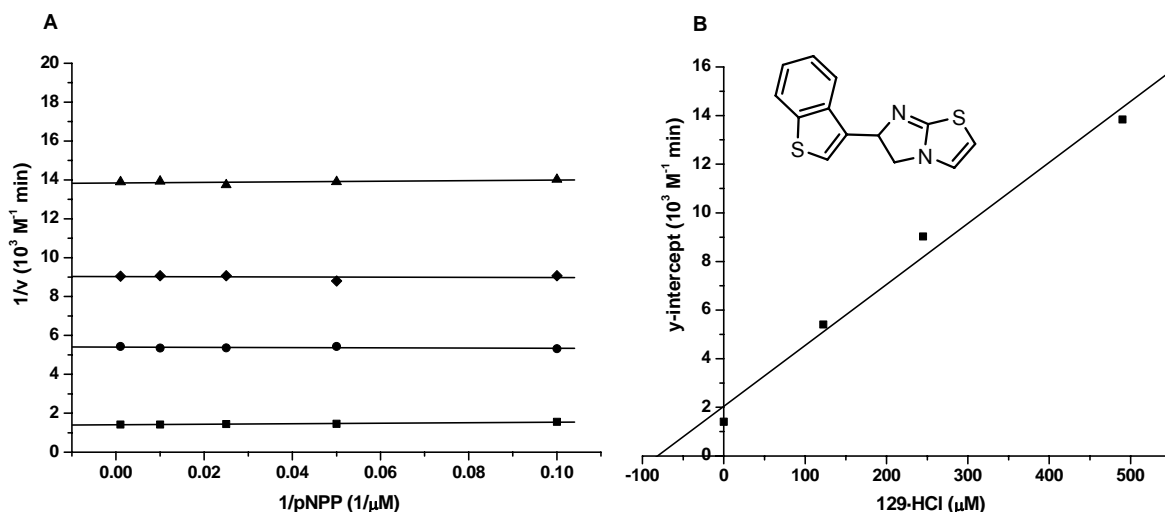
Figure 4. Inhibition of *p*NPP hydrolysis of TNAP by **129.HCl** at pH=7.8 and at 37°C without DMSO. A) Linewaever-Burk plot in the presence of 6 μg ml^{-1} TNAP with 10, 20, 40, 100 and 1000 μM *p*NPP and increasing concentration of 0 μM (■), 122.5 μM (●), 245 μM (♦) and 490 μM (▲)**129.HCl**. B) Plot of v_{max}^{-1} vs **129.HCl** concentration that enabled us to determine apparent K_i. The *x* intercept gives the negative value of K_i.
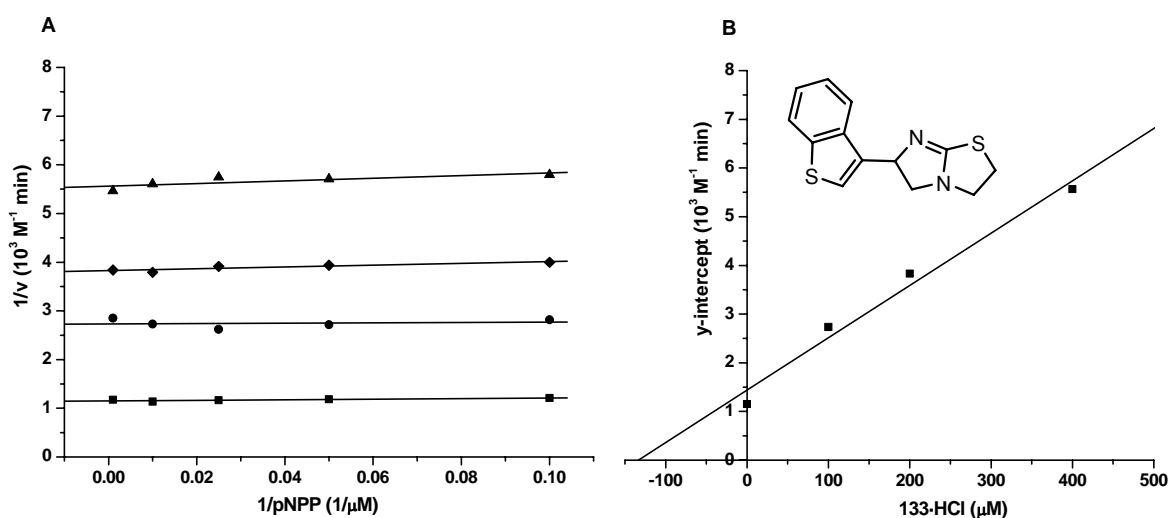
Figure 5. Inhibition of *p*NPP hydrolysis of TNAP by **133.HCl** at pH=7.8 and at 37°C without DMSO. A) Linewaever-Burk plot in the presence of 6 μg ml^{-1} TNAP with 10, 20, 40, 100 and 1000 μM *p*NPP and increasing concentration of 0 μM (■), 100μM (●), 200 μM (♦) and 400 μM (▲) **133.HCl**. B) Plot of v_{max}^{-1} vs **133.HCl** concentration that enabled us to determine apparent K_i. The *x* intercept gives the negative value of K_i.

Conclusion

Some Benzothiophene derivatives showed more pronouced inhibition properties towards BIAP than TNAP. Such compounds may have a clinical application, since the intestinal type of alkaline phosphatase increased in the urine of patients with renal disease.[57]   On the other hand, 6-benzothiopheno-imidazo[2,1-b]thiazole derivatives (benzothiopheno-tetramisole and benzothiopheno-2,3-dehydrotetramisole), proved to be efficient in the TNAP inhibition, which could be implemented in a drug therapy for osteoarthritis. Two water soluble racemic benzothiopheno–tetramisole and -2,3-dehydrotetramisole with apparent inhibiton constants K_i = 85 $\pm$ 6 μM and 135 $\pm$ 3 μM (n=3) comparable to that of enantiomeric levamisole 93 $\pm$ 4 μM were found, indicating some potential to synthesize and optimize enantiomeric benzothiopheno–tetramisole.

Experimental section

Materials. Reactants and solvents were supplied by Aldrich, Acros, Lancaster, Alfa Aeser and Fluka and purchased at the highest commercial quality and used without further purification. Porcine kidney tissue non-specific alkaline phosphatase (TNAP), bovine intestinal alkaline phosphatase (BIAP) and levamisole hydrochloride were purchased from Sigma and used without further purification. *p*-Nitrophenylphosphate was obtained from Fluka.

All reactions were carried out under an argon atmosphere with dry solvents under anhydrous conditions, unless otherwise stated. NMR spectra were recorded on a Bruker DPX-300 ([1]H: 300MHz; [13]C: 300MHz) instrument using $CDCl_3$ and DMSO as solvents. The chemical shifts (δ ppm) and coupling constants (Hz) are reported in the standard fashion. The following abbreviations are used to explain the multiplicities: s = singlet, d = doublet, t = triplet, q = quartet, m = multiplet, br = broad. Electrospray ionization (ESI) mass spectrometry (MS) experiments were performed on a thermo Finnigan LCQ Advantage mass. High-resolution mass spectra (HRMS) were recorded on a Finnigan Mat 95xL mass spectrometer using CI. Analytical thin-layer chromatography was effected on silica gel Merck 60 D254 (0.25 mm). Flash chromatographies were performed on Merck Si 60 silica gel (40-63 μm) Merck aluminum oxide 90 active neutral (63-200 μm). Elemental analyses were performed by the 'Service Central d'Analyses du CNRS' (Solaize, France).

Chemistry.

General procedure of 2-aryl-3(diluoromethyl)-benzo[*b*]thiophenes 64 and 68.
DAST (3.08 mL, 25.2 mmol) was added dropwise to the solid 2-aryl-benzo[*b*]thiophene -3-carboxaldehyde (0.84 mmol) **21** or **24** and the resulting red solution was stirred at room temperature for 16h. under argon. The mixture was then poured dropwise into ice-cold water (50 mL) and extracted with CH_2Cl_2 (2x50 mL). The organic phase was dried over $MgSO_4$, filtered and concentrated. The residue was purified by flash column chromatography (SiO_2) to obtain the pure desired compound.

2-phenyl-3-(difluoromethyl)-benzo[*b*]thiophene 64. Eluent: cyclohexane. Yield: 75%. ^{1}H NMR (CDCl$_3$) δ 8.16 (dd, *J* = 0.9Hz, 6.8Hz, 1H), 7.85 (dd, *J* = 0.9Hz, 6.8Hz, 1H), 7.53-7.38 (m, 7H), 6.77 (t, *J* = 54Hz, 1H, CF$_2$*H*). ^{13}C NMR (CDCl$_3$) δ 147.1, 139.1, 136.9, 132.1, 129.9, 129.5, 129.1, 125.2, 124.9 (t, *J* = 24.5Hz), 124.0, 122.2, 112.7 (t, *J* = 232Hz). ^{19}F NMR (CDCl$_3$): -108.9. MS (EI$^+$): *m/z* 260(MH$^+$).

2-(3'-pyridine)-3-(difluoromethyl)-benzo[*b*]thiophene 68. Eluent: cyclohexane/ AcOEt (8:2). Yield: 62%. ^{1}H NMR (CDCl$_3$) δ 8.77 (d, br., 2H), 8.16 (dd, *J* = 1.1Hz, 6.6Hz, 1H), 7.81 (dd, *J* = 1.0Hz, 6.6Hz, 1H), 7.75 (ddd, *J* = 1.7Hz, 1.7Hz, 7.9Hz 1H), 7.47-7.34 (m, 3H), 6.73 (t, *J* = 53.7Hz, 1H). ^{13}C NMR (CDCl$_3$) δ 150.4, 149.8, 142.5 (t, *J* = 9.82Hz), 139.1, 136.9, 136.6, 128.3, 125.9 (t, *J* = 25.1Hz), 125.6, 125.4, 123.8 (t, *J* = 2.2Hz), 123.5, 122.1, 112.0 (t, *J* = 234Hz). ^{19}F NMR (CDCl$_3$): -109.2. MS (EI$^+$): *m/z* 261(MH$^+$).

General procedure of 2-aryl-3(hydroxymethyl)-benzo[*b*]thiophenes 66 and 70.
NaBH$_4$ (0.6 mmol) was added to a solution of **21** or **24** (0.4 mmol) in MeOH (2 mL) at 0°C under argon. After stirring for 2h at 0°C, the reaction mixture was quenched with acetone, poured into NH$_4$Cl 10% (10 mL) and extracted with CH_2Cl_2 (2x10mL). The organic layers were ressembled, dried over $MgSO_4$, filtered and concentrated. The residu was purified by flash column chromatography (SiO_2) to obtain the pure desired compound.

2-phenyl-3-(hydroxymethyl)-benzo[*b*]thiophene 66.[40] Eluent: cyclohexane/AcOEt (9:1). Yield: 78%. ^{1}H NMR (CDCl$_3$) δ 7.96 (d, *J* = 7Hz, 1H), 7.86 (d, *J* = 7Hz, 1H), 7.61 (dd, *J* = 1.7Hz, 6.6Hz, 2H), 7.51-7.35 (m, 5H), 4.91 (s, 2H). ^{13}C NMR (CDCl^3) δ 143.1, 104.1, 139.2, 133.8, 130.4, 129.8, 128.9, 128.6, 124.7, 122.4, 122.3, 56.97. MS (EI$^+$): *m/z* 240(MH$^+$).

2-(3'-pyridine)-3-(hydroxymethyl)-benzo[*b*]thiophene 70. Eluent: cyclohexane/ AcOEt (7:3). Yield: 100%. ^{1}H NMR (DMSO-d_6) δ 8.86 (d, J = 2.2Hz, 1H), 8.66 (dd, J = 1.5Hz, 4.7Hz, 1H), 8.08-8.00 (m, 3H), 7.58 (ddd, J = 0.8Hz, 4.7Hz, 4.7Hz, 1H), 7.46 (m, 2H). ^{13}C NMR (DMSO-d_6) δ 149.4, 149.3, 140.0, 138.4, 136.8, 136.7, 133.4, 129.6, 125.1, 124.7, 123.9, 123.3, 122.3, 54.85. MS (EI$^+$): *m/z* 241(MH$^+$).

General procedure of 2-aryl-3-oxime--benzo[*b*]thiophenes 67 and 71. Pyridine (1.26 mmol) was added to a solution of **21** or **24** (0.353 mmol) and NH$_2$OH.HCl (1.47 mmol) in EtOH (1 mL). The mixture was refluxed for 1h30. After cooling to room temperature, CH$_2$Cl$_2$ (15 mL) was added and the solution was poured into cold water (30 mL). After addition of CH$_2$Cl$_2$ (15 mL), the organic phase was separated, dried over MgSO$_4$ and concentrated under vacuum at 20°C. Purification by chromatography (SiO$_2$) provided pure products.

2-phenyl-3-oxime-benzo[*b*]thiophene 67. Eluent: cyclohexane/ AcOEt (9:1). Yield: 85%. ^{1}H NMR (CDCl$_3$) δ 8.63 (d, J = 7.7Hz, 1H), 8.40 (s, 1H), 7.85 (d, J = 7.7hz, 1H), 7.55-7.39 (m, 8H). ^{13}C NMR (CDCl$_3$) δ 147.8, 147.0, 138.8, 137.5, 133.1, 130.2, 129.1, 128.9, 125.6, 125.5, 125.2, 123.7, 122.0. MS (EI$^+$): *m/z* 253(MH$^+$).

2-(3'-pyridine) -3-oxime-benzo[*b*]thiophene 71. Eluent: cyclohexane/ AcOEt (7:3). Yield: 95%. ^{1}H NMR (DMSO-d_6) δ 11.49 (s, 1H), 8.75 (s, 1H), 8.70 (d, J = 4.4Hz, 1H), 8.58 (d, J = 7.4Hz, 1H), 8.18 (s, 1H), 8.06 (d, J = 7.7Hz, 1H), 7.99 (d, J = 7.7Hz, 1H), 7.60-7.45 (m, 3H). ^{13}C NMR (DMSO-d_6) δ 150.0, 149.7, 143.5, 141.0, 138.3, 137.3, 136.9, 128.9, 125.6, 125.5, 125.4, 125.3, 123.9, 122.5. MS (EI$^+$): *m/z* 254(MH$^+$).

2-phenyl-benzo[*b*]thiophene-3-carboxylic acid 65. 21 (0.09g, 0.377 mmol) was dissolved in 5.4 mL of dioxane/H$_2$O (7:3). NaClO$_2$ (0.045 g, 0.5 mmol) and NH$_2$SO$_3$H (0.209 g, 2.15 mmol) was added and the mixture was stirred for 2h at room temperature. After addition of 10% NaHCO$_3$ and extraction with AcOEt, the organic layer was washed with HCl 2N. The organic layer was separated, dried over MgSO$_4$, filtered and evaporated. Purification by flash chromatography (SiO$_2$, cyclohexane/AcOEt 8:2) produced pure **65** in 68% yield (0.065 g). ^{1}H NMR (CDCl$_3$) δ 11.38 (s, 1H), 8.51 (d, J = 8.1Hz, 1H), 7.84 (d, J = 8.1Hz, 1H), 7.60-7.40 (m, 7H). ^{13}C NMR (CDCl$_3$) δ 169.2, 162.4, 155.1, 138.7, 138.2, 133.8, 129.8, 129.3, 128.3, 125.8, 125.2, 121.8. MS (EI$^+$): *m/z* 254(MH$^+$).

2-(3'-pyridine)-benzo[*b*]thiophene-3-carboxylic acid methyl ester 71. NaCN (0.195 g, 4 mmol) and MnO$_2$ (1.38 g, 15.8 mmol) were added to a solution of **24** (0.19

g, 0.8 mmol) in MeOH (30 mL). The mixture was stirred at room temperature overnight. CH_2Cl_2 (100 mL) was then added and the resulting precipitate filtered on celite. The filtrate was concentrated and dissolved in H_2O/CH_2Cl_2. The organic phase was washed with water, dried over $MgSO_4$ and evaporated. Purification by flash chromatography (SiO_2, cyclohexane/AcOEt 9:1) gave pure **71** in 93% yield (0.2 g). ^1H NMR ($CDCl_3$) δ 8.73 (s, 1H), 8.62 (d, J = 4.0Hz, 1H), 8.41 (d, J = 7.9Hz, 1H), 7.79 (d, J = 7.9Hz, 2H), 7.49-7.31 (m, 3H), 3.74 (s, 3H). ^{13}C NMR ($CDCl_3$) δ 163.7, 149.7, 147.9, 138.7, 138.2, 136.8, 130.3, 125.7, 125.4, 125.0, 123.8, 122.8, 121.8, 51.7. MS (EI^+): *m/z* 269(MH^+).

Compound 126. Benzo[*b*]thiophene **125** (9.7 mmol, 2.48 g) was refluxed for 1 h with 2-aminothiazole (9.7 mmol, 0.97 g) in 25 ml of 2-propanol. The resulting solid was filtered, triturated with a 10% Na_2CO_3 solution then filtered and dried. The crude product was purified by flash chromatography (EtOAc) to give **127** (2.1 g, 78%) as a milky solid. Data for compound **126:** ^1H NMR (DMSO) δ 9.63 (s, 1H), 9.16 (s, 1H), 8.53 (dd, 1H, $J = 1.5Hz$, 6.8Hz), 8.17 (dd, 1H, $J = 0.75Hz$, 7.1Hz), 7.55-7.5 (m, 2H), 7.44 (d, 1H, $J=4.5Hz$), 7.1 (d, 1H, $J=4.5Hz$), 5.88 (s, 2H); ^1H NMR (300Hz, DMSO) δ 185.9, 169.5, 162.2, 141.4, 139.5, 136.5, 131.3, 131.1, 126.5, 126.1, 124.7, 107.8, 55.5; MS(ESI): 275$[M+H]^+$; HR ESIMS calculated for $C_{13}H_{11}OS_2N_2^+=275.0313$; found= 275.03121.

Compound 127. To a mixture of **126** (7.6 mmol, 2.1g) and 5 ml of pyridine in 50 ml of chloroform was added 2 ml of acetic anhydride. The mixture was refluxed for 1.5 h and the chloroform was removed to leave oil. Then the residue was washed by ethyl ether and purified by flash chromatography (EtOAc) to afford **127** (1.6 g, 66%) as a brown solid. Data for compound **127:** ^1H NMR (300MHz, DMSO) δ 8.3 (s, 1H), 8.54 (dd, 1H, $J=0.9Hz$, 2.8Hz), 8.15 (dd, 1H, $J=1.9Hz$, 7.0Hz), 7.53-7.50 (m, 2H), 7.48 (d, 1H, $J = 4.7Hz$), 7.0 (d, 1H, $J = 4.7Hz$), 5.82 (s, 2H), 2.02 (s, 3H); 13C NMR (300Hz, DMSO) δ 187.7, 178.7, 167.2, 141.0, 139.6, 136.4, 131.8, 128.2, 126.4, 126.1, 124.8, 123.4, 108.3, 54.8, 27.0; MS(ESI): 317 $[M+H]^+$; HR ESIMS calculated for $C_{15}H_{13}O_2S_2N_2^+=317.0418$; found= 317.04179.

Compound 128. To a solution of **127** (3 mmol, 1 g) in 25 ml of methanol maintained at 10ºC was added in small portions 5 mmol of $NaBH_4$. The solution was stirred at room temperature for 2 h, solvent was removed under vacuum, and the residue was suspended in water and extracted with DCM. The DCM layer was dried with $MgSO_4$ and the solvent was removed to leave a solid which was purified by flash

chromatography (EtOAc/MeOH =95/5) to afford **128** (0.65 g, 65%) as a white solid. Data for compound **128**: ^{1}H NMR (300MHz, DMSO) δ 8.45 (d, 1H, J=7.4Hz), 8.00 (d, 1H, J=8.5Hz), 7.64 (s, 1H), 7.47-7.40 (m, 3H), 6.92 (d, 1H, J=4.7Hz), 5.95 (d, 1H, J=5.1Hz), 5.38 (s, 1H), 4.63 (dd, 1H J=2.4Hz, 13.4Hz), 4.12 (dd, 1H J=9.0Hz, 13.4Hz), 2.20 (s, 3H); ^{13}C NMR (300Hz, DMSO) δ 178.5, 166.5, 140.5, 138.2, 137.5, 129.1, 124.9, 124.5, 123.5, 123.4, 122.8, 107.6, 66.8, 54.7, 27.0; MS(ESI): 319 [M+H]$^+$; HR ESIMS calculated for $C_{15}H_{15}O_2S_2N_2^+$=319.0575; found= 319.05759.

Compound 129. 128 (0.63 mmol, 0.2g) was added in small portion to 2 ml of thionyl chloride at 5 ℃ over a period of 30 min. The mixture was stirred at room temperature for 1 h, Ac$_2$O (10 ml) was added, and the acetyl chloride which formed was removed under vacuum. The mixture was refluxed for another 0.5 h and the excess Ac$_2$O was removed under vacuum. The residue was washed by 10% Na$_2$CO$_3$ solution and extracted with DCM. The DCM layer was dried with MgSO$_4$ and the solvent was removed to leave a solid which was purified by flash chromatography (EtOAc) affording **129** (0.07 g, 43%) as a white solid. Then **129** was directly dissolved in 2 ml methanol and 37% hydrochloric acid in water was added. The mixture was stirred overnight and the solvent was removed to leave a slight green solid. After washing with acetone and dried, the hydrochloride salt of **129** was obtained. Data for compound **129.HCl**: ^{1}H NMR (300MHz, DMSO) δ 7.87 (dd, 1H, J=2.1Hz, 7.7Hz), 7.70 (dd, 1H, J=2.5Hz, 6.6Hz), 7.45 (s, 1H), 7.41-7.32 (m, 2H), 6.48 (d, 1H, J=4.5Hz), 5.90 (t, 1H), 5.77 (d, 1H, J=4.5Hz), 4.31 (t, 1H), 3.78 (t, 1H); ^{13}C NMR (300Hz, DMSO) δ 170.6, 141.6, 138.2, 137.5 124.8, 124.5, 123.6, 123.2, 122.8, 121.9, 102.1, 71.1 53.2; MS(ESI): 259 [M+H]$^+$; HR ESIMS calculated for $C_{13}H_{11}S_2N_2^+$=259.0364; found= 259.03637.

Compound 130. 2-Aminothiazoline (11.8 mmol, 1.2 g) was dissolved in 25 ml acetonitrile and small portions of 3-(2-bromoacetyl)benzo[b]thiophene **125** (11.8 mmol, 3 g) was added. The mixture was stirred at r.t. for 2 h and filtered. The precipitate was macerated with a 10% Na$_2$CO$_3$ solution then filtered and dried. The crude product was purified by flash chromatography (EtOAc) to afford **130** (2.88 g, 88.6%) as a white solid. Data for compound **130**: ^{1}H NMR (300MHz, DMSO) δ 9.08 (s, 1H), 8.59 (dd, 1H, J=1.5Hz, 7.7Hz), 8.10 (dd, 1H, J=1.1Hz, 8.5Hz), 7.55-7.44 (m, 2H), 4.85 (s, 2H), 3.72 (t,2H), 3.23 (t,2H); ^{13}C NMR (300Hz, DMSO) δ 191.0, 161.9, 139.8, 139.5, 136.6, 132.5, 126.2, 125.8, 124.9, 123.3, 52.5, 52.0, 27.2; MS(ESI): 277 [M+H]$^+$; HR ESIMS calculated for $C_{13}H_{13}OS_2N_2^+$=277.0469; found= 277.04684.

Compound 131. To a mixture of **130** (10.4 mmol, 2.88g) and 5 ml of pyridine in 50 ml of chloroform was added 2 ml of acetic anhydride. The mixture was refluxed for 1.5 h and the chloroform was removed to leave an oil. Then the residue was washed by ethyl ether and purified by flash chromatography (EtOAc) to afford **131** (2.52 g, 76%) as a brown solid. Data for compound **131:** ^{1}H NMR (300MHz, DMSO) δ 9.15 (s, 1H), 8.57 (dd, 1H, $J = 1.5$Hz, 8.7Hz), 8.12 (dd, 1H, $J = 1.3$Hz, 8.5Hz), 7.55-7.46 (m, 2H), 5.20 (s, 2H), 3.76 (t, 2H), 3.22 (t, 2H); ^{13}C NMR (300Hz, DMSO) δ 188.8, 180.7, 170.0, 140.6, 139.5, 136.5, 132.0, 126.3, 125.9, 124.8, 123.4, 54.0, 50.4, 27.5, 27.0; MS(ESI): 319 [M+H]+; HR ESIMS calculated for $C_{15}H_{15}O_2S_2N_2^+$=319.0575; found= 319.05751.

Compound 132. To a solution of **131** (4.7 mmol, 1.5 g) in 25 ml of methanol maintained at 10 ºC was added in small portions 5 mmol of NaBH$_4$. The solution was stirred at room temperature for 2 h, solvent was removed under vacuum, and the residue was suspended in water and extracted with DCM. The DCM layer was dried with MgSO$_4$ and the solvent was removed to leave a solid which was purified by flash chromatography (EtOAc/MeOH = 95/5) to afford **132** (0.6 g, 40%) as a yellowish solid. Data for compound **132:** ^{1}H NMR (300MHz, DMSO) δ 8.31 (d, 1H, J=7.2Hz), 7.99 (d, 1H, $J = 7.1$Hz), 7.63 (s, 1H), 7.45-7.35 (m, 2H), 5.89 (d, 1H, $J = 34.9$), 5.35 (s, 1H), 4.12 (q, 1H), 3.95 (q, 1H) 3.70 (q, 1H), 3.47 (q, 1H) 3.15-3.06 (m, 2H), 2.18 (s, 3H); ^{13}C NMR (300Hz, DMSO) δ 180.4, 169.9, 140.5, 138.8, 137.5, 124.8, 124.3, 123.3, 123.2, 122.9, 67.5, 54.0, 51.7, 27.4, 27.1; MS(ESI): 321 [M+H]$^+$; HR ESIMS calculated for $C_{15}H_{16}O_2S_2N_2Na^+$=343.0551; found= 343.05518.

Compound 133. A solution of **132** (0.63 mmol, 0.2g) in 15ml of chloroform was added to 2 ml of thionyl chloride at 5°C over a period of 30 min. The mixture was stirred at room temperature for 2 h, 20 ml of NaOH solution (1 M) was added, and the mixture was refluxed for 1 h. Organic layer was dried by MgSO$_4$, then filtered and the solvent removed. The residue was purified by flash chromatography (DCM/EtOAc = 1/1) to afford **133** (35 mg, 21.5%) as a milky solid. Then **133** was dissolved in 2 ml methanol and 37% hydrochloric acid in water was added. The mixture was stirred overnight and the solvent was removed to leave a slight grey solid. After washing with acetone and dried, the hydrochloride salt of **133** was obtained. Data for compound **133.HCl:** ^{1}H NMR (300MHz, DMSO) δ 7.86 (dd, 1H, J=2.8Hz, 7.0Hz), 7.74 (dd, 1H, J=2.1Hz, 6.0Hz), 7.46 (s, 1H), 7.40-7.32 (m, 2H), 5.85 (t, 1H), 3.85 (t, 1H), 3.74-3.56 (m, 2H), 3.44 (t, 1H), 3.23(q, 2H); ^{13}C NMR (300Hz, DMSO) δ 138.6, 123.3, 123.2, 122.5,

121.4, 47.8, 33.6, 30.9, 28.7, 28.6, 28.4, 21.7, 13.1; MS(ESI): 261 [M+H]$^+$; HR ESIMS calculated for $C_{13}H_{12}S_2N_2$=261.0520; found= 261.05207.

Screening test. To screen putative inhibitors, activity of BIAP as well as that of porcine kidney TNAP were measured in 25 mM piperazine, 25 mM glycylglycine, 5 mM $MgCl_2$, 5 µM $ZnCl_2$ at pH 10.4 and at 37°C.[58] The mixtures containing the buffer, BIAP (0.1-0.3 µgmL^{-1}), or TNAP (4-6 µgmL^{-1}), and the inhibitors (0.1mM for BIAP with final DMSO 1% (v/v), 0.4mM for TNAP with final DMSO 4% (v/v)) were incubated for 10 min at 37 °C without pNPP. Then, 0.05 mM pNPP was added at the last minute to initiate the reaction. The activity was quantified at 420 nm, using a molar absorption coefficient of 18.6 cm^{-1}mM^{-1} at pH 10.4.

Inhibition of the best benzothiophene inhibitor on BIAP and matrix-vesicle TNAP activity. From the screening test, the best benzothiophene inhibitor was selected. Its activity was measured at pH 10.4 and at 37°C in the presence of either 0.2 µgmL^{-1} BIAP or 10 µgmL^{-1} matrix vesicles (MVs) with 0.1 mM pNPP. The concentrations of inhibitor (0-1.2 mM) are indicated in Figure 1. MV-protein concentration was determined by the method of Bradford.[59] MV extracellular organelles produced by chondrocytes, osteoblasts and odontoblasts[45,60] initiate normal skeletal calcification and are characterized by high TNAP activity.[13,14] Collagenase released MVs were isolated from bone and epiphyseal cartilage slices of 17-day-old chicken embryos according to Balcerzak et al.[61]

Determination of the inhibition constant in physiological pH. To determine the inhibition constant K_i of the soluble inhibitors, porcine kidney TNAP activity was measured in 0.1 M Tris-HCl buffer with 5 mM $MgCl_2$ and 5 µM $ZnCl_2$ at pH 7.8 and at 37°C. The mixtures containing the buffer, TNAP (6 µg ml^{-1}), and the inhibitors (from 100 to 500 µM) were incubated for 10 min at 37 °C without pNPP. Then, pNPP was added at the last minute to initiate the reaction. The concentrations of pNPP were 10 µM, 20 µM, 40 µM, 100 µM and 1000 µM, respectively. The change in absorbance of released p-nitrophenolate chromophore was monitored at 420 nm, using a molar absorption coefficient of 9.2 cm^{-1}mM^{-1} at pH 7.8. In all cases, one unit of the alkaline phosphatase activity (U) was defined as the amount of enzyme hydrolysing 1µmol of pNPP per min under described conditions. All the experiments were repeated three times in an independent manner.

Acknowledgements

REFERENCES

(1) Sun, Y.; Anley, E. N. Jr. Calcium-containing crystals and osteoarthritis. *Curr. Opin. Orthop.* **2007**, 18, 472-477.

(2) Rosenthal, A.K. Update in calcium deposition diseases. *Curr. Opin. Rheumatol.* **2007**, 19, 158-162.

(3) Molloy, E.S.; McCarthy, G. M. Basic calcium phosphate crystals: pathways to joint degeneration. *Curr. Opin. Rheumatol.* **2006**, 18, 187-192.

(4) Rosenthal, A. K. Calcium crystal deposition and osteoarthritis. *Rheum. Dis. Clin. North. Am.* **2006**, 32, 401-412.

(5) Gordon, G. V.; Villanueva, T.; Schumacher, H. R; Gohel, V. Autopsy study correlating degree of osteoarthritis, synovitis and evidence of articular calfication. *J. Rheumatol.* **1984**, 11, 681-688.

(6) Carroll, G. J.; Stuart, R. A.; Armstrong, J. A.; Breidhahl, P. D.; Laing, B. A. Hydroxyapatite crystals are a frequent finding in osteoarthritis synovial fluid, but are not related to increased concentrations of keratan sulfate or interleukin 1beta. *J. Rheumatol.* **1991**, 18, 861-866.

(7) Derfus, B. A.; Kurian, J.B.; Butler, J.J.; Daft, L. J.; Carrera, G. F.; Ryan, L. M.; Rosenthal, A. K. The high prevalence of pathologic calcium crystals in preoperatives knees. *J. Rheumatol.* **2002**, 29, 570-574.

(8) Nalbant, S.; Martinez, J. A. ; Kitumnuaypong T. ; Clayburne, G. ; Sieck, M. ; Schumacher, H. R. Jr. Synovial fluid features and their relations to osteoarthritis severity: new findings from sequential studies. *Osteoarthritis Cartilage* **2003**, 11, 50-54.

(9) Johnson, K.; Terkeltaub, R. Inorganic pyrophosphate (PPI) in pathologic calcification of articular cartilage. *Front Biosc.* **2005**, 10, 988-997.

(10) Williams C. J. Familial calcium pyrophosphate dihydrate deposition disease and the ANKH gene. *Curr. Opin. Rheumatol.* **2003**, 15, 326-331.

(11) Netter, P.; Bardin, T.; Bianchi, A.; Richette, P.; Loeuille, D. The ANKH gene and familial calcium pyrophosphate dihydrate deposition disease. *Joint Bone Spine* **2004**, 71, 365-368.

(12) Ali, S. Y. Apatite crystal nodules in arthritic cartilage. *Eur. J. Rheumatol. Inflam.* **1978**, 1, 115-119.

(13) Golub, E. E.; Boesze-Battalgia, K. The role of alkaline phosphatase in mineralization. *Curr. Opin. Orthop.* **2007**, 18, 444-448.

(14) Balcerzak, M.; Hamade, E.; Zhang, L.; Pikula, S.; Azzar, G.; Radisson, J. Bandorowicz-Pikula, J.; Buchet R. The roles of annexins and alkaline phosphatase in mineralization process. *Acta Biochim. Pol.* **2003**, 50, 1019-1038.

(15) Van Belle, H. Alkaline Phosphatase. I Kinetics and inhibition by levamisole of purified isoenzymes from humans. *Clin. Chem.* **1976**, 22, 158-168.

(16) Schuermans, Y. Levamisole in rheumatoid arthritis. *Lancet* **1975**, 1(7898), 111.

(17) McGill, P. E. Levamisole in rheumatoid arthritis. *Lancet* **1976**, 2, 149.

(18) Miller, B. ; de Merieux, P.; Srinivasan, R.; Clements, P. ; Fan, P. ; Levy, J. ; Paulus, H. E. Double-blind placebo-controlled cross-over evaluation of levamisole in rheumatoid arthritis. *Arthritis Rheum.* **1980**, 23, 172-82.

(19) Rosenthal, M.; Breysse, Y.; Dixon, A.S.; Franchimont, P.; Huskisson, E. C.; Schmidt, K. L.; Schuermans, Y.; Veys, E.; Vischer, T. L.; Janssen, P. A.; Brugmans, J.; de Crepe, J.; Symoens, J.; Macnair, A. L.; Amery W.K., Veys E. Levamisole and agranulocytosis. *Lancet* **1977**, 1(8017), 904-905.

(20) Mielants, H.; Veys, E. M. A study of the haematological side-effects of

Levamisole in rheumatoid arthritis with recommendations. *J. Rheumatol.* **1978**, 5 suppl. 4, 77-83.

(21) Raeymaekers, A. H. M.; Allewinjn, F. T. N.; Vandenberk, J.; Demoen, P. J. A.; Van Offenwert, T. T. T.; Janssen Novel broad-spectrum anthelmintics. Tetramisole and related derivatives of 6-arylimidazo[2,1-*b*]thiazole. *J. Med. Chem.* **1966**, 9, 545-551.

(22) Bhargava, K. K.; Lee, M. H.; Huang, Y.-M.; Cunningham, L. S.; Agrawal, K. C.; Sartorelli, A. C tetramisole Analogues as inhibitors of alkaline phosphatase, an enzyme involved in the resistance of neaplastic cells to 6-thiopurines. *J. Med. Chem.* **1977**, 20, 563-566.

(23) Collington, E. W.; Middlemiss, D.; Panchal, T. A.; Wilson, D. A convenient synthesis of 4-(2-pyridyl)imidazolidine-2-thiones by the rearrangement of imidazo[1,5-a]pyridine -3-thione. *Tetrahedron Lett.* **1981**, 22, 3675-3678.

(24) Kumar, D. S.; Rashmi, R.; Satyavan, S. Synthesis of 2-substituted benzothiazoles as tetramisole analogs. *Monatsh. Chem.* **1981**, 112, 1387-1391.

(25) Nielek, S.; Tadeusz, L. 2,3,5,6-tetrahydro-6-(3-methylbenzofuran-2-yl) imidazo[2,1-*b*] thiazole. *Chem. Ber.* **1982**, 115, 1247-1251.

(26) Jones, G. S.; Hanson, R. N.; Davis, M. A. Selenium-sulfur analogs.Selenoisosteres of levamisole. *J. Hetero. Chem*. **1983**, 20, 523-526.

(27) Gouesnard, J.-P. Sodium nitrite reactivity. Part 3. Reaction with levamisole. *J. Chem. Soc. Perkin trans. 1* **1986**, 1901-1903.

(28) Brewer, M. D. ; Dorgan, J. J.; Manger, B. R.; Mamalis, P.; Webster, A. B. Isothiourea derivatives of 6-phenyl-2,3,5,6-tetrahydroimidazo[2,1-*b*]thiazole with broad-spectrum anthelmintic activity. *J. Med. Chem.* **1987**, 30, 1848-1853.

(29) Amarouch, H.; Loiseau, P. R.; Bonnafous, M.; Caujolle, R. ; Payard, M. ; Loiseau,

P. M.; Bories, C.; Gayral, P. 5,6-dihydroimidazo[2,1-b]thiazoles and 2,3-dihydroimidazo[2,1-*b*] benzothiazoles, analogs of levamisole. *Farm. Ed. Sci.* **1988**, 43, 421-437.

(30) Metaye, T.; Mettey, Y.; Lehuede, J.; Vierfond, J.-M.; Lalegerie, P. Comparative inhibition of human alkaline phosphatase and diamine oxidase by bromo-levamisole, cimetidine and various derivatives. *Biochem. Pharm.* **1988**, 37, 4263-4268.

(31) Weikert, R. J.; Bingham, S.; Emanuel, M. A.; Fraser-Smith, E. B.; loughhead, D. G.; Nelson, P. H.; Poulton, A. L. Synthesis and anthelmintic activity of 3'-benzoylurea derivatives of 6-phenyl-2,3,5,6-tetrahydroimidazo[2,1-*b*]thiazole. *J. Med. Chem.* **1991**, 34, 1630-1633.

(32) Comley, J. C. W.; Gutteridge, W. E.; Hudson, A. T.; Jenkins, D. C.; Miller, D. D.; Nicol, R. H.; Randall, A. W.; Stables, J. N.; Thornton, R. Synthesis and anti-filarial activity of 6-(-3-aminophenyl)-2,3,5,6-tetrahydroimidazo[2,1-*b*]thiazole derivatives. *Eur. J. Med. Chem.* **1992**, 27, 503-509.

(33) Kaugars, G.; Martin, S. E.; Nelson, S. J.; Watt, W. Synthesis of 2,3,5,6-tetrahydroimidazo[2,1-*b*]thiazoles. *Heterocycles* **1994**, 38, 2593-2603.

(34) Fournier Dit Chabert, J.; Joucla, L.; David, E.; Lemaire, M. An efficient phosphine-free palladium coupling for the synthesis of new 2-arylbenzo[*b*]thiophenes. *Tetrahedron* **2004**, 60, 3221-3230.

(35) David, E.; Perrin, J.; Pellet-Rostaing, S.; Fournier Dit Chabert, J.; Lemaire, M. Efficient acess to 2-aryl-3-substituted benzo[*b*]thiophenes. *J. Org. Chem.* **2005**, 70, 3569-3573.

(36) Fournier Dit Chabert, J.; Chatelain, G.; Pellet-Rostaing, S.; Bouchu, D.; Lemaire, M. Benzo[*b*]thiophene as a template for substituted quinolines and tetrahydroquinolines. *Tetrahedron Lett.* **2006**, 47, 1015-1018.

(37) David, E.; Rangheard, C.; Pellet-Rostaing, S.; Lemaire, M. Synthesis of

benz[*c*]benzothiopheno[2,3-*e*]azepine via Heck-type coupling and Pictet-Spengler reaction. *Synlett* **2006**, 13, 2016-2020.

(38) David, E.; Pellet-Rostaing, S.; Lemaire, M. Heck-like coupling and Pictet-Spengler reaction for the synthesis of benzothieno[3,2-*c*]quinolines. *Tetrahedron* **2007**, 63, 8999-9006.

(39) Fournier Dit Chabert, J.; Marquez, B.; Neville, L. ; Joucla, L. ; Broussous, S. ; Bouhours, P. ; David, E. ; Pellet-Rostaing, S. ; Marquet, B. ; Moreau, N. ; Lemaire, M. Synthesis and evaluation of new arylbenzo[*b*]thiophene and diarylthiophene derivatives as inhibitors of the NorA multidrug transporter of *staphylococcus aureus.* *Bioorg. Med. Chem.* **2007**, 15, 4482-4497.

(40) Nakamura, I.; Sato, T.; Tamamoto, Y. Gold-catalyzed intramolecular carbothiolation of alkynes: synthesis of 2,3-disubstituted benzothiophenes from (α-alkoxy alkyl) (ortho-alkynyl phenyl) sulfides. *Angew. Chem. Int. Ed.* **2006**, 45, 4473-4475.

(41) Conley, R. A., Heindel, N. D. Thianaphthen-2-one chemistry: the benzylidene thiolactone rearrangement: synthesis of 2-arylthianaphthene-3-carboxylic acids and esters. *J. Org. Chem.* **1976**, 41, 3743-3746.

(42) Al Nakib, T.; Meegan, M. J.; Burke, M. L. Synthesis of 1- [2 - benzo[*b*]thiophene - 3 - yl) - 2 - benzyloxyethyl] - 1H - imidazole and 1- [2- benzo[*b*]thiophene - 3 - yl) - 2 - benzyloxyethyl] - 1H -1,2,4 - triazole with antifungal activity. *J. Chem. Res.* **1994**, 1037-1045.

(43) Li, L.; Buchet, R.; Wu, Y.   Dimethyl sulfoxide-induced hydroxyapatite formation: A biological model of matrix vesicle nucleation to screen inhibitors of mineralization. *Anal. Biochem.* **2008**, 381, 123-128.

(44) Kirsch, T.; Nah, H.D.; Shapiro, IM.; Pacifici, M. Regulated production of mineralization-competent matrix vesicles in hypertrophic chondrocytes. *J. Cell. Biol.* **1997**, 137, 1149-1160.

(45) Anderson, H. C. Molecular biology of matrix vesicles. *Clin. Orthop. Relat. Res.* **1995**, 314, 266-280.

(46) Anderson, H. C.; Garimella, R.; Tague, S. E. The role of matrix vesicles in growth plate development and biomineralization. *Front Biosci.* **2005**, 10, 822-837.

(47) Pritzker, K.P. Crystal-associated arthropathies: what's new in old joints. *J. Am. Geriatr. Soc.* **1980**, 28, 439-45.

(48) Ali, S. Y. Apatite-type crystal deposition in arthritic cartilage. *Scan Electron Microsc.* **1985**, 4, 1555-1566.

(49) Anderson, H.C. Mechanisms of pathologic calcification. *Rheum. Dis. Clin. North. Am.* **1988**, 14, 303-319.

(50) Anderson, H. C. Matrix vesicles and calcification. *Curr. Rheumatol. Rep.* **2003**, 5, 222-226.

(51) Santos, N. C.; Figueira-Coelho, J.; Martins-Silva, J.; Saldanha C. Multidisciplinary utilisation of dimethyl sulfoxide: pharmacological, cellular and molecular aspects. *Biochemical Pharmacology* **2003**, 65 , 1035-1041.

(52) Pérez-Pastén, R.; Martinez-Galero, E.; Garduno-Siciliano, L.; Conde Lara, I.; Chamorro Cevallos G. Effects of dimethylsulfoxide on mice arsenite-induced dysmorphogenesis in embryo culture and cytoxicity in embryo cells. *Toxicology Letters* **2006**, 161, 167-173.

(53) Mereghetti, I.; Cagnotto, A.; Mnnini. T. Dimethyl sulfoxide: An antogonist in scintillation proximity assay [35S]-GTPgS binding to rat 5-HT6 receptor cloned in HEK-293 cells? *J. Neuroscience Methods* **2007**, 160, 251-255.

(54) Fossum, E. N.; Lisowski, M. J.; Macey, T. A.; Ingram, S. L.; Morgan. M. M. Microinjection of the vehicule dimethyl sulfoxide (DMSO) into the periaqueductal gray modulates morphine antinociception. *Brain Research* **2008** 1204, 53-58.

(55) Narisawa, S.; Harmey, D.; Yadav, M. C.; O'Neill, W. C.; Hoylaerts, M. F.; Millán J. L. Novel Inhibitors of Alkaline Phosphatase Suppress Vascular Smooth Muscle Cell Calcification. *J. Bone Min. Res.* **2007**, 22, 1700-1710.

(56) A. Kozlenkov, A.; Le Du, M. H.; Cuniasse, P.; Ny, T.; Hoylaerts, M. F.; Millan, J. L. Residues determining the binding specificity of uncompetitive inhibitors to tissue-Nonspecific alkaline phosphatase. *J. Bone Min. Res.* **2004**, 19, 1862-1871.

(57) Tsumura, M; Ueno, Y; Kinouchi, T; Koyama, I; Komoda, T. Atypical alkaline phosphatase isozymes in serum and urine of patients with renal failure. *Clinica Chimica Acta* **2001** 312, 169-178.

(58) Cyboron, G. W.; Wuthier, R. E. Purification and initial characterization of intrinsic membrane-bound alkaline phosphatase from chicken epiphyseal cartilage. *J. Biol. Chem.* **1981**, 256, 7262-7268.

(59) Bradford, M. M. A rapid and sensitive method for the quantitation of microgram quantities of protein utilizing the principle of protein-dye binding. *Anal. Biochem.* **1976**, 72, 248-254.

(60) Anderson, H. C. The role of matrix vesicles in physiological and pathological calcification *Curr. Opin. Orthop.* **2007**, 18, 428-433.

(61) Balcerzak, M.; Radisson, J.; Azzar, G.; Farlay, D.; Boivin, G.; Pikula, S. Buchet, R. A comparative analysis of   strategies for isolation of matrix vesicles. *Anal. Biochem.* **2007**, 361, 176-182.

DMSO-induced hydroxyapatite formation: A biological model of matrix-vesicle nucleation to screen inhibitors of mineralization

Lina Li[1,2], René Buchet[1*] and Yuqing Wu[2]

[1] Université de Lyon, Villeurbanne, F-69622, France; Université Lyon 1, Villeurbanne, F-69622, France; INSA-Lyon, Villeurbanne, F-69621, France; CPE Lyon, Villeurbanne, F-69616, France; CNRS UMR 5246 ICBMS, Villeurbanne, F-69622, France.

[2]State Key Laboratory for Supramolecular Structure and Materials, Jilin University, ChangChun, 130012, China.

RUNNING HEAD: DMSO-induced hydroxyapatite and screening test

ABSTRACT

To elucidate the inhibition mechanisms of hydroxyapatite (HA), a biological model mimicking the mineralization process was developed. Addition of DMSO (4% v/v) in synthetic cartilage lymph (SCL) medium containing 2 mM calcium and 3.42 mM inorganic phosphate at pH 7.6 and 37 °C produced HA as matrix vesicles (MVs) under physiological conditions. Such a model has the advantage to monitor HA nucleation process, without interfering with other processes at cellular or enzymatic levels. Turbidity measurements allowed us to follow the process of nucleation, while infrared spectra and X-ray diffraction permitted us to identify HA. Mineral formation induced by DMSO and by MVs in the SCL medium, produced crystalline HA in a similar manner. The nucleation model served to evaluate the inhibition effects of ATP, GTP, UTP, ADP, ADP-ribose, AMP and pyrophosphate. 10 µM pyrophosphate, 100 µM nucleotide triphosphate (ATP, GTP, UTP) and 1 mM ADP inhibited HA formation directly, while 1 mM ADP-ribose and 1 mM AMP did not. This confirmed that the pyrophosphate group, is a potent inhibitor of HA formation. Increasing pyrophosphate concentration from 100 µM to 1 mM induced calcium pyrophosphate dihydrate. We propose that DMSO-induced HA formation could serve to screen putative inhibitors of mineral formation.

Introduction

The search for specific inhibitors of mineralization necessitates a biological assay that mimics the initiation of mineral formation under physiological conditions. The biological mineralization is controlled by the cell and involves a fine balance between stimulatory and inhibitory factors [1]. To initiate the mineralization process, the cell has to be "mineralization competent". For example, only mature osteoblasts and terminally differentiated growth-plate chondrocytes undergo mineralization events [1]. The mineralization is initiated inside vesicles, either after secretion like matrix vesicles (MVs) or apoptotic bodies or before their secretion, inside the cell. Cell necroses may release mineralizable vesicles [2]. Cells undergoing pathological mineralization are reminiscent of osteoblast or chondrocyte-phenotype, expressing several proteins, necessary for mineralization [3]. Many secreted matrix proteins are involved in the initiation and directional growth of the mineral phase. Calcium and phosphate in metastable equilibrium can induce mineralization [3]. MVs are released from mineralization competent osteoblasts, odontoblasts and hypertrophied chondrocytes [4]. They are extracellular microstructures serving as sites for calcium and inorganic phosphate (P_i) accumulation followed by the formation of hydroxyapatite (HA) initiating mineralization in newly forming bone [5]. Since Ca^{2+}-binding annexins (AnxA1, AnxA2, AnxA5, AnxA6, AnxA11) are relatively abundant proteins in MVs [6-9], among them AnxA5 and AnxA6 are effective stimulators of mineral formation [10-12]. Alkaline phosphatase, also an enriched MV protein, in the presence of phosphomonoester substrates and calcium was able to initiate HA [13]. Several acidic proteins in the extracellular matrix such as bone salioprotein (BSP) [14-18], dentin phosphophoryn (DPP) [16,19], dentin matrix protein 1 (DMP1) [20], osteopontin [21], bone matrix gelatin [22] are potent nucleators of HA. It has been proposed that acidic proteins, as in the case of sericin, due to their negatively charged carboxylate groups are effective in the nucleation of HA and therefore nucleation is sensitive to the structural arrangement of carboxylate groups [23]. Phospholipids in Ca^{2+} and Pi containing synthetic cartilage lymph may stimulate Ca^{2+} acidic phospholipid complex [24], while phosphatidylserine in supersaturated calcium phosphate solutions promoted the formation of octacalcium phosphate [25]. Stabilization of the interaction between Ca^{2+} and negatively charged residues of phospholipids may favor the nucleation of HA. The aim of our work was to develop a nucleation model of

hydroxyapatite (HA; $Ca_{10}[PO_4]_6[OH]_2$) formation, which could serve to screen putative inhibitors of hydroxyapatite formation and to elucidate the mechanisms of inhibition. Since several inhibitors of HA formation can interact with enzymes and lipids, as substrates or ligands, we designed a nucleation model without proteins or lipids to monitor solely the inhibitory effect on the HA formation. Dimethyl sulfoxide has been used to treat arthritic disorders [26-29], and as a carrier to aid penetration of medicines in the skin [30-32]. We found that addition of DMSO (4% v/v) in synthetic cartilage lymph (SCL) medium containing calcium and inorganic phosphate produced hydroxyapatite as matrix vesicles. The nucleation model served to evaluate the inhibition effects of nucleotide derivatives such as ATP, GTP, UTP, ADP, ADP-ribose, AMP and pyrophosphate (PP_i), several of which are substrates for tissue non-specific alkaline phosphatase, ATPases, nucleotide triphosphate pyrophosphatase, phosphodiesterase 1, enzymes that are present in MVs. We showed that ATP, GTP, UTP, ADP and pyrophosphate inhibited directly HA formation, confirming that the HA inhibition by nucleotide triphosphates is not only caused by PPi, produced by the MV enzymes, but also by the nucleotide itself. We found that ADP-ribose and AMP did not inhibit HA formation, indicating that pyrophosphate moiety with a free phosphomonoester group was involved in the molecular mechanism of inhibition by nucleotides.

EXPERIMENTAL SECTION

Materials. Dimethyl sulfoxide (DMSO), a spectrophotometric grade solvent, ATP, ADP, AMP, ADP-ribose, GTP, UTP and pyrophosphate were purchased from Sigma-Aldrich.

Extraction of matrix vesicles. Collagenase-released MVs were isolated from bone and epiphyseal cartilage slices of 17-day-old chicken embryos according to Balcerzak et al [33]. Slices of bone tissues were digested at 37°C for about 3h in a synthetic cartilage lymph containing 2mM Ca^{2+} and collagenase (type IA, ICN Biomedicals Inc., 200 units/g of tissue with a volume of 4mL/g of tissue). The synthetic cartilage lymph (SCL) mimics physiological conditions [34] and its composition was 1.42mM NaH_2PO_4, 100 mM NaCl, 63.5 mM sucrose, 16.5 mM TES, 12.7 mM KCl, 5.55 mM D-glucose, 1.83 mM $NaHCO_3$, 0.57 mM $MgCl_2.6H_2O$ and 0.57 mM Na_2SO_4, pH 7.6. The partially

digested tissue was vortexed, and the suspension was centrifuged at 13,000 × g for 20 min at 4°C (centrifuge Beckman J32B, rotor JA20). The pellet was discarded, and the suspension was centrifuged again at 80,000 × g for 1 h at 4°C (centrifuge Kontron TGA, rotor 6538). The MV pellet was suspended as a stock suspension of 1.0 mg of vesicle protein/mL in SCL at 4°C for further use. Protein concentration in the vesicles was determined by the method of Bradford [35].

Mineralization assay. Light scattering [10,36] was employed for real time measurement of mineral formation induced by DMSO and MV. Different concentrations of DMSO (v/v) were added in SCL medium. MVs were suspended in SCL to a final concentration of 30μg of MV protein/mL. Different ions (Ca^{2+}, P_i, PP_i), substrates (AMP, ADP, ADP-ribose, ATP, GTP, UTP) were added and vortexed into the SCL medium to a total volume of 1ml. Their respective concentrations are indicated in the figure legends. The samples were then incubated at 37°C in the cuvettes without mixing, and the light scattering was read at 340 nm at a 15-min interval. Each experiment was repeated at least three times.

Identification of mineral complexes by infrared spectroscopy. From the mineralization assay, the formed minerals were centrifuged and washed three times with water, then dried under N_2. Dry material (1-4 mg) was incorporated into KBr (100 mg) to obtain pellets. The infrared spectra were measured by means of a Nicolet FITR spectrometer model 510 M. The optical resolution was 4 cm^{-1} and 128 scans were recorded. At least three independent infrared measurements were made and one IR spectrum was shown.

Identification of mineral complexes by X-ray diffractometry. To obtain a sufficient quantity of crystalline HA, 2ml solution with 4 % (v/v) DMSO in SCL medium containing 2mM Ca^{2+}, 3.42mM P_i, 5ml solution with 30μg/mL MVs protein, in the identical SCL medium were prepared. All the samples were incubated at 37 ºC for 48h. Mineral samples were centrifuged, washed and dried under similar conditions as infrared measurement. They were analyzed with a Bruker D8 Advance diffractometer using copper Kα radiation. It was compared with the standard data of HA from ICDD (International Centre for Diffraction Data), PDF (Powder Diffraction File) number 01-089-4405. The diffractometer was equipped with a VÅNTEC-1 Detector and a

geometrical goniometer (Theta-Theta). Diffraction angle 2θ was comprised between 4.5º and 70º. The voltage and current intensity were 33 kV and 45 mA, respectively. X-ray analysis was performed in the Henri Longchambon diffractometer centre in the University of Lyon 1, Villeurbanne, France. Two independent X-ray measurements for the MV-induced minerals and three independent X-ray measurements for the DMSO-induced minerals were performed.

Results and discussion

DMSO-induced formation of hydroxyapatite as matrix vesicles. Mineral formation was assessed by light scattering at 340nm, reflecting mineralization [10,36]. The observed induction time of turbidity of 30µg protein/mL MVs incubated in SCL medium containing 2mM Ca^{2+}, 3.42mM P_i was about 40-60 min (Fig 1A) as reported elsewhere [37]. The increase in the turbidity was solely associated with mineral formation since MVs without calcium or phosphate did not induce any turbidity. In the absence of MVs, SCL medium containing 2mM Ca^{2+} and 3.42mM P_i did not mineralize after several hours [37]. Replacement of MVs by 4 % (v/v) DMSO in SCL medium containing 2mM Ca^{2+}, 3.42mM P_i produced mineral formation as probed by the increase in turbidity (Fig. 1A). To confirm that the increase in the turbidity during incubation in SCL medium was not induced by the formation of amorphous minerals, minerals formed after 20h incubation were analyzed by infrared spectroscopy (Fig. 1B). The mineral amounts formed in SCL medium in the presence of MVs (Fig. 1B bottom trace) or in the presence of 4% (v/v) DMSO (Fig. 1B top trace) were identical. Their infrared spectra indicated unambiguously crystalline hydroxyapatite (HA) (Fig. 1B) as revealed by the characteristic HA bands located at 562 cm^{-1}, 602 cm^{-1}, 961 and 1033 cm^{-1} and around 1090-1111 cm^{-1} [38,39]. Mineral crystalline structures induced by 4 % (v/v) DMSO (Fig. 1C, trace *i*) and by 30µg/mL MVs protein (Fig. 1C, trace *ii*) both in SCL medium containing 2mM Ca^{2+}, 3.42mM P_i were analyzed by X-ray diffraction. Both exhibited diffraction peaks at 2θ = 26º, 32º, 40º, 47º, 50º, 53º, and around 64º (Fig.1C trace *i* and trace *ii*), which matched almost exactly the positions of peaks in the standard spectra of HA (ICDD: PDF 01-089-4405) (Fig.1C trace *iii)*. This indicated that the crystalline HA was formed in both systems. In the case of mineral induced by MVs, there was a broad band around 16º to 22º and a peak at 29.25º 2θ which could be due to a small quantity of brushite or octacalcium phosphate formed during the

mineralization process. The broad band was also observed in the case of mineral produced by MVs after a 16-hour incubation in SCL medium [12].
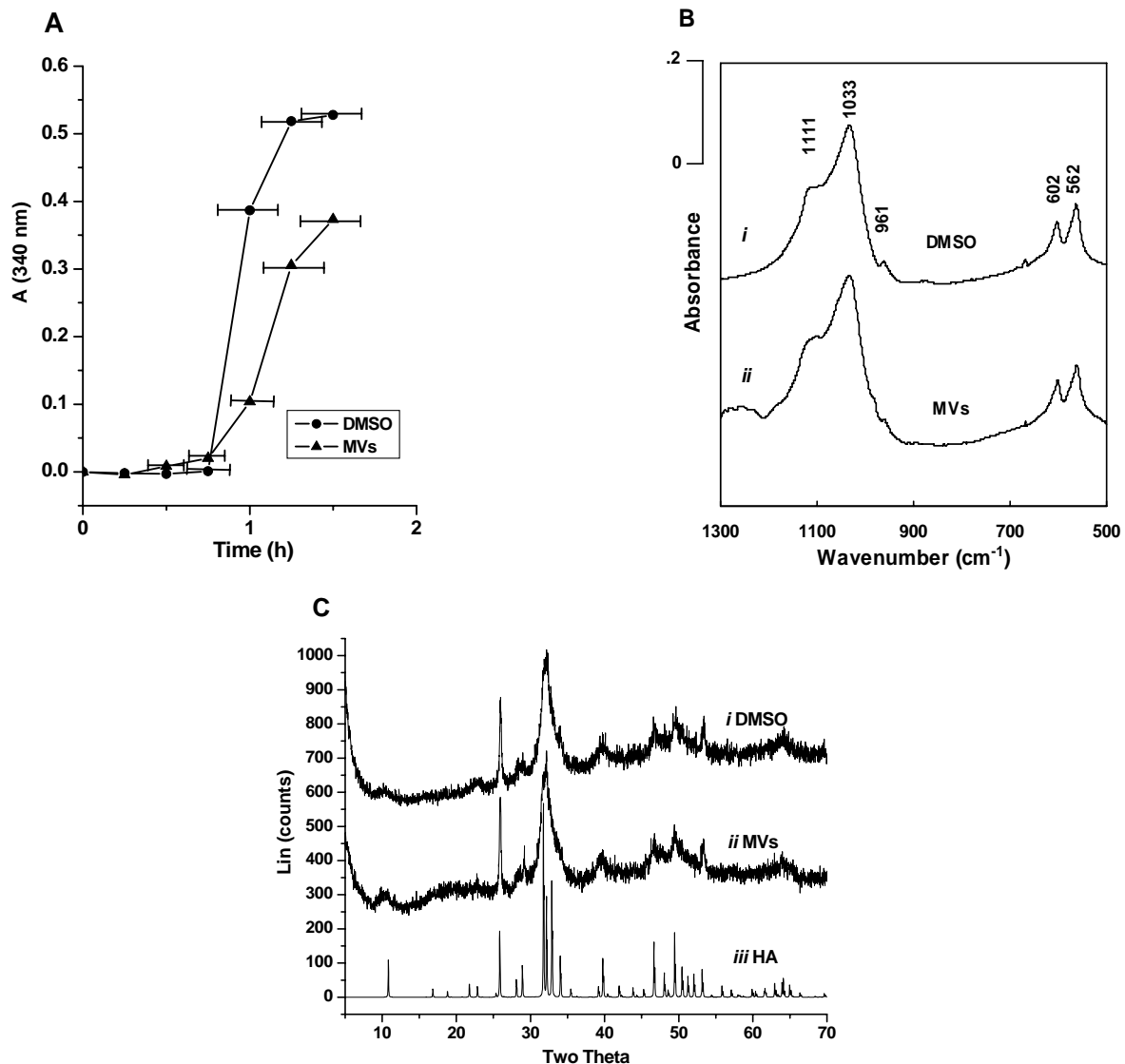
Figure 1: DMSO as matrix vesicles induced hydroxyapatite. A, Mineral formation was assessed by light scattering at 340nm : (●) SCL medium containing 2mM Ca^{2+}, 3.42mM Pi and 4 % DMSO; (▲) SCL medium containing 2mM Ca^{2+}, 3.42mM P_i and 30 µg protein/mL MVs. B, Identification of mineral formation by infrared spectroscopy: Trace i infrared spectrum of mineral deposits formed in SCL medium containing 2mM Ca^{2+}, 3.42mM P_i and 4 % DMSO; Trace ii infrared spectrum of mineral deposits formed in SCL medium containing 2mM Ca^{2+}, 3.42mM P_i and 30 µg protein/mL MVs. C. X-Ray diffraction pattern of mineral formed in SCL medium containing 2mM Ca^{2+}, 3.42mM P_i and 4 % DMSO (trace i) or in SCL medium containing 2mM Ca^{2+}, 3.42mM P_i and 30 µg protein/mL MVs (trace ii) . Trace iii is the standard hydroxyapatite from International Centre for Diffraction Data, Powder Diffraction File number 01-089-4405.

In the mineralization medium with 4% (v/v) DMSO, the increase of turbidity (Fig. 1A)

paralleled with the increase of HA formation, since there were no other minerals than HA as indicated by the infrared spectra of minerals formed and analyzed over time (Fig. 2A). The amount of HA was also raised with the DMSO concentration from 0.1 % to 20% (v/v) (Fig. 2B).
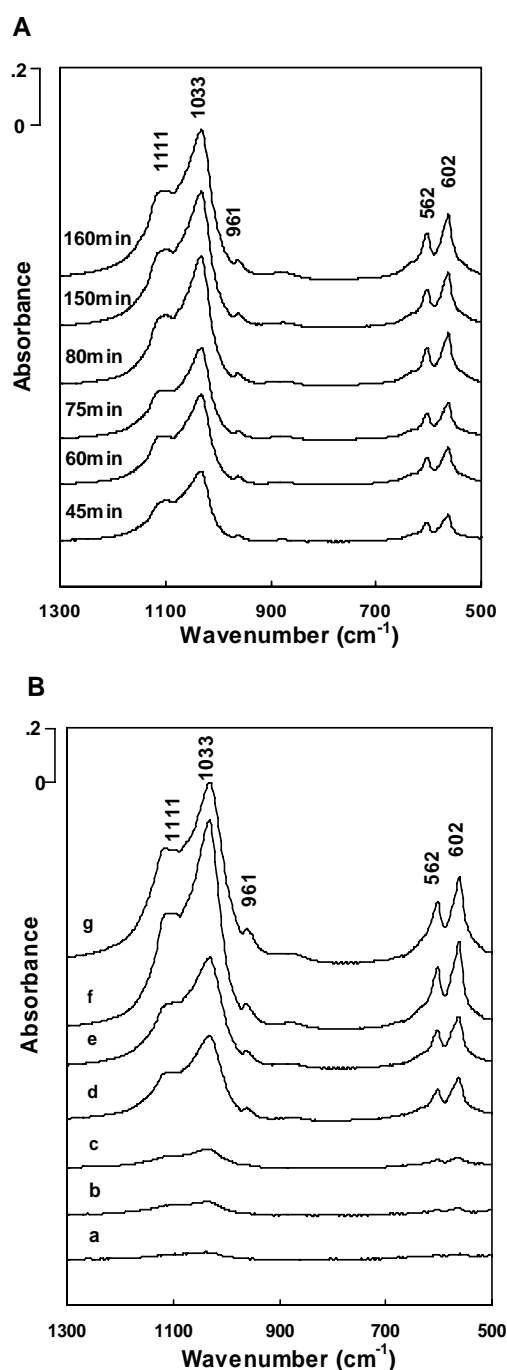
Figure 2: DMSO-induced formation of hydroxyapatite as monitored by infrared spectroscopy. A, SCL medium containing 2mM Ca^{2+}, 3.42mM P_i and 4 % DMSO were incubated at different time at 37 °C as indicated. Then the mineral was analyzed by infrared spectroscopy. B, SCL medium containing 2mM Ca^{2+}, 3.42mM P_i were incubated at 37 °C for 24h with increasing DMSO concentration (a) 0.1 %, (b) 0.5 %, (c) 1%, (d) 2 %, (e) 4 %, (f) 10 % and (g) 20%. Each mineral obtained at the indicated DMSO concentration was analyzed by infrared spectroscopy.

Effects of ATP, ADP, AMP and ADP-ribose on hydroxyapatite formation. ATP and ADP inhibited HA formation in the presence of alkaline phosphatase, while AMP did not [13]. Although pyrophosphate, a known inhibitor of HA formation [40-44], can be produced during hydrolysis of ATP due to the phosphodiesterase activity of alkaline phosphatase [37,45-47], it was not clear whether ATP itself could inhibit HA formation. Since it is difficult to induce HA in SCL medium, the DMSO-induced HA formation in SCL medium mimicking physiological conditions, served as a nucleation model to check the ability of ATP to inhibit HA formation. Addition of ATP in SCL medium containing 4% DMSO (v/v), 2mM Ca^{2+} and 3.42mM P_i, decreased turbidity in contrast to the control sample without nucleotide (Fig. 3A). After one-week incubation, the analysis of SCL medium in the presence of 1 mM ATP did not reveal any HA (Fig. 3B), confirming the inhibition of HA formation by the addition of ATP.
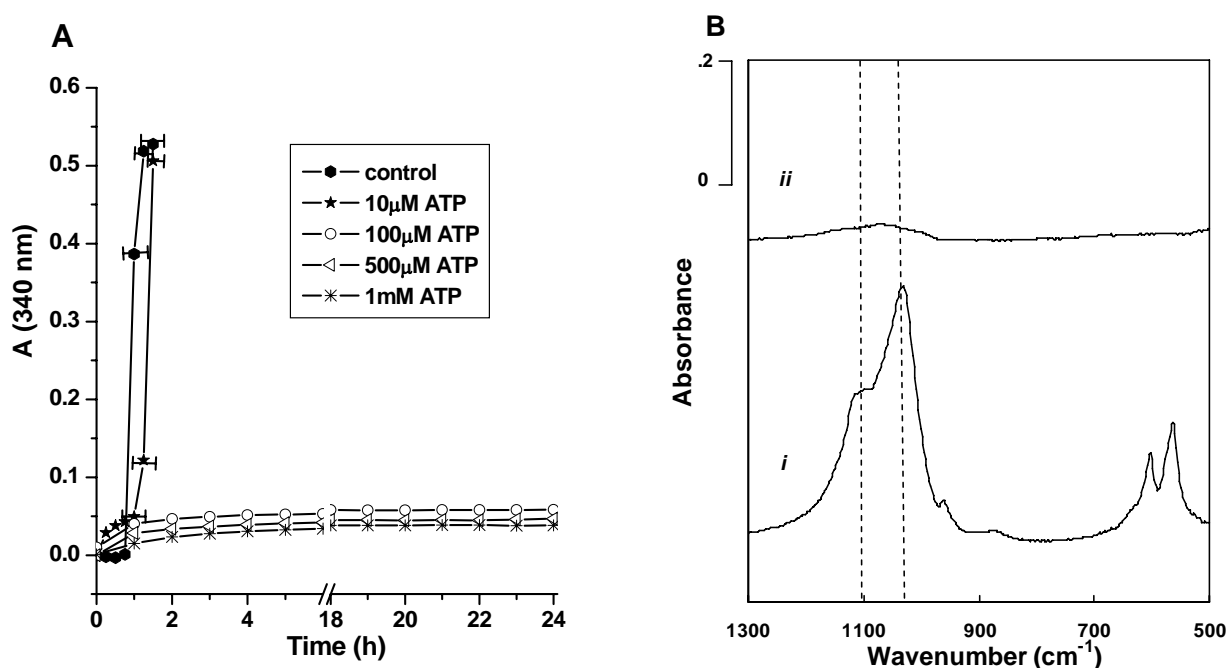
Figure 3: Mineral induction by DMSO with ATP. A, Mineral formation in SCL medium, containing 2mM Ca^{2+}, 3.42mM P_i, 4 % DMSO with ATP at the indicated concentration. The mineral formation was assessed by light scattering at 340nm. B, Infrared spectra of mineral formed in SCL medium containing 2mM Ca^{2+}, 3.42mM P_i, 4 % DMSO, after one-week incubation with 1 mM ATP (trace ii) or without ATP (trace i).

In the same medium, a control sample with 1 mM ADP inhibited mineralization over a 24h incubation time (Fig. 4A), while addition of 1 mM AMP instead of ADP led to HA

formation. Since the nature of phosphate groups can influence the inhibition of HA formation, ADP-ribose containing only phosphodiester bonds was used to test for its ability to affect mineralization. In contrast to ADP, ADP-ribose did not inhibit HA formation (Fig. 4A).
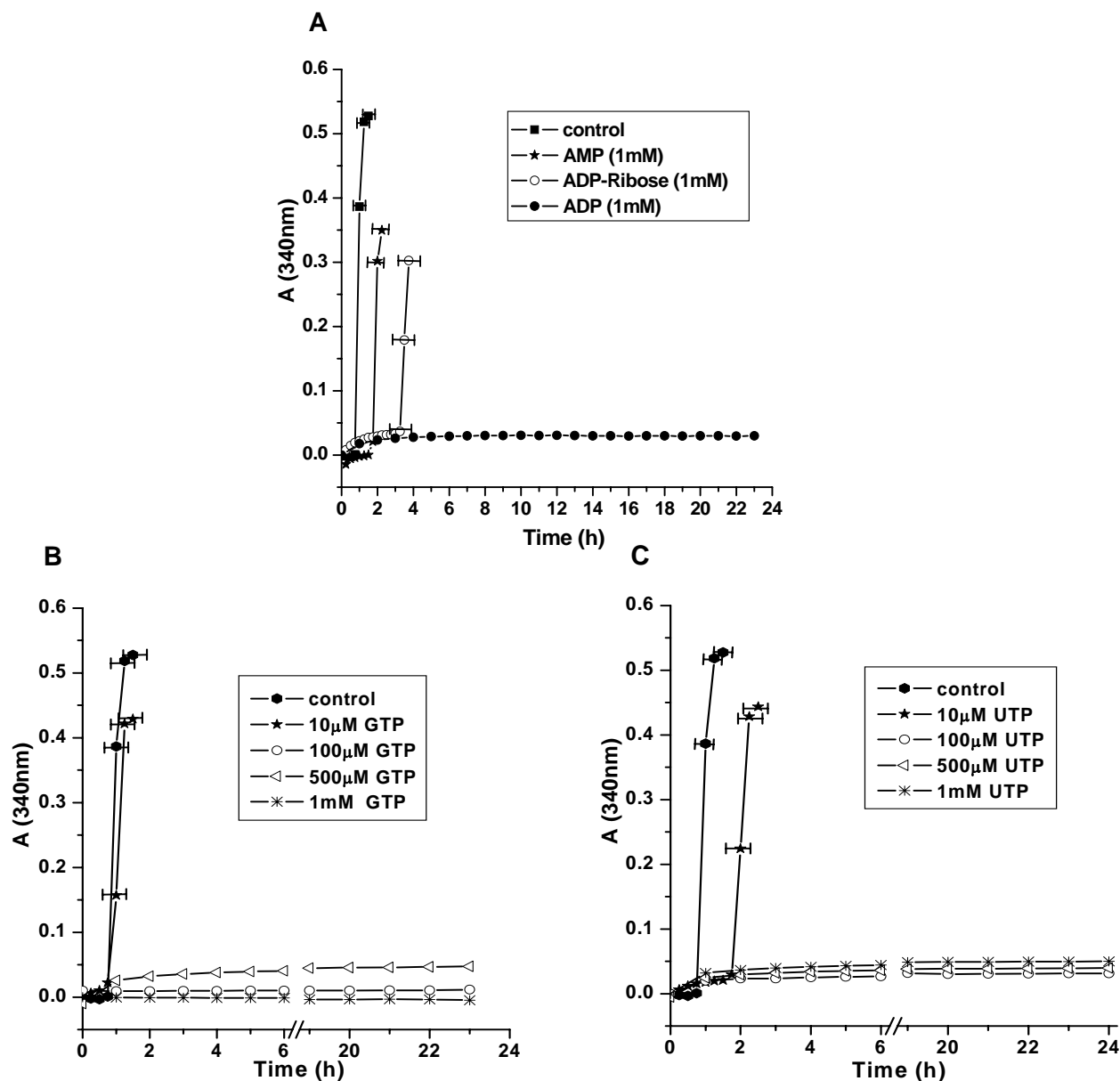
Figure 4: Mineral induction by DMSO with AMP, ADP, ADP-ribose, GTP and UTP. Mineral formation in SCL medium containing 2 mM Ca^{2+}, 3.42mM P_i and 4 % DMSO was assessed by light scattering at 340 nm : A, (■) without additional SCL supplementation, (★) with 1 mM AMP, (O) with 1 mM ADP-ribose, (●) with 1 mM ADP; B, Mineral formation in SCL medium, containing 2mM Ca^{2+}, 3.42mM P_i, 4 % DMSO with GTP at the indicated concentration. C, Mineral formation in SCL medium, containing 2mM Ca^{2+}, 3.42mM P_i, 4 % DMSO with UTP at the indicated concentration. The mineral formations were assessed by light scattering at 340 nm.

Effects of GTP, UTP and pyrophosphate on hydroxyapatite formation. Similar inhibitory effects were observed with GTP (Fig. 4B) and with UTP (Fig. 4C), inferring that neither purine nor pyrimidine moieties could affect mineral formation but that the pyrophosphate moiety could. To confirm this, PP_i was added in SCL medium containing 2mM Ca^{2+}, 3.42mM P_i and 4% DMSO (v/v). 10 µM of PP_i inhibited mineralization up to 20h incubation (Fig. 5A). After one week-incubation, a detectable amount of HA was formed as evidenced by infrared spectroscopy. No HA could be detected with 100 µM of PP_i in SCL medium containing 2mM Ca^{2+}, 3.42mM P_i and 4% DMS0 (v/v) after one-week incubation (Fig. 5B). Calcium dihydrate pyrophosphate mineral formation was obtained at 1 mM pyrophosphate concentration in SCL medium containing 2mM Ca^{2+}, 3.42mM P_i and 4% DMSO (v/v) (Fig. 5B).
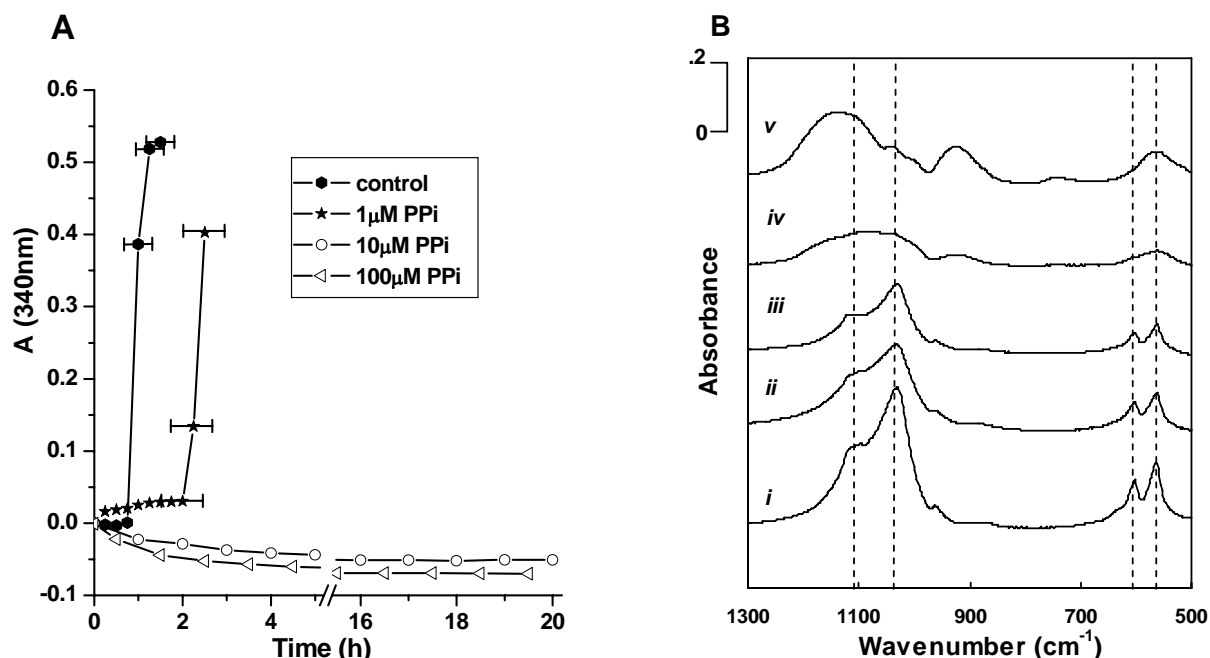
Figure 5: Mineral induction by DMSO with PP_i. A, Mineral formation in SCL medium, containing 2mM Ca^{2+}, 3.42mM P_i, 4 % DMSO with PP_i at the indicated concentration. The mineral formation was assessed by light scattering at 340nm. B, Infrared spectra of mineral formed in SCL medium containing 2mM Ca^{2+}, 3.42mM P_i, 4 % DMSO, after one-week incubation without (trace i), or with 1µM (trace ii), 10 µM (trace iii), 100 µM (trace iv), or 1 mM PP_i (trace v).

Conclusions

In vitro modeling of matrix vesicle nucleation. Calcium and phosphate in metastable equilibrium can induce mineralization. This process is facilitated by a nucleation process. During endochondral bone formation, the nucleation process is initiated

inside matrix vesicles, providing an optimum environment for the accumulation of calcium and phosphate leading to the formation of HA [4,5]. 4% DMSO (v/v) in SCL medium was able to induce HA formation, in a similar manner as matrix vesicles. HA formation was confirmed by infrared spectroscopy and by X-ray diffraction. The induction time of HA formation induced by 4% (v/v) DMSO in SCL medium was comparable to that produced by MVs in the same SCL medium. The nucleation model could serve to elucidate the mechanisms of inhibition since it monitored only the nucleation process, whereas matrix vesicles contain several enzymes which can interact with the inhibitors, especially when the inhibitors are enzyme substrates: nucleotides, pyrophosphate and other phosphate derivatives. The *in vitro* nucleation model permits us to screen HA crystallization inhibitors. Such inhibitors could suppress pathological calcification not only in the articular cartilage leading to osteoarthritis but also in soft tissues such as cardiovascular tissues and kidney.

Inhibitory mechanisms of HA formation by nucleotides. To validate the nucleation model, we investigated the inhibitory effects of several enzyme substrates and their derivatives during the formation of HA. Nucleotides were selected since extracellular ATP is involved in the regulation of bone and cartilage metabolism [48]. Extracellular nucleotides can inhibit bone mineralization by acting through P2Y2 receptors or by their enzymatic hydrolysis product, pyrophosphate [49]. The nature of phosphate substrate (ATP, AMP, etc…) hydrolyzed by the enzymes determines the type of mineral formed in MVs [50], especially when ATP hydrolyzed by MV enzymes provides pyrophosphate, a potent inhibitor of HA nucleation [40-44, 51]. Addition of ATP retarded mineral formation in MVs [52] due to its inhibitory effect on HA formation [52] or due to the inhibitory effect of pyrophosphate [40-44, 51] hydrolyzed from ATP by MV enzymes. Such direct inhibitory action on HA formation was well evidenced in DMSO-induced HA formation. Addition of any of the nucleotides ATP, GTP and UTP in SCL medium containing 4% (v/v) DMSO did not produce HA, confirming that nucleotide triphosphate itself is a potent inhibitor of HA. DMSO-induced HA formation was inhibited by the addition of pyrophosphate and ADP, while AMP addition did not, indicating that pyrophosphate prevented the formation of HA and that the purine group was not involved. ADP-ribose did not inhibit HA formation, suggesting that the inhibitory effect of pyrophosphate moiety depends on the number of negative charges surrounding the pyrophosphate, two in the case of ADP-ribose instead of three in the

case of ADP at pH 7.6. DMSO-induced nucleation of HA could serve as a screening model to evaluate the inhibitory properties of putative drugs to prevent pathological calcification.

ACKNOWLEDGMENT

REFERENCES

[1] T. Kirsch, Physiological and pathological mineralization: a complex multifactorial process, Curr. Opin. Orthop. 18 (2007) 425-427.

[2] B. Zimmermann, H.C. Wachtel, C. Noppe, Patterns of mineralization in vitro, Cell Tissue Res. 263 (1991) 483-93.

[3] C.H.A. Van de Lest, A.B. Vaandrager, Mechanisms of cell-mediated mineralization, Curr. Opin. Orthop. 18 (2007) 434-443.

[4] H.C. Anderson, The role of matrix vesicles in physiological and pathological calcification Curr. Opin. Orthop. 18 (2007) 428-433.

[5] H.C. Anderson, R. Garimella, S.E. Tague, The role of matrix vesicles in growth plate development and biomineralization, Front Biosci. (10) 2005, 822-837.

[6] X. Cao, B.R. Genge, L.N. Wu, W.R. Buzzi, R.M. Showman, R.E. Wuthier, Characterization , cloning and expression of the 67 KDa annexin from chicken growth plate matrix vesicles, Biochem Biophys. Res. Commun. 197 (1993) 556-561.

[7] T. Kirsch, H.D. Nah, D.R. Demuth, G. Harrison, E.E. Golub, S.L. Adams, M. Pacifici, Annexin V mediated calcium flux across membranes is dependent on the lipid composition: implications for cartilage mineralization, Biochemistry 36 (1997) 1149-1160.

[8] Z. Xiao, C.E. Camalier, K. Nagashima, K.C. Chan, D.A. Luca, M.J. de la Cruz, M. Gignac, S. Lockett, H.J. Issaq, T.D. Veenstra, T.P. Conrads, G.R. Jr Beck, Analysis of the extracellular matrix vesicle proteome in mineralizing osteoblasts,   J. Cell. Physiol. 210 (2007) 325-335.

[9] M. Balcerzak M, A. Malinowska, C. Thouverey, A. Sekrecka, M. Dadlez, R. Buchet, S. Pikula, Proteome analysis of matrix vesicles isolated from femurs of chicken embryo, Proteomics 8 (2008) 192-205.

[10] B.R. Genge, L.N.Y. Wu, R.E. Wuthier R.E, Kinetic analysis of mineral formation during in vitro modeling of matrix vesicle mineralization: effect of annexin A5, phosphatidylserine, and type II collagen, Anal Biochem. (367) 2007 159-166.

[11] B.R. Genge , L.N.Y. Wu, R.E. Wuthier, *In vitro* modelling of matrix vesicle nucleation. Synergistic stimulation of mineral formation by annexin A5 and phosphatidylserine. J. Biol. Chem. 282 (2007), 26035-24045.

[12] B.R. Genge, L.N.Y. Wu, R.E. Wuthier R.E, Mineralization of Annexin-5-containing Lipid-Calcium-Phosphate Complexes: MODULATION BY VARYING LIPID COMPOSITION AND INCUBATION WITH CARTILAGE COLLAGENS, J Biol Chem. 283 (2008) 9737-9748.

[13] E. Hamade, G. Azzar, J. Radisson, R. Buchet, B. Roux, Chick embryo anchored alkaline phosphatase and mineralization process in vitro. Influence of Ca^{2+} and nature of substrates, Eur. J. Biochem. 270 (2003) 2082-2090.

[14] G.K. Hunter, H.A. Goldberg, Nucleation of hydroxyapatite by bone salioprotein, Proc. Natl. Acad. Sci. USA 90 (1993) 8562-8565.

[15] H.A. Goldberg, K.J. Warner, M.J. Stillman, G.K. Hunter, Determination of the hydroxyapatite-nucleating region of bone salioprotein, Connect. Tissue Res. 35 (1996) 385-392.

[16] G.K. Hunter, P.V. Hauschka, A.R. Poole, L.C. Rosenberg, H.A. Goldberg, Nucleation and inhibition of hydroxyapatite formation by mineralized tissue proteins, Biochem. J. 317 (1996) 59-64.

[17] B. Ganss, R.H. Kim, J. Sodek, Bone sialoprotein, Crit. Rev. Oral. Biol. Med. 10 (1999) 79-98.

[18] C.E. Tye, K.R. Rattray, K.J. Warner, J.A. Gordon, J. Sodek, G.K. Hunter, H.A. Golberg, Delineation of the hydroxyapatite-nucleating domains of bone salioprotein, J. Biol. Chem. 273 (2003) 7949-7955.

[19] T. Saito, A.L. Arsenault, M. Yamauchi, Y. Kuboki, M.A. Crenshaw, Mineral induction by immobilized phosphoproteins, Bone 21 (1997) 305-311.

[20] S. Gajjeraman, K. Narayanan, J. Hao, C. Qin, A. George, Matrix macromolecules in hard tissues control the nucleation and hierarchical assembly of hydroxyapatite, J. Biol. Chem. 282 (2007) 1193-1204.

[21] S. Ito, T. Saito, K.J. Amano, In vitro apatite induction by osteopontin: interfacial energy for hydroxyapatite nucleation on osteopontin, Biomed. Mater. Res. 69 (2004) 11-16.

[22] K. Yamashita, T. Takagi, Calcification preceding new bone formation induced by demineralised bone matrix gelatin, Arch. Histol. Cytol. 55 (1992) 31-43.

[23] A. Takeuchi, C. Ohtsuki, T. Miyazaki, M. Kamitakahara, S. Ogata, M. Yamazaki Y. Furatani, H. Kinoshita, M.J.R. Tanihara, Heterogeneous nucleation of hydroxyapatite on protein: structural effect of silk sericin, Soc. Interface 22 (2005) 373-378.

[24] A.L. Boskey, M.R. Godberg, A.S. Posner, Calcium-phospholipid-phosphate complexes in mineralizing tissue, Proc. Soc. Exp. Biol. Med. 157 (1978) 590-593.

[25] G.H. Nancollas, A. Tsortos, A. Zieba, The nucleation and growth of calcium phosphate crystals at protein and phosphatidylserine liposome surfaces, Scanning Microsc. 10 (1996) 499-507.

[26] C.H. Demos, G.L. Beckloff, M.N. Donin, P.M. Olivier, Dimethyl sulfoxide in musculoskeletal disorder, Ann. NY Acad. Sci. 141 (1967) 517-523.

[27] R.A Jimenez, R. F. J. Willkens, Dimethyl sulfoxide: a perspective of its use in rheumatic diseases, Lab. Clin. Med. 100 (1982) 489-500.

[28] J.M. Trice, R.S. Pinals, Dimethyl sulfoxide: a review of its use in the rheumatic disorders, Semin. Arthritis Rheum. 15 (1985) 45-60

[29] E.D. Rosenstein, Topical agents in the treatment of rheumatic disorders, Rheum. Dis. Clin. North Am. 25 (1999) 899-918.

[30] S.W. Jacob, R. Herschler, Dimethyl sulfoxide after twenty year, Ann. NY Acad. Sci. 411 (1983) 14-18.

[31] C.F. Brayton, Dimethyl sulfoxide (DMSO): a review, Cornell Vet. 76 (1986) 61-90.

[32] A.A. Bookmann, S. Williams, J.Z. Shainhouse, Effect of a topical diclofenac solution for relieving symptoms of primary osteoarthritis of the knee: a randomized controlled trial, CMAJ 171 (2004) 333-338.

[33] M. Balcerzak, J. Radisson, G. Azzar, D. Farlay, G. Boivin, S. Pikula, R. Buchet, A comparative analysis of strategies for isolation of matrix vesicles, Anal. Biochem. 361 (2007) 176-82.

[34] L. N. Wu, B.R. Genge, D.G. Dunkelberger, R.Z. LeGeros, B. Concannon, R.E. Wuthier, Physicochemical characterization of the nucleational core of matrix vesicles, J. Biol. Chem. 272 (1997) 4404-4411.

[35] M.M. Bradford, A rapid and sensitive method for the quantitation of microgram quantities of protein utilizing the principle of protein-dye binding, Anal. Biochem. 72 (1976) 248-254.

[36] L.N. Wu, G.R. Sauer, B.R. Genge, W.B. Valhmu, R.E. Wuthier, Effects of analogues of inorganic phosphate and sodium ion on mineralization of matrix vesicles isolated from growth plate cartilage of normal rapidly growing chickens, J. Inorg. Biochem. 94 (2003) 221-235.

[37] L. Zhang, M. Balcerzak, J. Radisson, C. Thouverey, S. Pikula, G. Azzar, R. Buchet, Phosphodiesterase activity of alkaline phosphatase in ATP-initiated Ca^{2+} and phosphate deposits in isolated matrix vesicles J. Biol. Chem. 280 (2005) 37289-37296.

[38] G.R. Sauer, R.E. Wuthier R, Fourier transform infrared characterization of mineral phases formed during induction of mineralization by collagenase-released matrix vesicles in vitro, J. Biol. Chem. 268 (1988) 13718-13724.

[39] B.O. Fowler, Vibrational assignments for calcium, strontium, and barium hydroxyapatites utilizing isotopic substitution, Inorganic Chem. 13 (1974) 194-207.

[40] N.C. Blumenthal, Mechanisms of inhibition of calcification, Clin. Orthop. Relat. Res. 247 (1989) 279-289.

[41] T.C. Register, R.E. Wuthier, Effect of pyrophosphate and two diphosphonates on 45Ca and 32P$_i$ uptake and mineralization by matrix vesicle-enriched fractions and by hydroxyapatite, Bone 6 (1985) 307-312.

[42] A. Tanimura, D.H. McGregor, H.C. Anderson, Matrix vesicles in arthrosclerotic calcification, Proc. Soc. Exp. Biol. Med. 172 (1983) 173-177.

[43] H.C. Tenenbaum, Levamisole and inorganic pyrophosphate inhibit beta-glycerophosphate induced mineralization of bone formed in vitro, Bone Miner. 3 (1987) 13-26.

[44] R.A. Terkeltaub, Inorganic pyrophosphate generation and disposition in pathophysiology, Am. J. Physiol. Cell. Physiol. 381 (2001) C1-C11.

[45] A.A. Rezende, J.M. Pizauro, P. Cinacaglini P.; Leone F.A. Phosphodiesterase activity is a novel property of alkaline phosphatase from osseous plate, Biochem. J. 301 (1994) 517-522.

[46] P.J. O'Brien, D. Herschlag, Functional interrelationships in the alkaline phosphatase superfamily: phosphodiesterase activity of Escherichia coli alkaline phosphatase, Biochemistry 40 (2001) 5691-5699.

[47] J.G. Zalatan, T.D. Fenn, A.T. Brunger, D. Herschlag D, Structural and functional comparisons of nucleotide pyrophosphatase phosphodiesterase and alkaline

phosphatase: Implications for mechanisms and evolution, Biochemistry 45 (2006) 9788-9803.

[48] C. Thouverey, F. Bleicher, J. Bandorowicz-Pikula, Extracellular ATP and its effects on physiological and pathological mineralization, J. Curr. Opin. Orthop. 18, (2007) 460-466.

[49] I.R. Orriss, J.C. Utting, A. Brandao-Burch, K. Colston, B.R. Grubb, G. Burnstock, T.R. Arnett, Extracellular nucleotides block bone mineralization in vitro: evidence for dual inhibitory mechanisms involving both P2Y2 receptors and pyrophosphate, Endocrinology 148 (2007) 4208-4216.

[50] R. Garimella, X. Bi, H.C. Anderson, N.P. Camacho, Nature of phosphate substrate as a major determinant of mineral type formed in matrix vesicle-mediated in vitro mineralization: An FTIR imaging study, Bone 38 (2006) 811-817.

[51] R.J. Zaka, C. Williams, The inorganic phosphate/inorganic pyrophosphate axis in the mineralization of cartilage and bone. Curr. Opin. Orthop. 18 (2007) 454-459.

[52] A.L. Boskey, B.D. Boyan, Z. Schwartz, Matrix vesicles promote mineralization in a gelatin gel. Calcif. Tissue Int. 60 (1997) 309-315.

Sinomenine, theophylline, cysteine and levamisole: Comparisons of their effects on mineral formation induced by matrix vesicles

Lina Li[1-6], René Buchet [2-6] and Yuqing Wu[1*]

[1]State Key Laboratory for Supramolecular Structure and Materials, Jilin University, ChangChun 130012 China

[2]Université de Lyon, Villeurbanne, F-69622, France

[3]Université Lyon 1, Villeurbanne, F-69622, France

[4]INSA de Lyon, Villeurbanne, F-69621, France

[5]CPELyon, Villeurbanne, F-69616, France

[6]CNRS UMR 5246 ICBMS, Villeurbanne, F-69622, France

MicroAbstract: Sinomenine (SIN) an anti-rheumatic Chinese drug, did not inhibit tissue non-specific alkaline phosphatase (TNAP) but delayed hydroxyapatite (HA) formation induced by matrix vesicles (MVs). We concluded that its therapeutical action is probably due to a slowing down of HA formation in cartilage joints.

Introduction: SIN, an alkaloid extracted from a Chinese medicinal plant *sinomenium acutum,* has been used for the treatment of patients with rheumatic diseases including rheumatoid arthritis for many centuries. Due to the broad pharmacological profile of SIN, it is expected that several molecular mechanisms could be implicated in the beneficial therapeutic effects of SIN. So far, SIN, as an anti-arthritic drug has not been checked for its direct effect to prevent calcification.

Methods: MVs provide an easily quantifiable model to analyze the initiation of HA formation. The mineralization process induced by MVs at physiological pH and at 37 °C in the presence of SIN was compared with those induced by MVs with either cysteine, levamisole or theophylline. The light scattering method was employed for real time measurement of mineral formation induced by MVs (15-20 µg of MV protein) in synthetic cartilage lymph (SCL) buffer with different concentrations of ions (Ca^{2+}, P_i) or AMP at pH 7.6 and at 37 °C .

Results: Incubation of either 0.25-1 mM cysteine, theophylline or levamisole with MVs in SCL medium containing AMP and calcium but without phosphate, prolonged the induction time of mineral formation by inhibiting TNAP activity, while 0.25-1 mM SIN neither inhibited TNAP nor changed the induction time of mineral formation. However, SIN was able to delay mineral formation induced by MVs in SCL medium containing P_i instead of AMP in a similar manner as that induced by theophylline, but to a lesser extent than levamisole, while addition of cysteine activated the mineral formation.

Conclusions: Ion transports within MVs and TNAP activity are not coupled since they were affected in a different manner by cysteine, theophyline, levamisole and SIN. We propose that the anti-rheumatic and anti-inflammatory effects of SIN are caused by delaying pathological HA crystal formation in arthritic joints which may slow down the degeneration and alleviate the inflammatory response.

Introduction

Sinomenine (SIN, 7,8-didehydro-4hydroxy-3,7-dimethoxy-17-methylmorphinan-6-one) belongs to the family of morphinan and is an alkaloid extracted from a Chinese medicinal plant *sinomenium acutum.* SIN has been used for the treatment of patients with rheumatic diseases including rheumatoid arthritis (RA) for many centuries.[1-2] The anti-arthritic mechanism of SIN may be related to antiproliferative effects of synovial fibroblasts,[3] to the reduction of mRNA expression of proinflammatory cytokines including TNF-α and IL-1β based from findings in rats with adjuvant arthritis [3,4], or to the suppression of both Th1 and Th2 (to a lesser extent than Th1) immune response as observed in collagen-induced arthritis in mice.[5] SIN is also a potent anti-inflammatory and neuroprotective agent that acts through inhibition of microglial NADPH oxidase [6]. Due to the broad pharmacological profile of SIN, it is expected that several molecular mechanisms could be implicated in the beneficial therapeutic effects of SIN. So far, SIN, as an anti-arthritic drug has not been checked for its direct effect to prevent calcification. Whether calcium crystals cause or worsen osteoarthritis or whether osteoarthritis causes or worsen calcium crystal deposition is still debatable.[7] Nevertheless, calcium-containing crystals are present in synovial fluid extracted from the knee joints of up 70% of osteoarthritis patients.[8] Calcium crystals may promote or accelerate joint degeneration.[8] Injections of crystals into the knee joints of dogs induced a severe inflammatory response,[9] while calcium crystals induced the production of nitric oxide[10,11] and cytokines.[12-15] Matrix vesicles (MVs), extracellular organelles produced by chondrocytes, osteoblasts and odontoblasts[16,17] initiate normal skeletal calcification. They are also present at the initial sites of hydroxyapatite (HA) mineral deposition in a variety of pathologic calcifications.[17-19] Osteoarthritic articular chondrocytes release MVs,[19-22] which are responsible for the pathological formation of HA[19-23] or calcium pyrophosphate dihydrate (CPPD) minerals[23-28] in degenerative joints. To address the effect of SIN on the calcification process, MVs were selected since they provide an easily quantifiable model to analyze the initiation of HA.[28,29] The mineralization process induced by MVs at physiological pH and at 37°C in the presence of SIN was compared with that induced by MVs with either cysteine, levamisole or theophylline. Cysteine,[29-32] levamisole[33-36] and theophylline[37-42] are inhibitors of alkaline phosphatase. Levamisole has been used for curing RA.[43,44] It was proposed that cysteine could

serve as a therapeutical option for CPPD crystal deposition disease.[32] Theophylline as other methyl xanthines (caffeine, 2 methylxanthines) are antagonists of adenosine[45-46] and can be used to block adenosine receptors. We found that the incubation of either cysteine, theophylline or levamisole with MVs in synthetic cartilage lymph (SCL) medium containing AMP and calcium but without phosphate, prolonged the induction time of mineral formation by inhibiting TNAP activity. In contrast, SIN did not inhibit TNAP. However, SIN was able to delay mineral formation induced by MVs in SCL medium containing P_i instead of AMP in a similar manner as that induced by theophylline, but to a lesser extent than levamisole, while addition of cysteine activated the mineral formation. Such findings indicate that P_i and Ca^{2+} transports were affected in a different manner by the different inhibitors. It was concluded that SIN, by delaying HA formation could indirectly boost its anti-inflammatory effect.

EXPERIMENTAL SECTION

Chemicals

Cysteine, levamisole and AMP were procured from Sigma, Theophylline was purchased from China National Parmaceutical Group Corporation. SIN was obtained from Chengdu Mansite Pharmaceutical Co., Ltd., China. The purity of theophylline and SIN was further confirmed by ^1H NMR and Mass Spectrum.

Preparation of synthetic cartilage lymph

Standard synthetic cartilage lymph (SCL) was prepared as stock solution and frozen at -20 °C until used. It contained 100 mM NaCl, 63.5 mM sucrose, 16.5 mM TES, 12.7 mM KCl, 5.55 mM D-glucose, 1.83 mM $NaHCO_3$, 0.57 mM $MgCl_2.6H_2O$ and 0.57 mM Na_2SO_4, pH 7.6.[47] 0-2 mM Ca, 0-3.42 mM Pi or 0-3.42 mM AMP were added as indicated.

Extraction and characterization of matrix vesicles

Collagenase released MVs were isolated from bone and epiphyseal cartilage slices of 17-day-old chicken embryos according to Balcerzak et al. [48] Slices of bone tissues

were digested at 37 °C for about 3h in a synthetic cartilage lymph (SCL) containing 2mM Ca^{2+} and collagenase (type IA, ICN Biomedicals Inc., 200 units/g of tissue with a volume of 4mL/g of tissue). The partially digested tissue was vortexed, and the suspension was centrifuged at 13,000 x g for 20 min at 4 °C (centrifuge Beckman J32B, rotor JA20). The pellet was discarded, and the suspension was centrifuged again at 80,000 x g for 1 h at 4°C (centrifuge Kontron TGA, rotor 6538). The MV pellet was resuspended in SCL without any Ca^{2+} and P_i to prevent the mineral formation. The MV suspension was prepared as a stock solution containing around 1-2 mg of vesicle protein/mL in SCL at 4 °C for further use. Protein concentration in the MVs was determined by the method of Bradford.[49] For electron-microscopy observation (Philips CM120 at 80kV accelerating voltage, Centre Technologique des Microstructures, Lyon 1), a drop of the suspension of MVs diluted to 25 µg of MV protein/mL was transferred to carbon-coated grids. Prior to the complete drying of MV samples, the grids were covered by an aliquot of 2% uranyl acetate solution according to the negative staining method and dried. Electrophoresis was performed in 10% (w/v) SDS-polyacrylamide gel after protein denaturation at 100 °C for 3 min in Laemmli buffer with 5 % (w/v) β-mercaptoethanol.[50] Proteins were stained with Coomassie Brilliant Blue R-250.

Alkaline phosphatase activity

To detect the different effect of soluble inhibitors of TNAP: cysteine, levamisole, theophylline as well as a Chinese medicine SIN, TNAP activity of MVs was determined in both alkaline and physiological conditions, using the buffer containing 25 mM piperazine, 25 mM glycylglycine, 5 mM $MgCl_2$, 5 µM $ZnCl_2$ at pH 10.4 and 0.1 M Tris-HCl buffer with 5 mM $MgCl_2$ and 5 µM $ZnCl_2$ at pH 7.5 respectively. The mixtures containing the buffer, 13 µg/ml protein of MVs and different concentrations (0-4 mM) of cysteine, levamisole, theophylline and SIN were incubated 10 min at 37 ºC without *p*NPP, then 0.1 mM *p*NPP was added at the last minute to initiate the reaction.[51] The activity was quantified at 420 nm, using a molar absorption coefficient of 18.6 $cm^{-1}mM^{-1}$ at pH 10.4 and of 9.2 $cm^{-1}mM^{-1}$ at pH 7.5. One unit of alkaline phosphatase activity was defined as the amount of enzyme required to hydrolyze 1 µmol p-nitrophenyl phosphate per min at 37 °C. The specific activity of MVs in the stock solution for mineralization was 15 U/mg as averaged from five different experiments.

Mineralization assay

The light scattering method[52] was employed for real time measurement of mineral formation induced by MVs (15-20 µg of MV protein) in SCL buffer with different concentrations of ions (Ca^{2+}, P_i) or substrates (AMP) at pH 7.6 to a final volume of 1 mL. SIN, theophylline, cysteine and levamisole were prepared as 10 mM stock solution in SCL buffer. Neither SIN nor any of three TNAP inhibitors up to 4 mM affected the pH of SCL buffer (pH7.6) by more than 0.04. The concentrations of ions, substrate and inhibitors are indicated in the figure legends. All the samples were mixed vigorously and then incubated at 37 °C in the cuvettes without any stirring. The real time light scattering was read at 340 nm automatically at 15-min intervals. Each experiment was repeated at least three times. The mineral formation of HA was confirmed by FTIR and x-ray.[53]

DMSO-induced hydroxyapatite assay

The DMSO-induced hydroxyapatite (HA) assay was prepared as elsewhere described.[53] 4% (v/v) DMSO in SCL medium containing 3.42 mM P_i and 2 mM Ca^{2+} induced hydroxyapatite formation within one hour.[53] 1-4 mM cysteine, levamisole, theophylline and SIN were employed in this system to determine the direct inhibition effect on HA formation, PP_i was selected and used as a negative control. The process of HA formation was monitored by the light scattering method, as described above.[52] The mineral formation of HA was also confirmed by FTIR and x-ray.[53]

RESULTS

Characterization of matrix vesicles.

Matrix vesicles (MVs) isolated from femurs of 17-old-day chick embryos exhibited 100-200 nm-diameter round shaped organelles as observed (Fig. 1A-C) on transmission electron microscopy. Gel electrophoresis revealed three major protein bands with apparent molecular weights of 45 kDa, 37 kDa and 31 KDa (Fig. 1D), typical of collagenase-released MVs.[54-57] MVs were able to mineralize and their apparent TNAP activities were around 15 U/mg MV protein, indicating an enriched amount of TNAP, a landmark of MVs. Taken together, these findings indicated that

the isolation of MVs led to functional and relatively pure MVs.
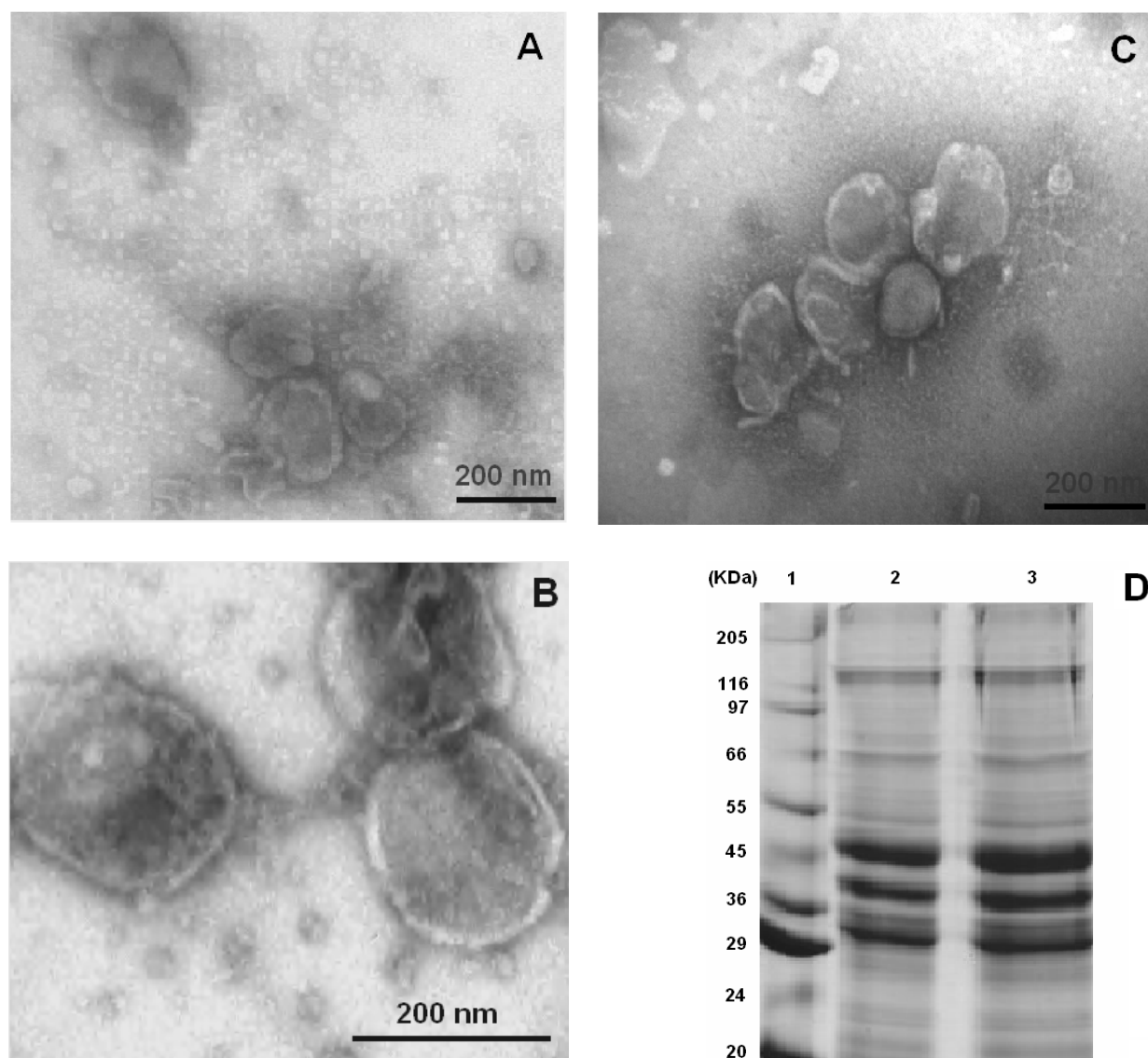
Figure 1: Characterization of MVs isolated from femurs of 17-day-old chicken embryos. A-C: Transmission electron micrographs of MVs negatively stained with uranyl acetate. Scale bar is as indicated. D: Gel electrophoresis (10% SDS–PAGE and stained with Coomassie brilliant blue) of MVs. *Lane 1*, protein standards; *lane 2*, 20 µg of MV protein profiles; *lane 3*, 30 µg of MV protein profiles.

Properties of SIN.

SIN, does not inhibit the *p*NPP hydrolysis by TNAP at 37 °C whether at pH 10.4 (Fig. 2A) or pH 7.5 (Fig. 2B), in contrast to TNAP inhibitors: cysteine[29-32], levamisole[33-36] and theophylline[37-42].
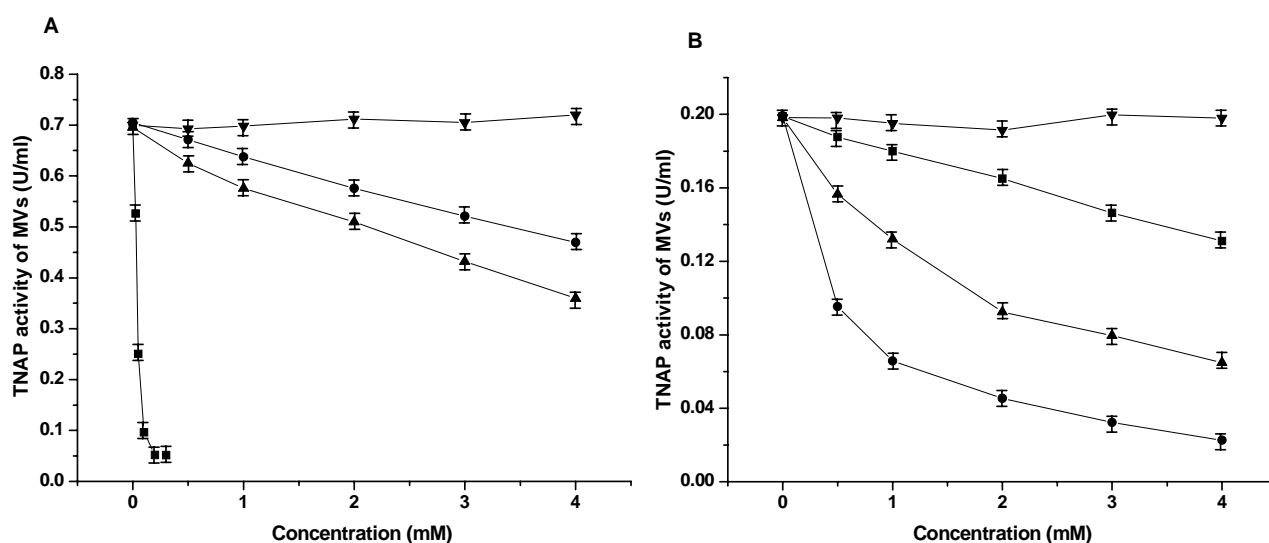
Figure 2: Inhibition of 0.1 mM pNPP hydrolysis by TNAP in matrix vesicles. 13 μg mL^{-1} MVs were incubated at 37 °C at pH 10.4 (Panel A) or at pH 7.5 (Panel B) in the absence or presence of increasing concentrations of cysteine (■), levamisole (●), theophylline (▲) and sinomenine (▼). At least three Independent measurements were performed.

Then, we checked whether SIN could interfere directly on the HA formation as PP_i. Using an assay based on DMSO-induced HA formation, we confirmed that PP_i is a known inhibitor of HA formation (Fig. 3A, PP_i). [53 58-62] Neither cysteine (Fig. 3A), nor levamisole (Fig. 3B), nor theophylline (Fig. 3C) nor SIN (Fig. 3D) affected DMSO-induced HA formation indicating that they did not influence directly the nucleation process of HA formation.
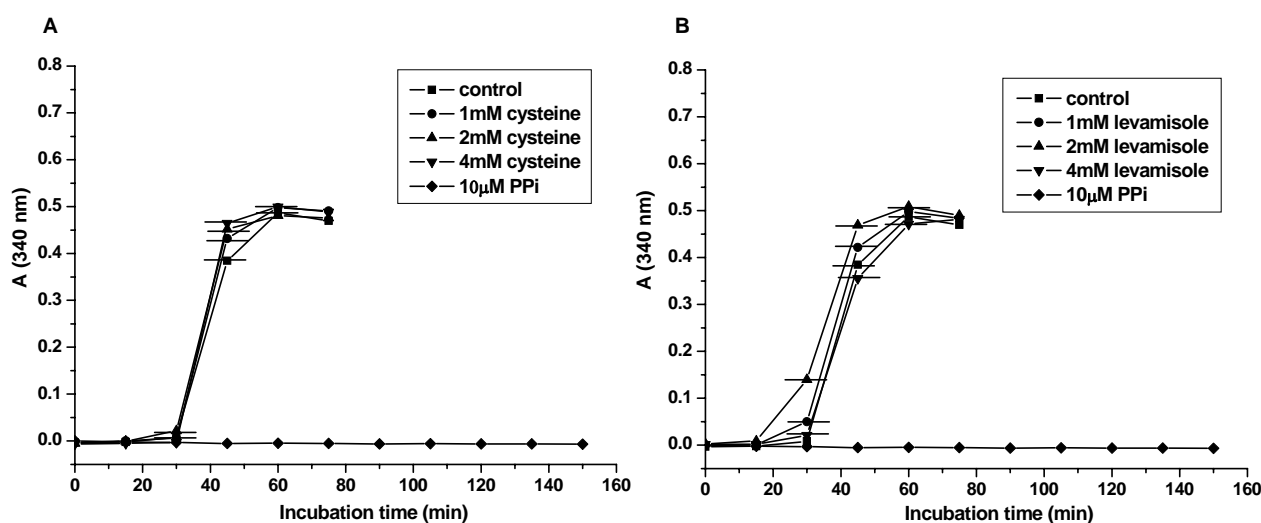
Figure 3: DMSO-induced hydroxyapatite assay. 4% (v/v) DMSO in SCL medium containing 3.42 mM P_i and 2 mM Ca^{2+} induces hydroxyapatite formation within one hour (control). Addition of 1-4 mM cysteine (Panel A), 1-4 mM levamisole (Panel B), 1-4 theophylline (Panel C) and 1-4 sinomenine (Panel D) also induced mineralization in the same manner as in SCL medium with 4% (v/v) DMSO without inhibitor (control). Addition of 10 μM PP_i did not produce any HA. Three independent measurements were performed.
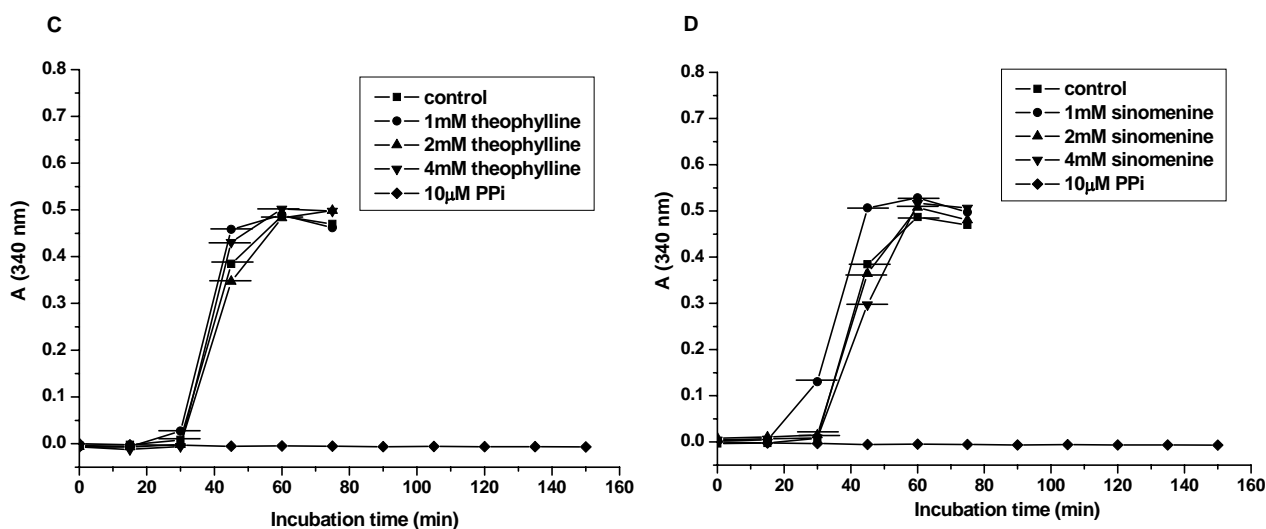
Inhibition of matrix vesicle induced mineral formation by SIN and by theophylline in the presence of AMP.

MVs with either SIN, theophylline, cysteine or levamisole were incubated at 37 °C in SCL medium containing 3.42 mM AMP and 2 mM Ca^{2+} without P_i. AMP is also a substrate for TNAP and its hydrolysis in the presence of Ca^{2+} can induce the formation of hydroxyapatite.[63] Under these conditions, mineral formation in the absence of any inhibitor was usually observed at around 20 hours (Fig. 4A, control). The time delay corresponded to the required time of AMP hydrolysis by MV enzymes producing P_i, Ca^{2+} and P_i transports into MVs, ion accumulations inside MVs and formation of HA. Mineralization started when the Ca x P_i product in MVs was optimum. Addition of 0.25 mM or 1 mM cysteine, a TNAP inhibitor[29-32], in the same SCL medium increased the time of MV-induced mineralization from 20 hours to 28 hours or to 44 hours respectively, demonstrating that AMP was partially hydrolyzed by TNAP (Fig. 4A). 0.25 mM and 1 mM levamisole increased also the induction time of mineralization from 20 hours to ~24 hours and to ~28 hours (Fig. 4B), but was less

effective than cysteine. 0.25 mM to 1 mM theophylline prolonged the incubation time from about 20 hours to 24 hours or to 34 hours respectively (Fig. 4C). 1 mM theophylline was more effective than 1 mM of levamisole on increasing the induction time of mineral formation but less than cysteine. 0.25-1 mM SIN didnot cause any obvious delay, consistent with the fact that SIN is not an inhibitor of TNAP. However, a larger concentration of SIN (2-4 mM) produced a longer induction time in mineral formation (Fig. 4D), although 2-4 mM SIN did not inhibit TNAP.

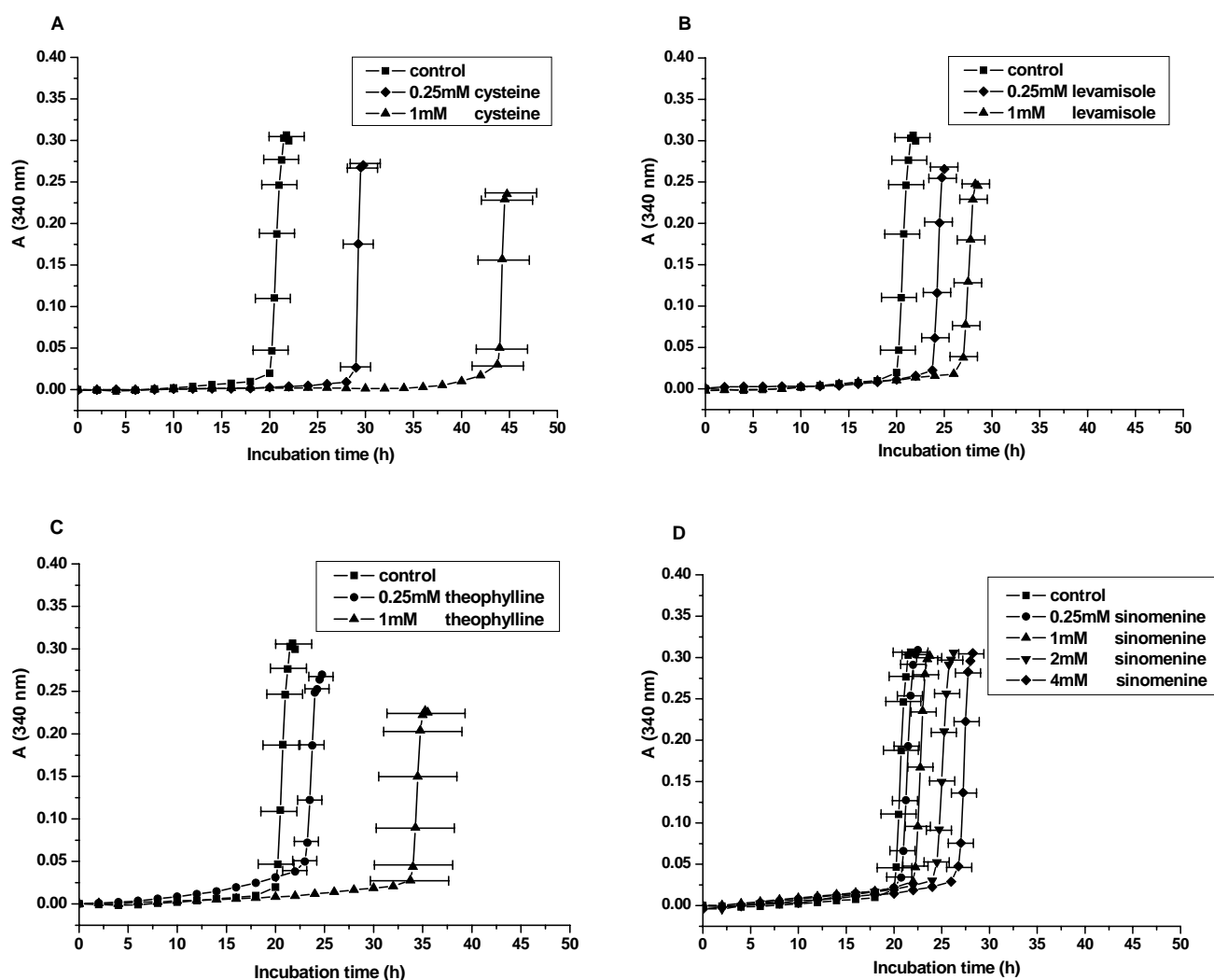Figure 4: Kinetics of mineral formation by matrix vesicles in SCL medium containing AMP. 15-20 µg/ml MVs were incubated at 37 °C in SCL buffer pH 7.4 containing 2 mM Ca^{2+}, 3.42 mM AMP with A) 0-1 mM cysteine; B) 0-1 mM levamisole; C) 0-1 mM theophylline; D) 0-4 mM sinomenine. At least three independent measurements were performed.

Inhibition of matrix vesicle induced mineral formation by sinomenine and theophylline in the presence of P_i.

Replacing 3.42 mM AMP (TNAP substrate) by 3.42 mM P_i in the SCL medium containing 2 mM Ca^{2+} and MVs, produced mineral formation at around 3 hours (Fig. 5A, control), being much shorter than that in the presence of AMP. Addition of cysteine activated slightly the mineralization (Fig. 5A), while addition of 1 mM to 4 mM levamisole increased the induction time of mineral formation from 3 hours to 7-10 hours respectively (Fig. 5B), confirming that at short incubation time levamisole inhibited P_i transport but this inhibition was lost at a longer incubation time[36]. Alternatively, this suggests that 1-4 mM levamisole partially inhibited the transport. 1-4 mM theophylline (Fig. 5C) as well as 1-4 mM SIN (Fig. 5D) both increased the induction time of mineral formation from about 3 hours to 5-8 hours.

Figure 5: Kinetics of mineral formation by matrix vesicles in SCL medium containing 3.42 mM P_i. 15-20 µg/ml MVs were incubated at 37 °C in SCL buffer pH 7.6 containing 2 mM Ca^{2+}, 3.42 mM P_i

with A) 0-4 mM cysteine; B) 0-4 mM levamisole; C) 0-4 mM theophylline; D) 0-4 mM sinomenine. At least three independent measurements were performed.

The change of P_i concentration from 3.42 to 1.42 mM decreased the amount of Ca x P_i product in MVs for mineralization and increased the induction time of mineral formation from 3 hours to about 7 hours (Fig. 6A). Addition of 1-4 mM levamisole (Fig. 6A), 1-4 mM theophylline (Fig. 6B) or 1-4 mM SIN (Fig. 6C) produced a longer induction time of mineral formation by several hours, up to 10 hours with the highest inhibitor concentrations.
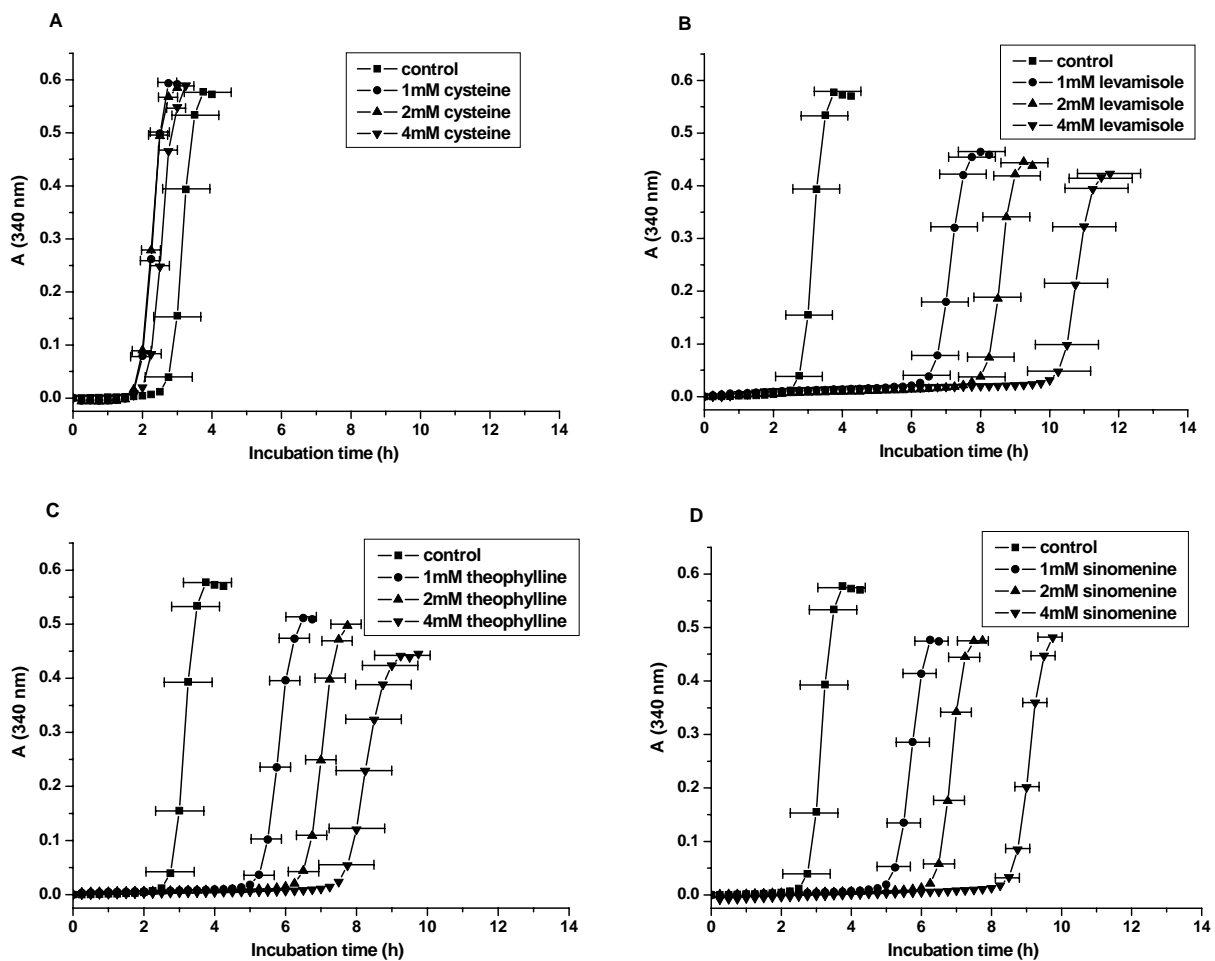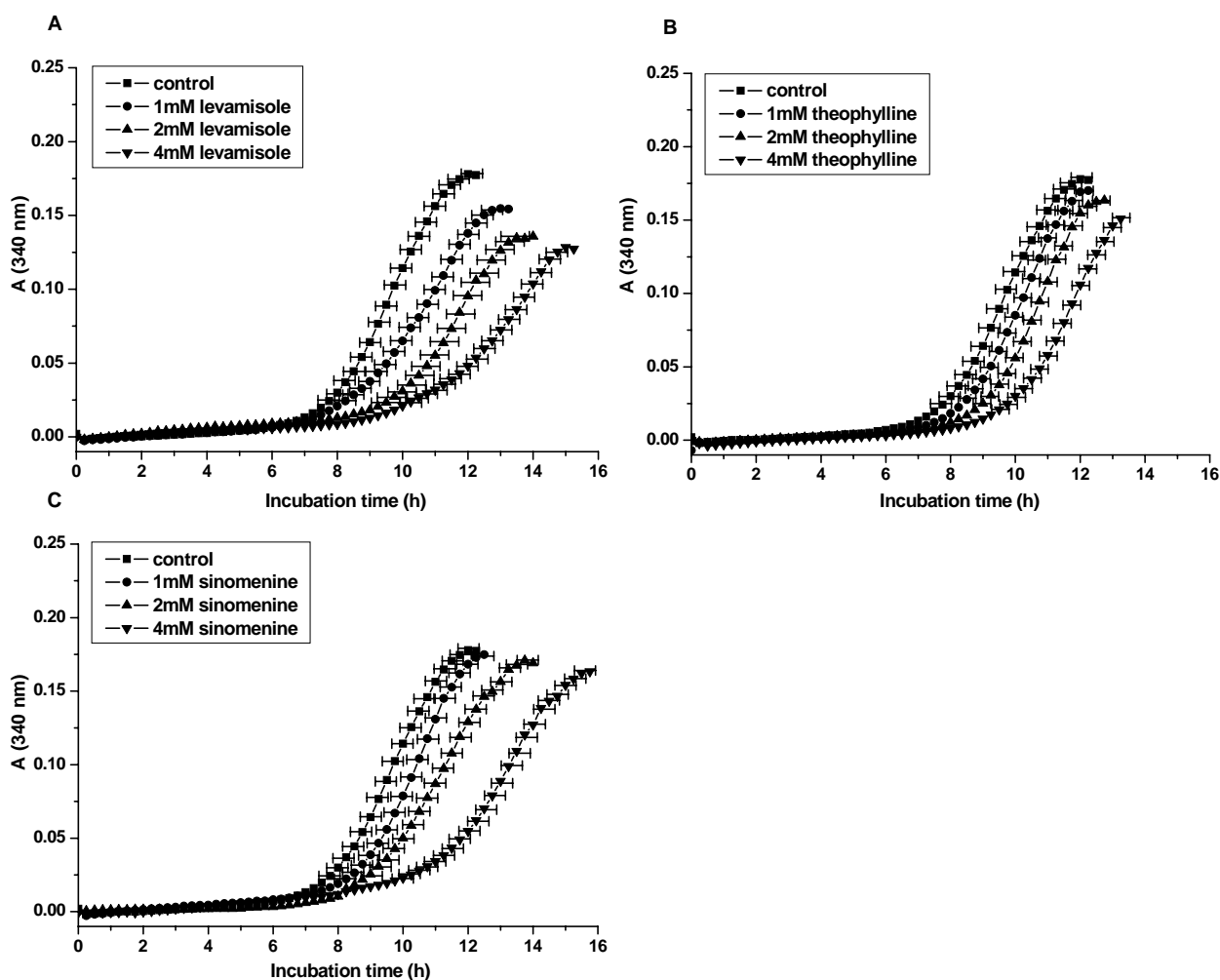

Figure 6: Kinetics of mineral formation by matrix vesicles in SCL medium containing 1.42 mM P_i. 15-20 µg/ml MVs were incubated at 37 °C in SCL buffer pH 7.6 containing 2 mM Ca^{2+}, 1.42 mM P_i with A) 0-4 mM levamisole; B) 0-4 mM theophylline; C) 0-4 mM sinomenine. At least three independent measurements were performed.

Inhibition of matrix vesicle induced mineral formation by sinomenine and theophylline in the presence of P_i and AMP.

To evaluate simultaneously P_i transport and AMP hydrolysis, the SCL medium containing MVs, 1.42 mM P_i, 2 mM AMP and 2 mM Ca^{2+} was used as mineralization buffer. The induction time of mineral formation produced by control MVs incubated without inhibitor at 37 °C was about 4 hours (Fig. 7), i.e. between the induction time observed with 3.42 mM AMP (20 hours) (Fig. 4A, control) and that obtained with 3.42 mM P_i (3 hours) (Fig. 5A, control). 1 mM cysteine decreased the induction time of mineral formation from 4 hours to 3 hours, while SIN, levamisole and theophylline delayed the mineralization process from 4 hours to 5-6 hours (Fig. 7).
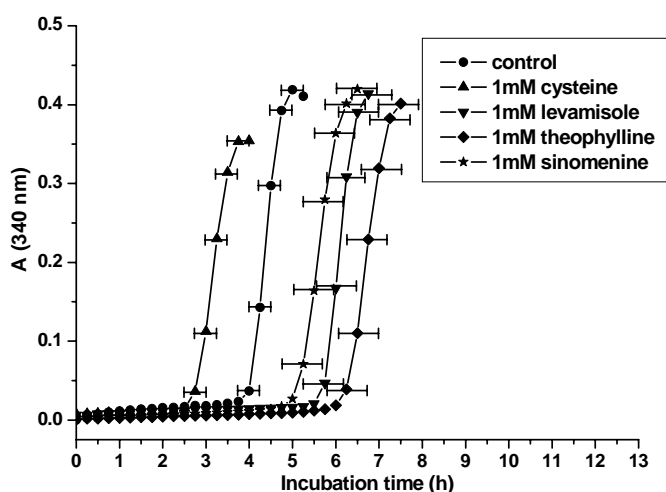
Figure 7: Kinetics of mineral formation by matrix vesicles in SCL medium containing 1.42 mM P_i and 2 mM AMP. 15-20 µg/ml MVs were incubated at 37 °C in SCL buffer pH 7.4 containing 2 mM Ca^{2+}. Further additions as indicated : (●) control: 1.42 mM P_i and 2 mM AMP; (▲) 1mM cysteine, 1.42 mM P_i and 2 mM AMP; (▼) 1mM levamisole, 1.42 mM P_i and 2 mM AMP; (◆)1mM theophylline, 1.42 mM P_i 2 mM AMP; (★)1mM sinomenine, 1.42 mM P_i and 2 mM AMP. At least three independent measurements were performed.

Discussions

Selection of mineralization model. The mechanism regulating physiological mineralization is very similar to that regulating pathological mineralization.[64] Under physiological conditions, MV-mediated mineralization occurs during bone formation. Under pathological calcifications, MVs are also present at the initial sites of HA

deposition.[17] In addition, calcification in atherosclerotic plaques occurs in association with extracellular vesicles similar to MVs.[17,65] The proteome of MVs has been recently identified,[65,66] providing more insight into the mechanisms of mineral formation and drug targets to prevent calcified diseases. MVs contain an enriched amount of several proteins implicated in the mineralization such as TNAP.[67,68] Recently, novel inhibitors of TNAP were found and were able to suppress *in vitro* calcification by cultured *Enpp*$^{1-/-}$ vascular smooth cells.[69] It was concluded that TNAP constitutes a good druggable target for the treatment and/or prevention of ectopic calcification.[69]

Inhibitors of alkaline phosphatase and mineral formation induced by matrix vesicles. Inhibitors of TNAP, cysteine[29-32], levamisole[33-36] and theophylline[37-42], increased the induction time of HA formation from 20 hours to 28-40 hours depending on the type and the concentration of inhibitor in mineralization medium containing AMP as a TNAP substrate. However, SIN which is not a TNAP inhibitor did not affect the induction time of HA formation significantly except at relatively higher concentrations. The induction time of mineral formation in the absence of P_i in the mineralization medium corresponded to the time required to hydrolyze AMP by TNAP within MVs, accumulate P_i and form HA. AMP hydrolysis is rapid but the mineral ion uptake did not occur until 20 hours and well after most of the AMP was hydrolyzed.[70] The driving force of Ca^{2+} and P_i uptakes inside MVs is controlled by gradient concentrations of Ca^{2+} and P_i. Both gradient concentrations are dependent (not necessarily in the same manner) on their respective bindings to the nucleation core[54] inside MVs as well as on $Ca_{10}(PO_4)_6(OH)_2$ formation depleting free Ca^{2+} and P_i inside MVs. At the highest concentration used (1 mM), the inhibitors were not efficient enough to inhibit completely AMP hydrolysis by TNAP, since HA formation was observed in all the cases, but it took a longer time than in the absence of inhibitors. Alternatively, other enzymes may also hydrolyze AMP. Concomitant addition of 2 mM AMP and 1.42 mM P_i shortened the induction time of HA from about 20 hours (with 3.42 mM AMP) to 4 hours, being consistent with the higher P_i concentration gradient that increased ion uptakes and HA formation.

Inhibitors of mineral formation through ion uptake. In mineralization medium containing 2 mM Ca^{2+} and 3.42 mM P_i, the induction time of HA formation by MVs reflected the time required for both Ca^{2+} and P_i uptakes inside MVs, their accumulations and their transformations into HA. Both D- and L- isomers of

tetramisole were able to inhibit Ca^{2+} and P_i uptakes by MVs, indicating that both enantiomers of tetramisole can act on distinct sites other than a TNAP since only L-isomer can inhibit TNAP.[36] In keeping with this finding, we observed longer induction time of HA formation in mineralization medium containing 2 mM Ca^{2+}, 3.42 mM P_i and 1-4 mM levamisole, as compared in the absence of levamisole. 1-4 mM cysteine, an inhibitor of TNAP, decreased slightly the induction time of mineral formation induced by MVs in SCL medium containing 2 mM Ca^{2+} and 3.42 mM P_i. Both theophylline and SIN were able to slow down mineral formation as indicated by the increase of the induction time of HA formation from 3 to about 7 hours depending on their different concentrations. Our findings indicated that levamisole and theophylline can inhibit TNAP and slow down HA formation in MVs, even in the presence of P_i, suggesting that both can interfere with Ca^{2+} and P_i uptakes. Consistent with the fact that TNAP is not coupled with Ca^{2+} and P_i uptakes[70,71], the TNAP inhibitor cysteine activated mineral formation, while SIN which is not a TNAP inhibitor slowed down HA formation.

Anti-rheumatic and anti-inflammatory mechanism of sinomenine. Our findings indicated that SIN can slow down MV-induced HA formation in a concentration-dependent manner, probably by interfering with Ca^{2+} and P_i uptakes into MVs. Such a phenomenon is consistent with recent reports that SIN exerts several cardioprotective actions on heart by inhibiting Ca^{2+} channel and simultaneously decreases K^+ and Na^+ channel currents under disease conditions.[72,73] We propose that SIN exerts its anti-rheumatic effect by slowing down pathological HA crystal formation in arthritis joints which may slow down the degeneration and inflammatory response. The anti-inflammatory effect of SIN may result indirectly from a decrease of HA deposition. Whether this mechanism occurs solely, or in a concomitant manner with other action mechanisms induced by SIN remains to be elucidated.

ACKNOWLEDGMENT

REFERENCES

1 Yamasaki H 1976 Pharmacology of sinomenine, an anti-rheumatic alkaloid from Sinomenium acutum. Acta Med Okayama **30:**1–20.

2 Liu L, Resch K, Kaever V 1994 Inhibition of lymphocyte proliferation by the anti-arthritic drug sinomenine. Int J Immunopharmacol **16:**685-691.

3 Liu L, Buchner E, Beitze D, Schmidt-Weber CB, Kaever V, Emmrich F, Kinne RW 1996 Ammelioration of rat experimental arthritides by treatment with the alkaloid sinomenine. Int J Immunopharmacol **18:**529-543.

4. Wang Y, Zhou L, Li R 2002 Study progress in sinomenium acutum (Thunb.) Rehd. et Wils. Zhong Yao Cai **25:**209-211.

5. Feng H, Yamaki K, Takano H, Inoue K, Yanagisawa R, Yoshino S 2007 Effect of sinomenine on collagen-induced arthritis in mice. Autoimmunity **40:**532-539.

6 Qian L, Xu Z, Zhang W, Wilson B, Hong J-S, Flood PM 2007 Sinomenine, a natural dextrorotatory morphinan analog, is anti-inflammatory and neuroprotective through inhibition of microglial NADPH oxidase. J Neuroinflammation **4:**23.

7 Rosenthal AK 2006 Calcium Crystal Deposition and Osteoarthritis. Rheum Dis Clin North Am **32:**401-412.

8 Sun Y, Hanley Jr EN 2007 Calcium–containing crystals and osteoarthritis. Curr Opin Orthop **18:**472-478.

9 McCarty DJ 1970 Crystal-induced inflammation of the joints. Annu Rev Med **21:**357-366.

10 EA HK, Uzan B, Rey C, Liote F 2005 Octacalcium phosphate crystals directly

stimulate expression of inducible nitric oxide synthase through p38 and JNK mitogrn-activated protein kinases in articular chondrocytes. Arthritis Res Ther **7:**R915-R926.

11 Liu-Bryan R, Pritzker K, Firenstein GS, Terkeltaub R 2005 TLR2 signaling in chondrocytes drives calcium pyrophosphate dihydrate and monosodium urate crystal-induced nitric oxide generation. J Immunol **174:**5016-5023.

12 Cooke MM, McCarthy GM, Sallis JD, Morgan MP. 2003 Phosphocitrate inhibits calcium hydroxyapatite induced mitogenesis and upregulation of matrix metalloproteinase-1, interleukin-1beta and cyclooxygenase-2 mRNA in human breast cancer cell lines. Breast Cancer Res Treat **79:**253-263.

13 Gueme PA, Terkeltaub R, Zyraw B, Lotz M 1989; Inflammatory microcrystals stimulate interleukin-6 production and secretion by human monocytes and synoviocytes. Arthritis Rheum **32:**1443-1452.

14 Nadra I, Mason JC, Philippidis P et al. 2005 Proinflammatory activation of macrophages by basic calcium phosphate crystals via protein kinase C and MAP kinase pathways: a vicious cycle of inflammation and arterial calcification? Cir Res **96:**1248-1256.

15 Reginatto AM, Olsen BR 2007 Genetics and Experimental models of crystal-induced arthritis. Lessons learned from mice and men: is it crystal clear? Curr Opin Rheumatol **19:**134-145.

16 Anderson HC, Garimella R, Tague SE 2005 The role of matrix vesicles in growth plate development and biomineralization. Front Biosci **10:**822-837.

17 Anderson HC 2007 The role of matrix vesicles in physiological and pathological calcification. Curr Opin Orthop **18:**428-433.

18 Anderson HC 1983 Calcific diseases. A concept. Arch Pathol Lab Med **107:**341-348.

19 Anderson HC 1988 Mechanisms of pathological calcification. Rheum Dis Clin North Am **14:**303-319.

20 Pritzker KP 1980 Crystal-associated arthropathies: what's new in old joints. J Am Geriatr Soc **28:**439-445.

21 Ali SY 1985 Apatite-type crystal deposition in arthritic cartilage. Scan Electron Microsc **4:**1555-1566.

22 Anderson HC 2003 Matrix vesicles and calcification. Curr Rheumatol Rep **5:**222-226.

23 Derfus BA, Kranendonk S, Camacho N, Mandel N, Kushnaryov V, Lynch K, Ryan L 1998 Human osteoarthritic cartilage matrix vesicles generate both calcium pyrophosphate dihydrate and apatite in vitro. Calcif Tissue Int **63:**258-262.

24 Derfus BA, Kurtin SM, Camacho NP, Kurup I, Ryan LM 1996 Comparison of matrix vesicles derived from normal and osteoarthritic human articular cartilage. Connect Tissue Res **35:**337-342.

25 Cheung HS, Kurup IV, Sallis JD, Ryan LM 1996 Inhibition of calcium pyrophosphate dihydrate crystal formation in articular cartilage vesicles and cartilage by phosphocitrate. J Biol Chem **271:**28082-28085.

26 Derfus BA, Camacho NP, Olmez U, Kushnaryov VM, Westfall PR, Ryan LM, Rosenthal AK 2001 Transforming growth factor beta-1 stimulates articular chondrocyte elaboration of matrix vesicles capable of greater calcium pyrophosphate precipitation. Osteoarthritis Cartilage **9:**189-194.

27 Gohr C 2004 *In vitro* models of calcium crystal formation. Curr Opin Rheumatol **16:**263-267.

28 Thouverey C, Bechkoff G, Pikula S, Buchet R 2008 Inorganic pyrophosphate as a

regulator of hydroxyapatite or calcium pyrophosphate dihydrate mineral deposition by matrix vesicles. Osteoarthritis Cartilage. Doi:10.1016/j.joca.2008.05.020

29 Cox RP, MacLeod CM 1963 Repression of alkaline phosphatase in human cell cultures by cystine and cysteine. Proc Natl Acad Sci USA **49:**504-510

30 Agus SG, Cox RP, Griffin MJ 1966 Inhibition of alkaline phosphatase by cysteine and its analogues. Biochim Biophys Acta **118:**363-370.

31 Zhu CM, Chen QC, Lin HN et al. 1999 Kinetics of inhibition of green crab (Scylla serrata) alkaline phosphatase by L-cysteine. J Protein Chem **18:**603-607.

32 Pauline PL, Florence WL, Tssui RV, Jindrah H. Tupy and Pritzker KPH 2007 Inhibition of alkaline phosphatase by cysteine: Implications for calcium pyrophosphate dihydrate crystal deposition disease. J Rheumatol **34:**1313-1322.

33 Borgers M 1973 The Cytochemical Application of New Potent Inhibitors of Alkaline Phosphatases. J Histochem Cytochem **21:**812-824.

34 Van Belle H 1976 Alkaline Phosphatase. I Kinetics and inhibition by levamisole of purified isoenzymes from humans. Clin Chem **22:**972-976.

35 Reynolds JT and Dew GW 1977 Comparison of the inhibition of avian and mammalian bone alkaline phosphatases by levamisole and compound R8231. Experientia **33:**154-155.

36 Register TC, Warner GP, Wulthier RE 1984 Effect of L and D tetramisole on 32Pi and 45Ca uptake and mineralization by matrix vesicle-enriched fractions from chicken epipheseal cartilage. J Biol Chem **259:**922-928.

37 Zizian BV, Gauthier B 1978 Characteristics of the inhibition of serum alkaline phosphatase by theophylline. Clin Biochem **11:**57-61.

38 Farley JR, Ivey JL, Baylink DJ 1980 Human skeletal alkaline phosphatase. Kinetic studies including pH dependence and inhibition by theophylline. J Biol Chem

255:4680-4686.

39 Dai X, Snow LD 1991 Differential theophylline inhibition of alkaline phosphatase and 5'-nucleotidase of bovine milk fat globule membranes. Int J Biochem **23:**743-747.

40 Rezende LA, Ciancaglini P, Pizauro JM, Leonoe FA 1998 Inorganic pyrophosphate-phosphohydrolytic activity associated with rat osseous phosphate alkaline phosphatase. Cell Mol Biol **44:**293-302.

41 Glogowski J, Danforth DR, Ciereszko A 2002 Inhibition of alkaline phosphatase activity of boar semen by pentoxifylline, caffeine and theophylline. Andrology **23:**783-792.

42 Kozlenkov A, Le Du MH, Cuniasse P, Ny T, Hoylaerts MF, Millan JL 2004 Residues determining the binding specificity of uncompetitive inhibitors to tissue-nonspecific alkaline phosphate. J Bone Miner Res **19:**1862-1872.

43 Schuermans Y. 1975 Levamisole in rheumatoid arthritis. Lancet **1:**111.

44 McGill PE 1976 Levamisole in rheumatoid arthritis. Lancet **2:**149

45 Jacobson KA, Van Rhee AM 1997 Development of selective purinoreceptor agonists and antagonists. In Jacobson KA, Jarvis MF editors. Purinergic approaches in experimental therapeutics. New York: Wiley 101-128.

46 Montesinos MC, Yap JS, Desai A, Posadas I, McGrary CT, Cronstein BN 2000 Reversal of the anti-inflammatory effects of methothrexate by the non selective adenosine receptor antagonists theophylline and caffeine. Arthritis Rheum **43:**656-663.

47 Wu LN, Genge BR, Dunkelberger DG, LeGeros RZ, Concannon B, Wuthier RE 1997 Physicochemical characterization of the nucleational core of matrix vesicles. J Biol Chem **272:**4404-4411.

48 Balcerzak M, Radisson J, Azzar G, Farlay D, Boivin G, Pikula S, Buchet R 2007 A comparative analysis of strategies for isolation of matrix vesicles. Anal Biochem **361:**176-182.

49 Bradford MM 1976 A rapid and sensitive method for the quantitation of microgram quantities of protein utilizing the principle of protein-dye binding. Anal Biochem **72:**248-254.

50 Laemmli UK 1970 Cleavage of structural proteins during the assembly of the head of bacteriophage T4. Nature **227:**680–685.

51 Cyboron GW, Wuthier RE 1981 Purification and initial characterization of intrinsic membrane-bound alkaline phosphatase from chicken epiphyseal cartilage, J Biol Chem **256:**7262-7268.

52 Wu, LN, Sauer GR, Genge BR, Valhmu WB, Wuthier RE 2003 Effects of analogues of inorganic phosphate and sodium ion on mineralization of matrix vesicles isolated from growth plate cartilage of normal rapidly growing chickens. J Inorg Biochem **94:**221-235.

53 Li L, Buchet R, Wu Y. 2008 DMSO-induced hydroxyapatite formation: A biological model of matrix-vesicle nucleation to screen inhibitors of mineralization. Anal Biochem **381:**123-128.

54 Wu LN, Yoshimori T, Genge BR, Sauer GR, Kirsch T, Ishikawa Y, Wuthier RE 1993 Characterization of the nucleational core complex responsible for mineral induction by growth plate cartilage matrix vesicles. J Biol Chem **268:**25084-25094.

55 Wuthier RE, Chin JE, Hale JE, Register TC, Hale LV, Ishikawa Y 1985 Isolation and characterization of calcium-accumulating matrix vesicles from chondrocytes of chicken epiphyseal growth plate cartilage in primary culture. J Biol Chem **260:**15972-15979.

56 Kirsch T, Ishikawa Y, Mwale F, Wuthier RE 1994 Roles of the nucleational core complex and collagens (types II and X) in calcification of growth plate cartilage matrix vesicles. J Biol Chem **269:**20103-20109.

57 Zhang L, Balcerzak M, Radisson J, Thouverey C, Pikula S, Azzar G, Buchet R 2005 Phosphodiesterase activity of alkaline phosphatase in ATP-initiated Ca^{2+} and phosphate deposits in isolated matrix vesicles. J Biol Chem **280:**37289-37296.

58 Blumenthal NC 1989 Mechanisms of inhibition of calcification. Clin Orthop Relat Res **247:**279-289.

59 Register TC, Wuthier RE 1985 Effect of pyrophosphate and two diphosphonates on 45Ca and $32P_i$ uptake and mineralization by matrix vesicle-enriched fractions and by hydroxyapatite. Bone **6:**307-312.

60 Tanimura A, McGregor DH, Anderson HC. 1983 Matrix vesicles in arthrosclerotic calcification. Proc Soc Exp Biol Med **172:**173-177.

61 Tenenbaum HC 1987 Levamisole and inorganic pyrophosphate inhibit beta-glycerophosphate induced mineralization of bone formed in vitro. Bone Miner **3:**13-26.

62 Terkeltaub RA 2001 Inorganic pyrophosphate generation and disposition in pathophysiology. Am J Physiol Cell Physiol **281:** C1-C11.

63 Hamade E, Azzar G, Radisson J, Buchet R, Roux B 2003 Chick embryo anchored alkaline phosphatase and mineralization process in vitro. Influence of Ca^{2+} and nature of substrates. Eur J Biochem **270:** 2082-2090.

64 Kirsch T 2007 Physiological and pathological mineralization: a complex multifactorial process. Curr Opin Orthop **18:** 425-427.

65 Xiao Z, Camalier CE, Nagashima K, Chan KC, Luca DA, de la Cruz MJ, Gignac M, Lockett S, Issaq HJ, Veenstra TD, Conrads TP, Beck GR Jr. 2007 Analysis of the

extracellular matrix vesicle proteome in mineralizing osteoblast. J Cell Physiol **210:**325-335.

66 Balcerzak M, Malinowska A, Thouverey C, Sekrecka A, Dadlez M, Buchet R, Pikula S 2008 Proteome analysis of matrix vesicles isolated from femurs of chicken embryo. Proteomics **8:**192-205.

67 Balcerzak M, Hamade E, Zhang L, Pikula S, Azzar G, Radisson J, *et al*. 2003 The roles of annexins and alkaline phosphatase in mineralization process. Acta Biochim Pol **50:**1019-1038.

68 Golub EE, Boesze-Battaglia K 2007 The role of alkaline phosphatase in mineralization. Curr Opin Orthop**18:**444-448.

69 Narisawa S, Harmey D, Yadav MC, O'Neil WC, Hoylaerts MF, Millan JL 2007 Novel inhibitors of alkaline phosphatase suppress vascular muscle cell calcification. J Bone Miner Res **22:**1700-1710.

70 Genge BR, Sauer GR, Wu LNY, Mclean FM, Wuthier RE 1988 Correlation between loss of alkaline phosphatase activity and accumulation of calcium during matrix vesicles-mediated mineralization. J Biol Chem **263:**18513-18519.

71 Montesuit C, Caverzasio J, Bonjour JP 1991 Characterization of a Pi transport system in cartilage matrix vesicles. Potential role in the calcification process. J Biol Chem **266:**17791-17797.

72 Satoh H 2005 Electropharmacological actions of the constituents of Sinomeni Caulis et Rhizome and Mokuboi-to in guinea pig heart. Am J Chin Med **33:**967–979.

73 Nishida S and Satoh H 2007 Vascular Pharmacology of Mokuboito (Mu-Fang-Yi-Tang) and Its Constituents on the Smooth Muscle and the Endothelium in Rat Aorta. Evid Based Complement Alternat Med. **4:**335-341.

CHAPTER IV

Concluding remarks and Perspectives

Although chiral recognition of biologically important substrates by enzymes and other biological macromolecules is well known, the detailed molecular mechanisms involved in these specific interactions are only partially elucidated. During the preparation of my Ph D thesis, BSA was selected as a protein model which can recognize specific stereoisomer interactions since it has been used as chiral stationary phase for years in HPLC [1,2]. It was confirmed that BSA was able to recognize specifically the enantiomeric form of amino acids, by determining enantioselective ratios (K_L/K_D) of amino acid derivatives such as dansyl-D,L-phenylalanine, dansyl-D,L-tryptophan and dansyl-D,L-serine. The findings indicated that the complex binding was controlled by both the size and the chirality of side groups of amino acids. The L-enantiomers of dansyl-phenylalanine and dansyl-tryptophan with aromatic side-chain were more selective to bind to BSA in comparison to dansyl-L-serine with aliphatic side-chain. This supports the view that the steric bulkiness and the aromaticity of the side group are important parameters in the chiral recognition mechanism. Indeed, the shapes of the ligand and the cleft of the binding site control the selectivity of the interaction. The weak interactions, such as in this case hydrophobic interaction of the aromatic moiety, can increase the selectivity of the interaction as well as hydrogen bond formation involving NH (as in tryptophanyl residue). One question that one may ask is the general nature of the interactions involving amino acids such as ligand binding to proteins. In fact, not only BSA can recognize specifically enantiomeric amino acids as demonstrated but also the alkaline phosphatase can distinguish enantiomeric amino acids since its isozymes are inhibited by L-phenylalanine and L-tryptophan [3-5].

One application of the ligand recognition by enzymes, such as alkaline phosphatase is the search for new inhibitors. The search for inhibitors is of prime importance for characterizing enzymes (isolation and purification, function and roles, etc…) and for medical applications (many drugs target specifically enzymes, diagnostic tools are often based on Western blot or on enzymatic activity). In this respect, alkaline phosphatase is a good example for two reasons. The first reason is that there are several isoforms of alkaline phosphatase, which do not necessarily interact in the same manner with the inhibitors, thereby providing new insight into the specificity of

the interactions. Some isoforms are tissue specific while others not, necessitating the need to design specific inhibitors. For example levamisole can inhibit tissue non-specific alkaline phosphatase (TNAP) while it does not inhibit bovine intestinal alkaline phosphatase (BIAP) [6]. The second reason is that TNAP is a marker in mineral formation and it is enriched in matrix vesicles (MVs) implicated in the initiation of mineral formation. Such inhibitors could be used to prevent pathological ectopic calcification. Dansyl derivatives and a library of benzothiophene compounds, as well as tetramisole derivatives were tested for the eventual inhibition of BIAP and of TNAP activities. During the search for inhibitors, a series of benzothiophene compounds was found to inhibit TNAP or BIAP. Due to their poor solubility, DMSO (up to 4% v/v) was added to better mix and solubilize the benzothiophene compounds. However, increasing DMSO concentration led more or less in several instances to a decrease of inhibition effect. Nevertheless, these findings based on a relatively large set of benzothiophene compounds, suggested that several benzothiophene compounds have the potential to inhibit TNAP, although artifacts due to their poor solubility cannot be completely neglected. Therefore, a series of racemic benzothiophene with levamisole moiety, water-soluble compounds were checked for the inhibition of TNAP. One advantage to find water soluble inhibitors is that the active site of TNAP is outside the cell in contact with aqueous extracellular medium and this minimizes their insertion into the hydrophobic portion of plasma membranes of cells. Two water-soluble benzothiophene derivatives were found to inhibit TNAP.

As reported before, putative specific inhibitors could serve as a therapeutical option for curing osteoarthritis [7-12], which is associated with excessive and uneven calcification produced during ageing, calcification diseases, environmental stress, etc… Indeed, levamisole, a TNAP inhibitor, has been used to cure osteoarthritis [13-15]. However, the calcification process could be also induced by other factors (Fig. 1).

MVs, which initiate mineralization, could be a therapeutical target to cure calcified diseases since it is not only enriched with TNAP but also with other enzymes implicated in P_i as well as in Ca^{2+} homeostasis. We hypothesized that some useful drugs for curing arthritis or rheumatoid disease could target several specific sites within MVs by interfering with their distinct functions.
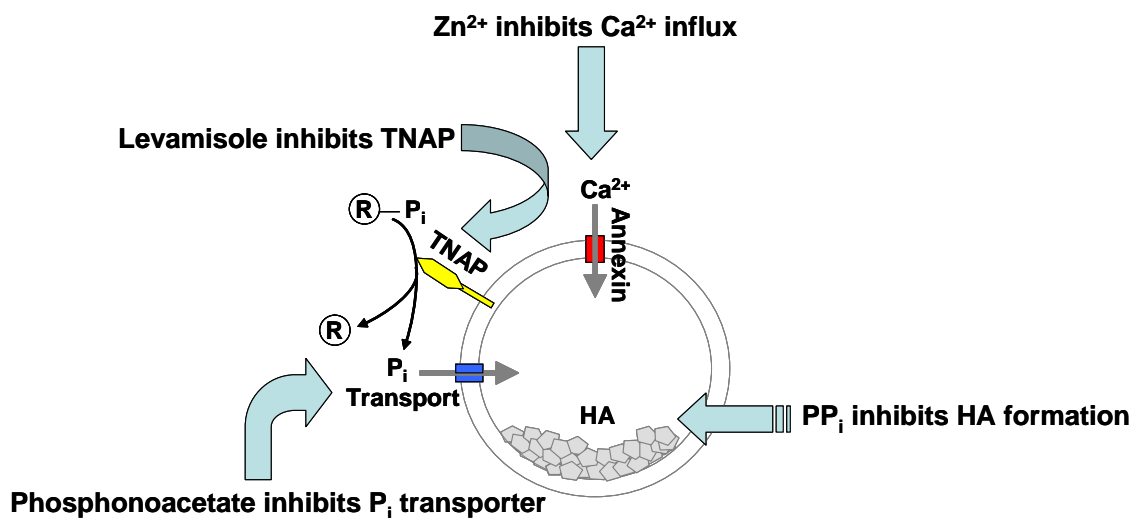
Fig 1 Matrix vesicle induces the initial step of mineral formation. Four putative drug targets are indicated to prevent mineral formation: 1) TNAP; 2) Annexins Ca^{2+} channels; 3) P_i transporters and 4) HA formation.

Figure 1 shows how MVs can initiate HA. To sustain HA formation, P_i and Ca^{2+} must be continuously supplied into MVs through their specific ion transporters. Extracellular P_i may be not sufficient to continuously promote HA formation; therefore, several enzymes such as TNAP are implicated in the P_i supplementation. The situation is rendered complicated by the presence of PP_i, a known inhibitor of HA formation, which can be hydrolyzed by TNAP. Thus to prevent calcified diseases associated with HA deposits initiated by MVs, at least four distinct sites could be targeted. 1) TNAP, producing P_i from a phosphate substrate inhibited by levamisole [13-15].   2) Annexins, calcium channels inhibited by Zn^{2+} [16]. 3) P_i transporters inhibited by phosphonoacetate or arsenate [17,18]. 4) HA formation directly prevented by PP_i [19,20]. Although MVs can address adequately several mechanisms of mineralization [21], they do not address cellular issues, such as inflammation responses. Nevertheless, it was found that the anti-inflammatory and anti-rheumatic Chinese medicine sinomenine, which is not an inhibitor of TNAP activity, slowed down the calcification in a similar manner as theophylline but to a lesser extent than levamisole. The inhibition effects were probably caused by interfering with P_i or Ca^{2+} transports.

Therefore, it is tempting to suggest that sinomenine may have distinct effects: inhibition of mineralization and anti-inflammatory response. Whether excessive calcification can lead to inflammation or inflammation can induce calcification is still not clear. HA, the main mineral component of bones, can be directly inhibited by PP_i. In this respect, I developed a new model containing 4% (v/v) DMSO in mineralization medium which can produce HA and served to screen inhibitors for HA formation. HA deposit has been found in arthritic cartilage. Therefore, direct inhibition of HA may serve as a therapeutical target to prevent calcium crystal deposits in cartilage.

The search for inhibitors which prevent pathological calcification is not only restricted to their actions on TNAP activity, but also on HA formation [19,20], on Pi transporter [17,18] or Ca^{2+} transport channel [22-24]. Such inhibitors could be very important therapeutic targets for osteoarthritis. However, other factors such as inflammatory responses or levels of expression of proteins involved in mineralization still need to be recognized by using cellular models such as osteoblasts, osteoclasts and chondrocytes.

REFERENCES

[1] Allenmark, S., Bomgren, B., Boren, H. (1983) Direct liquid chromatographic separation of enantiomers on immobilized protein stationary phases III. Optical resolution of a series of N-aroyl D,L-amino acids by high-performance liquid chromatography on bovine serum albumin covalently bound to silica. J. Chromatogr. A; 264: 63-68.

[2] Allenmark, S. (1986) Optical Resolution by Liquid Chromatography on Immobilized Bovine Serum Albumin. J. Liq. Chromatogr.; 9: 425-442.

[3] Fishman, W.H., Sie, H.G. (1971) Organ-specific inhibition of human alkaline phosphatase isoenzymes of liver, bone, intestine and placenta; L-phenylalanine, L-tryptophan and L-homoarginine. Enzymologia; 41: 140-167.

[4] Lin, C.W., Sie, H.G., Fishman, W.H. (1971) L-tryptophan. A non-allosteric organ-specific uncompetitive inhibitor of human placental alkaline phosphatase. Biochem. J.; 124: 509-516.

[5] Kozlenkov, A., Du, M.H., Cuniasse, P., Ny, T., Hoylaerts, M.F. and Millan, J.L. (2004) Residues Determining the Binding Specificity of Uncompetitive Inhibitors to Tissue-Nonspecific Alkaline Phosphatase. J. Bone Miner. Res.; 19: 1862-1872.

[6] Van Belle, H. (1976) Alkaline phosphatase. I. Kinetics and inhibition by levamisole of purified isoenzymes from humans. Clin. Chem; 22: 972-976.

[7] Ali, S.Y., Wisby, A. (1978) Apatite crystal nodules in arthritic cartilage. Europ. J. Rheumatol. Inflam.; 1: 115-119.

[8] Einhorn, T.A., Gordon, S.L., Siegel, S.A., Hummel, C.F., Avitable, M.J., Carty, R.P. (1985) Matrix vesicle enzymes in human osteoarthritis. J. Orthop. Res.; 3: 160-169.

[9] Hoyland, J.A., Thomas, J.T., Denn, R., Marriott, A., Ayad, S., Boot-Handford, R.P., Grant, M.E., Freemont, A.J. (1991) Distribution of type X collagen mRNA in normal and osteoarthritic human cartilage. Bone Miner.; 15: 151-163.

[10] Hashimoto, S., Ochs, R.L., Komiza, S., Lotz, M. (1998) Linkage of chondrocyte apoptosis and cartilage degradation in human osteoarthritis. Arthritis Rheum.; 41: 1632-1638.

[11] Masuhara, K., Bak Lee, S., Nakai, T., Sugano, N., Ochi, T., Sasaguri, Y. (2000) Matrix metalloproteinases in patients with osteoarthritis of the hip. Int. Orthop.; 24: 92-96.

[12] Lang, A., Hörler, D., Baici, A. (2000) The relative importance of cysteine peptidases in osteoarthritis. J. Rheumatol.; 27: 1970-1979.

[13] Tenenbaum, H.C. (1987) Levamisole and inorganic pyrophosphate inhibit beta-glycerophosphate induced mineralization of bone formed in vitro. Bone Miner.; 3: 13-26.

[14] Schuermans, Y. (1975) Levamisole in rheumatoid arthritis. Lancet; 1: 111.

[15] McGill, P.E. (1976) Levamisole in rheumatoid arthritis. Lancet; 2: 149.

[16] Gerke, V. and Moss, S.E. (2002) Annexins: From Structure to Function. Phys. Rev. 82: 331-371.

[17] Solomon, D.H., Wilkins, R.J., Meredith, D. and Browing, J.A. (2007) Characterization of Inorganic phosphate transport in bovine articular chondrocyres. Cell. Phys. Biochem. 20: 99-108.

[18] Wu, L.N., Sauer, G.R., Genge, B.R., Valhmu, W.B., Wuthier, R.E. (2003) Effects of analogues of inorganic phosphate and sodium ion on mineralization of matrix vesicles isolated from growth plate cartilage of normal rapidly growing chickens. J. Inorg. Biochem.; 94: 221-235.

[19] Register, T.C., Wuthier, R.E. (1985) Effect of pyrophosphate and two diphosphonates on 45Ca and 32P$_i$ uptake and mineralization by matrix vesicle-enriched fractions and by hydroxyapatite. Bone; 6: 307-312.

[20] Li, L., Buchet, R., Wu, Y. (2008) DMSO-induced hydroxyapatite formation: A biological model of matrix-vesicle nucleation to screen inhibitors of mineralization. Anal. Biochem.; 381: 123-128.

[21] C Gohr. (2007) *In vitro* models of calcium crystal formation, Curr. Opin. Rheumatol. 16 (2004) 263-267.

[22] Register, T.C., Warner, G.P., Wulthier, R.E. (1984) Effect of L and D tetramisole on 32Pi and 45Ca uptake and mineralization by matrix vesicle-enriched fractions from chicken epipheseal cartilage. J. Biol. Chem.; 259: 922-928.

[23] Chen, N.X., O'Neill, K.D., Chen, X., Moe, S.M. (2008) Annexin Mediated Matrix Vesicle Calcification in Vascular Smooth Muscle Cells. J. Bone Miner. Res.; doi: 10.1359/jbmr.080604.

[24] Kim, H.J., Kirsch, T. (2008) Collagen/annexin V interactions regulate chondrocyte mineralization. J. Biol. Chem.; 283: 10310-10317.

LIST OF PUBLICATIONS

Experimental papers:

-**Li L**, Chen K, Chang L, Jia S, Huang X, Wu Y. (2004) Spectroscopic Studies on the Chiral Discrimination of DNS-Amino Acids by Proteins. *Spectroscopy and Spectral Analysis*, 24: 119-120.

-Hao Y, **Li L**, Wu Y, Liu J, Luo G. (2004) Two-dimensional correlation spectroscopic studies on the recognition mechanism of a glutathione peroxidase mimic, bis-cyclodextrin diselenide. *Vibrational Spectroscopy*, 36: 185-189.

-Jia S, Hao Y, **Li L**, Chen K, Wu Y, Liu J, Wu L, Ding Y. (2005) High Chiral Discrimination of 2,2′-Ditellurobis(2-deoxy-β-cyclodextrin) in Recognition of Dansyl-D/L-phenylalanine. *Chemistry Letters*, 34: 1248-1249.

-Zhai C, Ma L, **Li L**, Wu Y, Li W, Wu L. (2006) Study on Interracial Adsorption Behavior of Bovine Serum Albumin on Air-water Interface and Its Interaction with Chiral Probes D/L-N-[4-(1-Pyrene) butyroyl]-phenylalanine. *Chemical Journal of Chinese Universities*, 27: 1545-1548.

-**Li L**, Wu Y and Buchet R. (2008) Chiral Discrimination of Bovine Serum Albumin toward Dansyl-derivatives of D,L-phenylalanine, D,L-tryptophan and D,L-serine in Solution. *Manuscript submitted.* *

-**Li L**, Chang L, Rostaing S, Lemaire M, Buchet R and Wu Y. (2008) Tetramisole derivative Inhibitors of tissue non-specific alkaline phosphatase and of basic calcium phosphate crystals. *Manuscript submitted.**

-**Li L**, Wu Y, Buchet R. Kinetic and inhibition studies of dansyl-L-phenylalanine and L-phenylalanine on calf intestinal alkaline phosphatase. *Spectroscopy and Spectral Analysis.* Accepted.

-**Li L**, Buchet R, Wu Y. (2008) Dimethyl sulfoxide-induced hydroxyapatite formation: A biological model of matrix vesicle nucleation to screen inhibitors of mineralization. *Analytical Biochemistry*, 381: 123–128. *

-**Li L**, Buchet R and Wu Y. (2008) Sinomenine, theophylline, cysteine and levamisole: Comparisons of their effects on mineral formation induced by matrix vesicles. *Manuscript submitted.**

*Publications reported in the PhD thesis.

Oral presentation

-**Li L**. Spectroscopic Studies on the Chiral Discrimination of DNS-Amino Acids by Proteins. The 13th National Conference on Molecular Spectroscope in Xiamen, China, November 2004.

Poster presentation

-**Li L**, Buchet R, Wu Y. (2008). Spectroscopic studies on the DMSO-induced hydroxyapatite formation and screening test. The 15th National Conference on Molecular Spectroscope in Beijing, China, October 2008.

Specific recognition and enzymatic inhibition: chemical and biochemical aspects of mineralization mechanisms

The specific recognition of three amino acid derivatives by bovine serum albumine (BSA) indicated that BSA could interact selectively with stereoisomers. Such property was also observed in the case of alkaline phosphatase, which could have medical applications. Tissue non-specific alkaline phosphatase (TNAP), a marker in mineral formation, is enriched in matrix vesicles (MVs) implicated in the initiation of mineral formation. Molecular recognition was exploited by searching inhibitors acting at four distinct levels of mineralization: 1) the enzyme TNAP, 2) hydroxyapatite (HA) formation, 3) the organelle MV, 4) the calcium and phosphate fluxes. Such specific inhibitors could serve as therapeutical options for curing osteoarthritis. We found that benzothiophene derivative tetramisoles are water soluble specific inhibitors of TNAP. A new model which can produce HA as MVs was developed and inhibitors of HA formation were screened, providing evidence that several nucleotides are inhibitors of HA formation. MVs which initiate calcification in osseous tissues undergoing both physiological and pathological calcifications served to determine the effects of Chinese drugs on mineralization. We demonstrated that the anti-rheumatic Chinese medicine sinomenine having no effect on TNAP and theophylline a TNAP inhibitor, both slowed down the HA formation by interfering probably with P_i or Ca^{2+} transports. Although the mineralization models do not address cellular issues, they presented great potential to screen putative drugs to cure osteoarthritis.

Keywords: Alkaline phosphatase, anti rheumatic, benzothiophene, inhibitors, matrix vesicles, mineralization, osteoarthritis, recognition, sinomenine, theophylline, pathological calcification.

特效识别和酶活性抑制：矿化机理的化学和生物化学方面

牛血清白蛋白对三种手性氨基酸衍生物的特效识别表明，该蛋白分子能够与立体异构体发生选择性作用。同样，我们观察到具有医学应用价值的碱性磷酸酶也有类似的特性。组织非特异性碱性磷酸酶(TNAP)作为矿物形成的标记，富集于引发矿化的基质囊泡中。分子识别研究被应用并扩展至探寻四个不同方面的矿化的特效抑制剂分子：1) TNAP，2) 羟磷灰石(HA)的形成，3) 基质囊泡细胞器，4) 钙离子和无机磷酸的流通量。这些特效的抑制剂分子可以作为骨关节炎的治疗靶点。我们发现苯并噻吩修饰的四咪唑是TNAP 特效的水溶性抑制剂。同时，我们构建了一个类似基质囊泡可以诱导羟磷灰石形成的新模型，并利用此模型筛选了 HA 的抑制剂，证明了几种核苷酸对 HA 的抑制作用。我们选取在生理和病理条件下都能引发骨组织钙化的基质囊泡，来检测不同中药对矿化过程的影响。结果表明，抗风湿类中药青藤碱对 TNAP 没有抑制作用，但却与 TNAP 的一种抑制剂——茶碱类似，可以通过抑制钙和磷的传输来减缓矿化的形成。尽管矿化的模型没有提供细胞的信息，但却为筛选骨关节炎的可行性药物发挥了巨大的潜在作用。

关键词：碱性磷酸酶，抗风湿，苯并噻吩，抑制剂，基质囊泡，矿化，骨关节炎，识别，青藤碱，茶碱，病理钙化。

RESUME en français
Trois dérivés d'amino acides sont reconnus d'une manière stéréo sélective par l'albumine du sérum bovin. Cette propriété a été observée dans le cas de la phosphatase alcaline de tissu non spécifique, (TNAP). Des inhibiteurs agissant à trois niveaux distincts sur les processus de minéralisation ont été cherchés: 1) TNAP ; 2) Formation de l'hydroxyapatite (HA); 3) Vésicules maticielles (VMs). Nous avons trouvé que des dérivés de benzothiophènes et de tétramisoles, solubles dans l'eau, sont des inhibiteurs spécifiques de TNAP. Un modèle qui permet de produire du HA, a été développé et a confirmé que les nucléotides sont des inhibiteurs de formation de HA. Nous avons montré que le médicament anti-rhumatisme sinomenine, n'ayant aucun effet sur le TNAP, ainsi que la théophylline ralentissaient tous les deux la formation de HA induits par les VMs. Ces modèles de minéralisation présentent un grand potentiel lors du criblage de médicaments pour le traitement de l'ostéoarthrose.

MOTS-CLES
Alcaline phosphatase, anti rhumatisme, benzothiophene, calcification pathologique, inhibiteurs, minéralisation, ostéoarthrose, reconnaissance, sinomenine, theophylline, vésicules matricielles.

TITRE en anglais
Specific recognition and enzymatic inhibition: chemical and biochemical aspects of mineralization mechanisms

RESUME en anglais
Three amino acid derivatives were stereoselectively recognized by bovine serum albumin. Such property was also observed in the case of tissue non-specific alkaline phosphatase (TNAP), a marker in mineral formation. Inhibitors acting at three distinct levels on mineral formation were searched: 1) TNAP; 2) Hydroxyapatite (HA) formation; 3) Matrix vesicle (MV). We found that benzothiophene derivative of tetramisole are water soluble inhibitors of TNAP. A model producing HA as MVs was developed and served to screen HA inhibitors, confirming that several nucleotides inhibited HA formation. We demonstrated that the anti-rheumatic Chinese medicine sinomenine, having no effect on TNAP and theophylline, slowed down HA induced by MVs. The mineralization models presented a great potential to screen putative drugs to cure ostoarthritis.

DISCIPLINE
Biochimie

MOTS-CLES
Alkaline phosphatase, anti rheumatic, benzothiophene, inhibitors, matrix vesicles, mineralization, osteoarthritis, recognition, sinomenine, theophylline, pathological calcification.

Université Claude Bernard Lyon 1
UFR Chimie – Biochimie
UMR CNRS UCBL 5246 – ICBMS
43 Boulevard du 11 Novembre 1918
69622 Villeurbanne Cedex, FRANCE

Jilin University
State key lab for supramolecular
structure and materials
2699 Qianjin Street
130012 ChangChun, CHINE